

**Identifying the role of Mer receptor tyrosine kinase
in glioblastoma multiforme**

Inauguraldissertation

zur

Erlangung der Würde eines Doktors der Philosophie

vorgelegt der

Philosophisch-Naturwissenschaftlichen Fakultät

der Universität Basel

von

Yuhua Wang

aus China

Basel 2012

Genehmigt von der Philosophisch-Naturwissenschaftlichen Fakultät der Universität Basel. Im Auftrag von Dr. Brian A. Hemmings, Prof. Dr. Kurt Ballmer und Prof. Dr. Nancy Hynes.

Basel, den 13.12.2011

Prof. Dr. Martin Spiess

(Dekan)

Table of content

A. List of abbreviation	i
--------------------------------	----------

B. Summary	ii
-------------------	-----------

1. Introduction

1.1	Gliomas	1
1.1.1	Genetics of malignant gliomas	2
1.1.2	Radioresistance and invasion of glioma cells	4
1.1.3	The current status of glioma treatment	6
1.2	Cancer cell invasion	8
1.2.1	Mesenchymal motility	9
1.2.2	Amoeboid motility	10
1.2.3	Collective motility	12
1.2.4	Switching between modes of motility	12
1.3	The Tyro3/Axl/Mer receptor tyrosine kinase family	13
1.3.1	Tyro3 signaling	21
1.3.2	Axl signaling	22
1.3.3	MerTK signaling	25
1.3.4	Dysregulation of TAM-TKs in cancers	29

2. Scope of the thesis	39
-------------------------------	-----------

3. Results and discussion	40
----------------------------------	-----------

Mer receptor tyrosine kinase promotes invasion and survival in glioblastoma multiforme

3.1	Abstract	41
-----	----------	----

3.2	Introduction	42
3.3	Materials and methods	43
3.4	Results	48
3.5	Discussion	58
3.6	Supplementary data	66
4.	General discussion	72
5.	References	79
6.	Appendix	105
6.1	MAP Kinase-Interacting Kinase 1 Regulates SMAD2- Dependent TGF- β Signaling Pathway in Human Glioblastoma Michal Grzmil, Pier Jr Morin, Maria Maddalena Lino, Adrian Merlo, Stephan Frank, Yuhua Wang , Gerald Moncayo, and Brian A. Hemmings	
6.2	Generation of MerTK monoclonal antibody	118
7.	Acknowledgements	122
8.	Curriculum Vitae	123

A. List of abbreviations

Less frequently used abbreviations are defined upon their first use in the text.

BBB	Blood-brain-barrier
bFGF	Basic fibroblast growth factor
ECM	Extracellular matrix
EGFR	Epidermal growth factor receptor
Gas6	Growth arrest-specific gene 6
GBM	Glioblastoma multiforme
MAPK	Mitogen-activated protein kinase
MerTK	Mer tyrosine kinase
MLC2	Myosin light chain 2
MMPs	Matrix metalloproteinases
mTOR	Mammalian target of rapamycin
PDGFR	Platelet-derived growth factor receptor
PI3K	Phosphoinositide-3-kinase
PKB	Protein kinase B
PTEN	Phosphatase and tensin homolog
ROCK	Rho-associated serine-threonine protein kinase
RTK	Receptor tyrosine kinase
TAM	Tyro3, Axl and Mer
VEGF	Vascular endothelial growth factor
2D	2-dimensional
3D	3-dimensional

B. Summary

GBM is one of the most aggressive human cancers. Primary GBM, which comprises more than 90% of biopsied or resected brain tumors, arises *de novo* without an antecedent history of low-grade disease. In contrast, secondary GBM progresses from previously diagnosed low-grade astrocytomas. Despite the implementation of intensive therapeutic strategies and supportive care, the median survival of GBM patients over the past decade has remained at ~ 12-14 months. A classification scheme based on a comprehensive understanding of the genetic alterations and gene expression changes underlying glioma formation has categorized glioblastoma into four distinct molecular subtypes: classical, mesenchymal, neural, and proneural. In addition, the role of cancer stem-like cells is being actively investigated. A transformed neural stem or glial progenitor cell can give rise to tumors, but mature astrocytes can also undergo de-differentiation. The diffusive infiltration nature of malignant glioma cells poses a serious clinical challenge because such cells are widely believed to be responsible for tumor recurrence after surgery, radiation, and chemotherapy.

MerTK is a member of the TAM receptor tyrosine kinase family, which is characterized by a conserved sequence within the kinase domain and a combination of two N-terminal immunoglobulin (Ig)-like domains and two fibronectin type III (FNIII) repeats in their extracellular regions. Although protein S and Gas6 are the putative ligands of TAM kinases, several other proteins have been proposed recently to activate TAM receptors, suggesting the existence of additional mechanisms for TAM activation. Full activation of MerTK requires the autophosphorylation of tyrosines 749, 753 and 754 within the kinase domain and co-immunoprecipitation experiments indicate that several signaling molecules associate with phosphorylated tyrosine 872 of MerTK in the catalytic domain. MerTK appears to be required

for ingestion of apoptotic cells by phagocytes such as monocytes/macrophages, and also by retinal pigment epithelial cells and dendritic cells. Overexpression of MerTK has been reported in many cancer types, including breast and prostate cancer, lymphoma and leukemia. Recently, MerTK was found to be upregulated in the mesenchymal subtype of primary GBMs and depletion of MerTK increases astrocytoma cell chemosensitivity. Nevertheless, the mechanisms of MerTK activation and its activity in brain tumor progression remain unclear.

In this study, MerTK was found to be overexpressed in GBM and GBM-derived spheres compared with non-neoplastic brain tissue and normal human astrocytes, and this is mitigated upon differentiation. Low expression of MerTK was also observed in conventional immortalized GBM cell lines. Co-staining MerTK with the astrocytic marker GFAP (glial fibrillary acidic protein) indicates that MerTK is expressed in the GFAP⁺ cell lineage in GBM samples. MerTK maintains the amoeboid rounded morphology of GBM cells under stem cell culture conditions and MerTK is upregulated in U373 GBM cells cultured in serum-free NBM (neural basal medium). *In vivo* studies have shown that glioma cells migrate in an amoeboid mode due to structural constraints in the neural ECM. Immunofluorescence staining of U373 cells shows intensive blebbing of the cell membrane, which is a typical morphological marker of amoeboidly migrating cells. Knockdown of MerTK not only disrupts rounded cell morphology but also decreases cell infiltrative capacity and increases cell sensitivity to etoposide-induced apoptosis. It was further shown that MerTK autophosphorylation is essential for its anti-apoptotic and pro-invasive activities. Depletion of MerTK attenuates the expression and phosphorylation of MLC2. The results obtained have uncovered a novel activity of MerTK in GBM progression and these findings promote MerTK as a potential therapeutic target in the treatment of GBM, in combination with radio/chemotherapy.

1. Introduction

1.1 Gliomas

Gliomas, the most common type of brain tumor, have their origin either in the brain or in the spine. They arise from mature glial cells, which normally support and protect neural cells, or from their less-differentiated precursors (Fig. 1) (1). Thanks to improvements in standard care, survival of patients with glioblastoma, which is the most aggressive glioma, has improved in the last decade from an average of 10 months to 14 months after diagnosis (2).

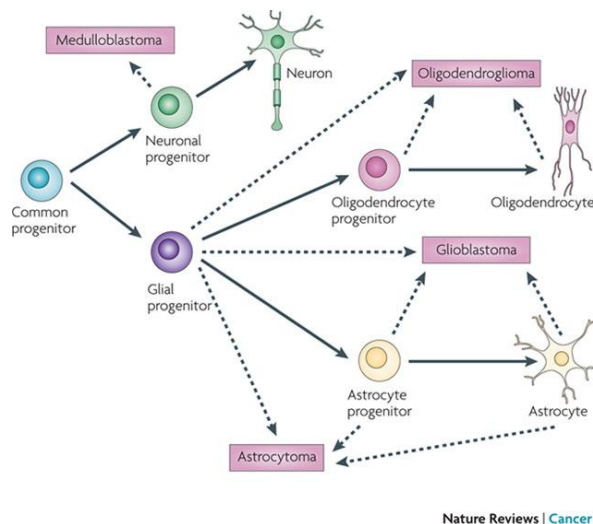


Figure 1. The neuroglial lineage tree. Self-renewing, common progenitors are thought to produce committed neuronal and glial progenitors that eventually differentiate into mature neurons, astrocytes and oligodendrocytes. Although the precise cells of origin for diffuse glioma variants and medulloblastoma remain largely unknown, a selection of likely candidates for each (*dashed arrows*) is indicated. (Taken from (1)).

According to the World Health Organization (WHO) classification, 4 grades (I, II, III and IV) of glioma are distinguished. In contrast to lower grades (I and II), high-grade (III and IV) tumors are more aggressive and have a worse prognosis. Histologically, high-grade gliomas display features such as nuclear atypia, increased proliferation, microvascular proliferation and necrosis (1). Radiologically, malignant gliomas appear as masses with irregular contours (Fig. 2). Roughly 90% of GBM (Grade IV) arise *de novo*, while 10% originate from lower grade astrocytoma and are known as “secondary” GBM (3).

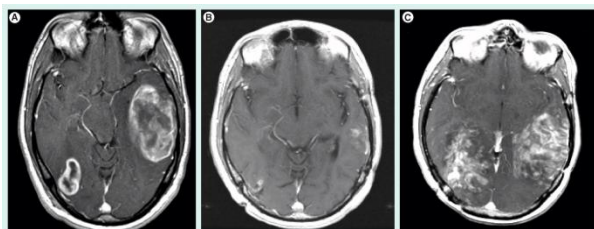


Figure 2. Axial T1-weighted post-contrast magnetic resonance image (MRI) sequences of a patient with glioblastoma. (A) At diagnosis an enhancing multifocal temporal and right parietoccipital tumor is seen. (B) The patient received combined chemo- and radiation-therapy and achieved a response. (C) The tumor recurred 2 years after diagnosis in a diffusely infiltrating fashion and the patient died. (Taken from (9)).

1.1.1 Genetics of malignant gliomas

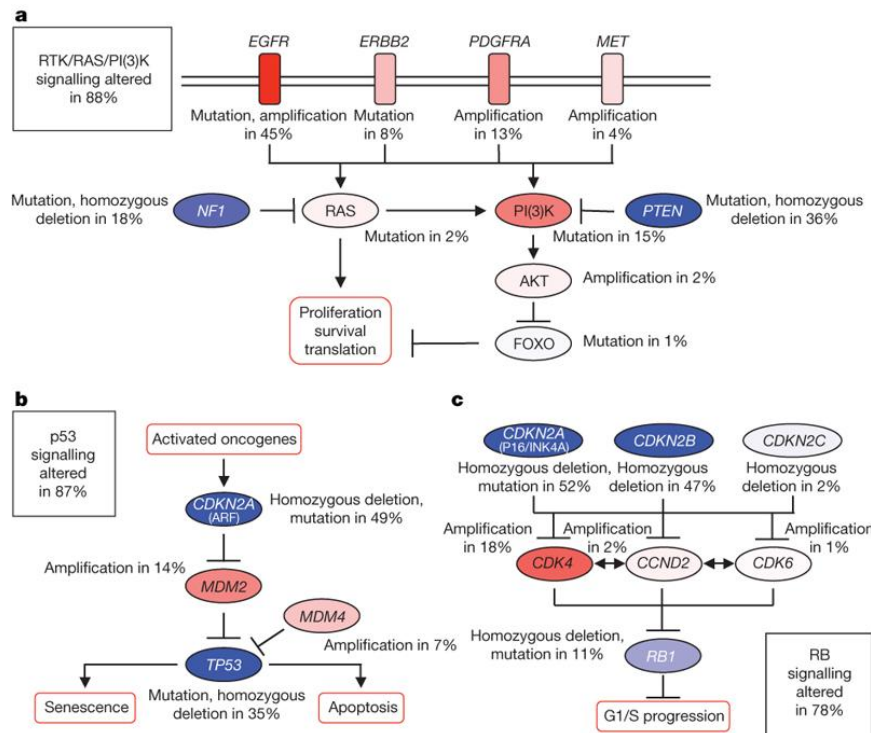


Figure 3. Frequent genetic alterations in three critical signaling pathways. a-c, Primary sequence alterations and significant copy number changes for components of the RTK/RAS/PI3K (a), p53 (b) and RB (c) signaling pathways are shown. Red indicates activating genetic alterations, with frequently altered genes showing deeper shades of red. Conversely, blue indicates inactivating alterations, with darker shades corresponding to a higher percentage of alterations. For each altered component of a particular pathway, the nature of the alteration and the percentage of tumors affected are indicated. Boxes contain the final percentages of glioblastomas with alterations in at least one known component gene of the designated pathway (Taken from (4)).

Like many other cancer cells, gliomas harbor multiple chromosomal aberrations, nucleotide mutations and epigenetic modifications that drive the development and progression of malignant transformation. Although the traditional pathological diagnosis provides a valuable approach to distinct tumor grades within categories of the same tumor type, the highly

heterogeneous nature of GBM tumors results in an inconsistency of clinical outcome within the same group of patients. This indicates the existence of further subtypes within each grade. In order to identify and classify the major gene alterations in GBM, The Cancer Genome Atlas (TCGA) performed multi-dimensional study of over 206 primary GBM tumor tissues (4). Comprehensive characterization defined three main signaling pathways that are dysregulated in the majority of GBM tumors, including the RTK/RAS/PI3K, p53 and retinoblastoma (RB) signaling pathways (4) (Fig. 3). A further important recent development by TCGA was the

genome-wide analysis of 500 untreated primary GBM tumor samples. Based on the expression file and genetic data, GBM is now classified into 4 subtypes according to their genetic alterations: classical, mesenchymal, neural, and proneural (5) (Fig. 4). All examples of the “classical”

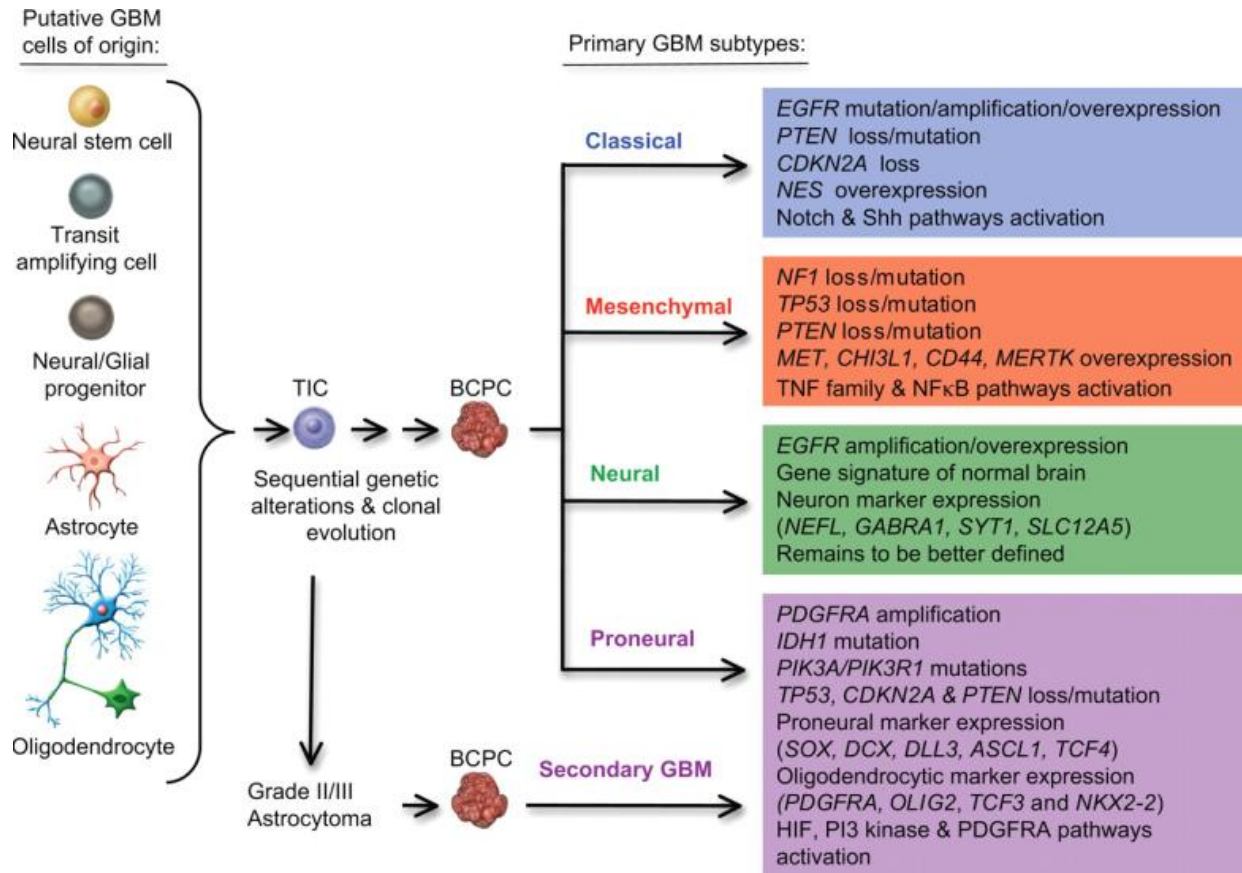


Figure 4. Sequential genetic changes observed in the pathogenesis of different subtypes of glioblastoma. Some cells in the normal brain undergo genetic alterations, which leads to a population of tumor-initiating cells (TICs), which can then further accumulate genetic and epigenetic changes and become brain cancer-propagating cells (BCPC). The latter cells are responsible for the formation of glioblastoma. TNF, tumor necrosis factor; HIF, hypoxia-inducible factor; IDH, isocitrate dehydrogenase (Taken from (2)).

subtype have a chromosome 7 amplification paired with chromosome 10 loss. EGFR amplification is found in 97% of the classical subtype and the homozygous deletion of *CDKN2A* encoding for both *p16INK4A* and *p14ARF* is also frequently associated with this subclass. Efficacy of the standard treatment for GBM patients after surgery such as radio/chemotherapy also shows a high correlation with classical GBM. Secondly, the mesenchymal subclass shows high expression of mesenchymal markers coupled with frequent inactivation of *NF1*, *TP53* and

PTEN. These tumors are responsive to intensive chemo/radiation therapies. The proneural subtype is named after the distinct expression of genes in oligodendrocytic and proneural development. Aberrant expression of *PDGFRA* and a high frequency of *IDH1* mutation are the two major features of this GBM subtype. Unfortunately, these tumors show the least response to standard treatment. Finally, the neural subtype of GBM tumors has high expression of neural markers and shows a low degree of infiltration. Notably, all subtypes commonly demonstrate dysregulation of the p53, RB and RTK signaling pathways, and tumors do not change subclass after recurrence (5).

1.1.2 Radioresistance and invasion of glioma cells

Although radiotherapy improves the survival of GBM patients compared with the best supportive care (6), radioresistance is an age-old problem with many cancers, including malignant gliomas. A major challenge with malignant gliomas is that tumor cells escaping surgical removal are able to invade adjacent brain tissue, even with intensive radio/chemotherapy. In fact, DNA damage was shown to enhance the potential for radioresistance and invasiveness of residual tumor cells after surgery (7-9), but the mechanisms underlying tumor radioresistance remain unclear.

Rapidly expanding research on glioma-initiating cells with stem cell characteristics, such as long-term self-renewal and the capacity to differentiate, has provided new insight into the molecular mechanisms of infiltration, radioresistant glioma growth and recurrence. Although it has been shown that CD133⁻ cells can give rise to CD133⁺ *in vivo* (10, 11), CD133 is still the most frequently used marker for identification of glioma stem cells. The DNA damage checkpoint is preferentially activated in CD133⁺ tumor cells isolated from glioma xenografts and

primary GBM tumor tissues, and radiation-induced DNA damage is more efficiently repaired than in CD133⁺ tumor cells (7). Furthermore, inhibition of the checkpoint kinases Chk1 and Chk2 sensitizes glioma stem cells to ionizing radiation-induced death, indicating that suppression of the DNA-damage checkpoint may improve the efficacy of radiotherapy in GBM (7). Other markers such as SSEA-1(12), Nestin, Sox2 and Musashi-1 are also used. Nevertheless, further investigation of the molecular biology of glioma stem cells is required.

The invasive nature of glioma cells poses a severe challenge for GBM treatment. The diffusing process of glioma cells has characteristics of non-neural carcinoma cells infiltrating into the stroma, namely cell detachment from the tumor mass, adhesion to surrounding ECM, and degradation or deformation of ECM that allows cell movement (13). Brain parenchyma lacks many elements of other organs, such as collagen, fibronectin and type I laminin, and is comprised largely of the polysaccharide hyaluronan and a proteoglycan-based matrix (13). The uniqueness of the neural ECM may explain the lack of dispersion of tumor cells migrating into the brain and also suggests that glioma cells infiltrate into surrounding tissues by distinct mechanisms (14).

Glioma cells migrate along white matter tracts, leading in many cases to invasion of the opposite brain hemisphere. Alternatively, they move along the basal lamina of brain blood vessels or between the glia limitans and the pia mater. The expression of lysosomal hyaluronidases and secretion of proteases by glioma cells leads to the degradation of pre-existing ECM. Coupled with the overproduction of neural ECM components, the secretion of novel ECM molecules and the expression of new cell-surface receptors for ECM signals, this leads to a remodeling of the surrounding matrix and the bypassing of molecular and structural inhibitory factors in the neural parenchyma. The result is the dissemination of glioma cells in the brain (14).

However, a clinical trial using MMP inhibitor cocktails was not effective because the inhibition of proteolysis caused an amoeboid phenotype in tumor cells, which could then infiltrate through the limited extracellular space (15). In the absence of spatial constraints in 2D, glioma cells migrate as fibroblasts by the formation of extended lamellipodium without nuclear distortion (15). In contrast, given the submicrometer size of the extracellular matrix in neuropil, glioma cells invade, like neural progenitor cells, dependent on myosin II activity (15). Although inhibition of myosin II strikingly devastates glioma cell migration (15), there is no doubt that the motility mechanism of tumor cells within the brain is flexible and reacts to the extracellular environment.

In addition to the effects of ECM on tumor invasion, there is cross-talk between glioma cells and neurons, glial, endothelial and immune cells in the tumor microenvironment (16, 17). Soluble factors secreted by these cells, including EGF, TGF- α , TGF- β , bFGF, may promote glioma cell proliferation, survival and motility (16, 18). It has been widely shown that hypoxia conditions accelerate tumor cell migration. Lack of oxygen can activate and stabilize hypoxia-inducible factor HIF-1 α , a well-known transcriptional regulator of glioma angiogenesis and invasion (19, 20). Knockdown of HIF-1 α was reported to reduce hypoxia-induced glioma cell migration and invasion (21).

1.1.3 The current status of glioma treatment

The dysregulated signaling pathways (Fig. 3) identified in glioma have provided insights into many neoplastic molecular alterations and, thus, novel therapeutic targets. This has led to the first generation of molecular drugs that inhibit these pathways in the clinical setting. These

Table 1. Some targets and molecular agents currently in clinical development for high-grade glioma

Primary target	Agent	Other targets	Mechanism of action
EGFR	Gefitinib (ZD1839) Erlotinib (OSI-774) Lapatinib (GW-572016) PF-00299804 BIBW2992 Cetuximab Nimotuzumab	HER-2 HER-2, HER-4 HER-2, HER-4	TKI TKI TKI TKI (irreversible) TKI (irreversible) Monoclonal antibody Monoclonal antibody
EGFRVIII	CDX110		Vaccine
Farnesyl transferase	Lonafarnib (SCH 66336) Tipifarnib (R115777)		FTI FTI
FGFR	Brivanib (BMS-582664) Vorinostat (SAHA) Valproic acid LBH589	VEGFR2	TKI HDAC inhibitor HDAC inhibitor HDAC inhibitor
HGF/SF	AMG102		Monoclonal antibody
HSP-90	17-AAG		Blocks HSP-90 ATP binding
Integrins $\alpha v\beta 3$, $\alpha v\beta 5$	Cilengitide (EMD121974)		Synthetic RGD peptide
c-Met	XL184	VEGFR	TKI
mTOR	Sirolimus (rapamycin) Everolimus (RAD001) Temozolimus (CCI-779) Ridaforolimus (AP23573)		mTOR inhibitor mTOR inhibitor mTOR inhibitor mTOR inhibitor
PDGFR- α	IMC3G3		Monoclonal antibody
PDGFR- β	Imatinib Dasatinib Tandutinib (MLN518)	BCR/Abl, c-Kit Src, BCR/Abl, c-Kit, ephrin A2 Flt3, c-Kit	TKI TKI TKI
PI3K	XL765	mTOR	STKI
PKC	Enzastaurin (LY31761)		STKI
VEGF-A	Aflibercept (VEGF Trap) Bevacizumab	VEGF-B, PlGF	Soluble decoy receptor Monoclonal antibody
VEGFR-2	Cediranib (AZD2171) CT-322 Pazopanib Sorafenib Sunitinib Vandetanib (ZD6474) XL-184	All VEGFR subtypes, PDGFR- β , c-Kit All VEGFR subtypes All VEGFR subtypes, PDGFR- α and β , c-Kit VEGFR-3, B-Raf, PDGFR- β , c-Kit, Ras, p38 α PDGFR- β , Flt3, c-Kit EGFR c-Met, RET, c-Kit, Flt3, Tie-2	TKI Adnectin TKI TKI TKI TKI TKI

TKI, tyrosine kinase inhibitor; FGFR, fibroblast growth factor receptor; FTI, farnesyltransferase inhibitor; VEGFR2, vascular endothelial growth factor receptor 2; HDAC, histone deacetylase; SAHA, suberoylanilide hydroxamic acid; HGF/SF, hepatocyte growth factor/scatter factor; HSP-90, heat shock protein 90; 17-AAG indicates 17-allylamino-17-demethoxygeldanamycin; RGD, arginine-glycine-aspartate; STKI, serine-threonine kinase inhibitor; PKC, protein kinase C; PlGF, placental growth factor.

agents can be classified into several groups that inhibit growth factor receptors, intracellular signaling pathways or angiogenesis (13).

The most attractive therapeutic target is EGFR, which is overexpressed in over 40% of primary GBM, especially of the classical subtype (Fig. 4). The *EGFR* gene with a deletion of

exon 2-7 (EGFRvIII) is ligand-independent constitutively activated (22, 23) and promotes cell proliferation, invasion and survival in many cancer types (24-26).

The PDGFR subtypes α and β and PDGF isoforms (AA, AB, BB, CC, DD) are also overexpressed and hyperactivated in malignant gliomas, especially in the proneural subtype (Fig. 4) (27). The autocrine or paracrine loop of PDGF was shown to promote glioma cell proliferation and angiogenesis (13, 28). In addition to growth factor receptors, key components of intracellular signaling pathways such as Ras, PI3K/PKB, MAPK, mTOR also provide attractive therapeutic targets (13). Moreover, given the high vascularization of GBM tumors, anti-angiogenic drugs blocking interactions between secreted pro-angiogenic molecules and their receptors can be additional tools for GBM treatment (29).

GBM is notorious for its biological diversity and histological heterogeneity and, thus, single agents targeting one “key” component are unable to cure GBM patients (30). Multi-targeting single agents would be a more effective strategy for GBM treatment (Table 1, taken from (2)), but the majority of the targeted molecular drugs for GBM examined clinically have been disappointing, with no evident prolongation of survival (31). More personalized treatment supported by expanding knowledge of glioma genetics will hopefully improve therapeutic target selection in the future.

1.2 Cancer cell migration and invasion

The ability of cancer cells to migrate into or invade surrounding tissues is one of the most life-threatening aspects of cancer. Migration requires modification of cell body shape and the remodeling of the ECM. Cancer cells disseminate from the primary tumor mass either as single cells, with amoeboid or mesenchymal motility, or as cell sheets, strands and clusters by

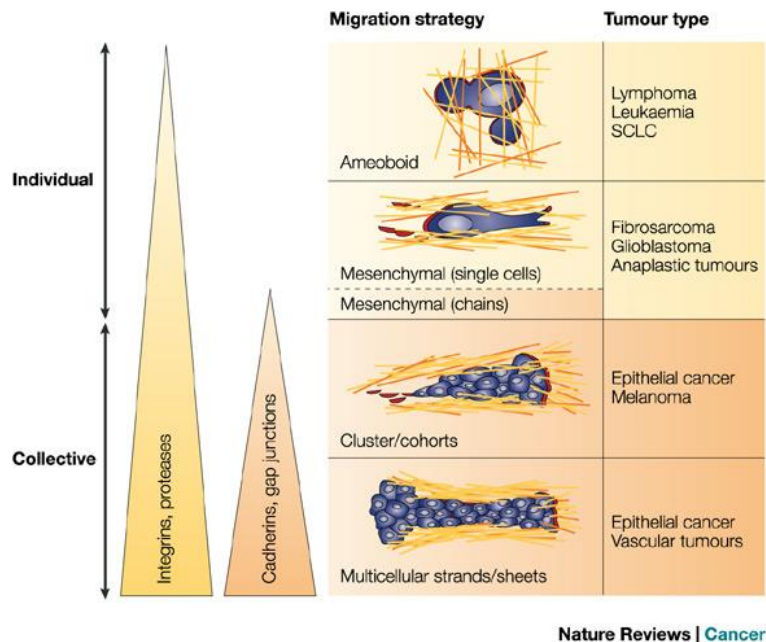


Figure 5. Diversity of tumor invasion mechanisms. (Taken from (33)).

collective migration. These processes are usually influenced by transmembrane adhesion receptors, matrix-degrading enzymes, and cell–cell interaction molecules (Fig. 5). Unlike Epithelial Mesenchymal Transition (EMT), which is a very rigid process following relatively extensive alterations in gene expression, the amoeboid and mesenchymal types of invasiveness are interchangeable modes that allow tumor cell motility according to the extracellular environment. The motility mode may change at different stages of the invasive process, in parallel to alterations in the microenvironment. Further study of the mechanisms mediating Mesenchymal Amoeboid Transition/Amoeboid Mesenchymal Transition (MAT/AMT) may provide novel key insights into tumor cell invasion/metastasis and trigger concepts for more efficient therapeutic drugs.

1.2.1 Mesenchymal motility

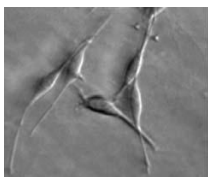


Figure 6. Mesenchymal morphology of K4 sarcoma cells. (Adapted from (32)).

Mesenchymally migrating cells have a fibroblast-like spindle-shaped morphology with the formation of actin-rich filopodia and lamellipodia at the leading edge (32). Generally, mesenchymal migration occurs in five steps: 1. protrusion formation at the leading edge; 2. cell-matrix interaction and formation of local contacts; 3. remodeling of ECM

by recruitment of surface proteases and focalized proteolysis; 4. cell contraction by actomyosin dependent on myosin II activity; 5. detachment of the trailing edge (33). In 3D view, cells are polarized and display an elongated shape and move with a velocity of approximately 0.1-0.5 $\mu\text{m}/\text{min}$ (34) (Fig. 6). Polymerization of actin is mediated by Rho-family small GTPase Rac and cdc42 through regulation of WASP/WAVE proteins (35, 36). The association of Arp2/3 with N-WASP and WAVE results in Arp2/3 activation and subsequently enhances the nucleation of actin filaments and branch formation at the leading edge (37). Focal contacts are mediated by integrins that link ECM to the actin cytoskeleton. Integrin clusters recruit many adaptor proteins, such as paxillin, vinculin, zyxin as well as protein kinases like Src and FAK, which further stabilizes focal adhesion (38). Activation of MMPs and uPA is also necessary for mesenchymal migration. Autocrine or paracrine of MMPs have been shown to promote cancer cell invasion *in vitro* and *in vivo* (39-42).

1.2.2 Amoeboid motility

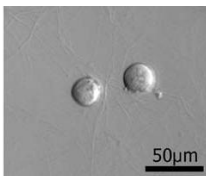


Figure 7. Amoeboid morphology of A3 sarcoma cells. (Adapted from (32)).

Amoeboid migration refers to the specific moving mechanism of the amoeba, which is characterized by actomyosin-mediated cycles of expansion and

contraction of the cell body. Amoeboidly migrating cells have a rounded cell morphology in 3D (Fig. 7). In higher eukaryotes, amoeboid-like movement is maintained in leukocytes and some cancer cells (43-46). The differences between amoeboid and mesenchymal migration are summarized in Table 2 (Taken from (33)).

Table 2. Differences in cellular and molecular migration mechanisms

Table 2 Differences in cellular and molecular migration mechanisms		
Characteristic	Mesenchymal	Amoeboid
Cell shape	Elongated, fibroblast-like (length 50–200 μm)	Roundish/elliptoid (length 10–30 μm)
Growth in culture	Adhesive	Growth in suspension
Migration velocity	Low (0.1–1 $\mu\text{m}/\text{min}$)	Low to high (0.1–20 $\mu\text{m}/\text{min}$)
Cell-matrix interactions	Integrins and proteases focalize	Integrins and proteases are non-focalized
Structure of actin cytoskeleton	Cortical and stress fibres	Cortical
Adhesion force generated	High, fibre pulling and bundling	Low, minor fibre bending
Proteolytic extracellular-matrix remodelling	Present to extensive	Not present
Cellular migration mechanism	Traction dependent	Propulsive, cytoplasmic streaming
Mechanism overcoming matrix barriers	Path generation, formation of proteolytic ECM defects	Path finding, propulsion and cytoplasmic forward flow ('streaming'); squeezing through narrow regions (constriction ring)
Prototypic non-neoplastic cell	Fibroblast, smooth-muscle cell	Lymphocyte, neutrophil
Neoplastic cells, carcinoma	Fibrosarcoma, glioblastoma, dedifferentiated epithelial cancer	Lymphoma, small-cell lung carcinoma, small-cell prostate cancer

Unlike mesenchymal migration, with tight local contacts, amoeboid tumor cells adhere loosely to substrates due to low integrin activity (47-50). Instead of degrading ECM, amoeboid-like invasion is dependent on actomyosin contractility promoted by Rho/ROCK signaling pathways (46, 51). Activated Rho can phosphorylate ROCK, which inactivates myosin-light-chain phosphatase (MLCP) or directly phosphorylates MLC2 (52, 53). In addition, myosin-light-chain kinase (MLCK) has an antagonistic effect on MLCP, which can also activate MLC2 (53). Phosphorylation of MLC2 at Ser19 followed by Thr18 enhances the ATPase activity of myosin II, promoting its interaction with actin filaments and thereby increasing cell contractility (54). The penetration of pre-existing ECM by amoeboid tumor cells without proteolysis requires sufficient motive force and cell tension. The intracellular pressure leads either to detachment from the matrix or to the formation of membrane blebs. The formation of blebs is driven by inflow of the cytoplasm and not by the actin polymerization that leads to lamellipodia in mesenchymal motility (55).

1.2.3 Collective motility

In contrast to single-cell migration, collective motility of tumor cells involves the movement of whole clusters, sheets or strands, a process that often occurs during embryogenesis and the development of mammalian glands (56-58). Of the variants of collective migration shown in Figure 5, “cluster/cohorts” are detached and disseminating cell collectives, such as those observed in the highly differentiated epithelial cancers of breast and colon. “Multicellular strands/sheets” do not detach or metastasize. However, these cells still have invasive features (33). Collective invasion is characterized by a high concentration of autocrine growth factors and proteolytic enzymes that promote tumor growth and invasion.

1.2.4 Switching between modes of motility

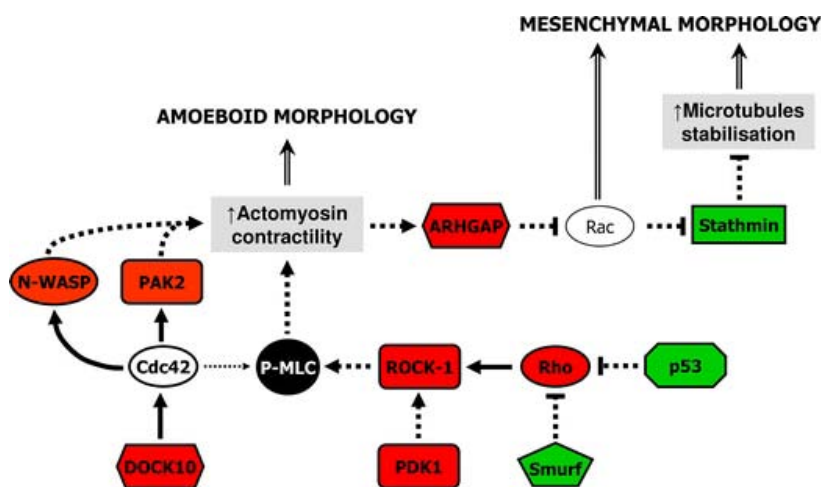


Figure 8. Interactions between the components of signaling pathways documented to be involved in the MAT/AMT transitions of cells in a 3D environment. The inhibition of the activity of the proteins highlighted in red was shown to trigger amoeboid to mesenchymal transitions. Inactivation of the proteins depicted in green induces a conversion from the mesenchymal to the amoeboid mode of invasiveness. *Solid lines* direct connections, *dashed lines* indirect connections. (Taken from (32)).

In *in vitro* and *in vivo* studies, an MMP inhibitor cocktail treatment induced the transition to a typical amoeboid rounded morphology, indicating the compensatory nature of invasion by tumor cells (43). In addition, inhibition of integrin activity was also shown to promote Collective Amoeboid

Transition (CAT) (59). Since amoeboid invasion largely relies on Rho/ROCK signaling

pathways, suppression of either Rho or ROCK will trigger a transition from a rounded morphology to an elongated mesenchymal shape (46). Rac1-mediated cell polarity and lamellipodia formation are believed to be the key regulators of mesenchymal invasion. Inhibition of Rac impairs the assembly of focal adhesion and therefore renders the amoeboid motility (60).

Smurf1 protein is an E3-ubiquitin ligase that degrades RhoA and impairs Rho/ROCK signaling (61). Inhibition of Smurf1 in mesenchymal BE colon cells is sufficient to induce MAT (62). Additionally, p53 was reported to act downstream of cdc42, which is involved in many pathways important in the regulation of cell motility. The loss of p53 activity can trigger MAT along with increased RhoA activity (63). The components of the signaling pathways involved in MAT/AMT are illustrated in Figure 8.

1.3 The Tyro3/Axl/Mer receptor tyrosine kinase family

The human genome encodes 90 tyrosine kinases that modulate a wide range of fundamental cellular events, including proliferation, growth, metabolism, apoptosis and motility (64). The 58 RTKs are classified into 20 families that transduce signals from the extracellular environment to the cytoplasm and nucleus by binding to ligands. TAM receptor tyrosine kinase family members are among the few that are specific to vertebrates (65). TAM receptors are characterized by a conserved sequence KW(I/L)A(I/L)ES within the kinase domain, as well as two fibronectin type III repeats and two immunoglobulin-like domains in the extracellular region (66) (Fig. 9). Overall, the protein sequences of the human TAM receptors within the kinase domain are 54-59% identical (72-75% similar), while the protein sequences in the extracellular domain are 31-36% identical (52-57% similar) (67). The predicted molecular weights of TAM receptors are 97, 98 and 110 kDa, respectively. However, the actual sizes range from 100 to 140 kDa for Axl and

Tyro3 and 165-205 kDa for MerTK due to posttranslational modifications, especially glycosylation (68-70). Tyro3 and Axl are ubiquitously expressed in tissues, whilst MerTK is mainly expressed in the hematopoietic system (66). High expression of MerTK is also found in ovary, prostate, testis, lung, retina, and kidney. Lower levels of MerTK are found in heart, brain, and skeletal muscle (66). In addition, TAM receptors are markedly expressed in many cancer types (Table 3).

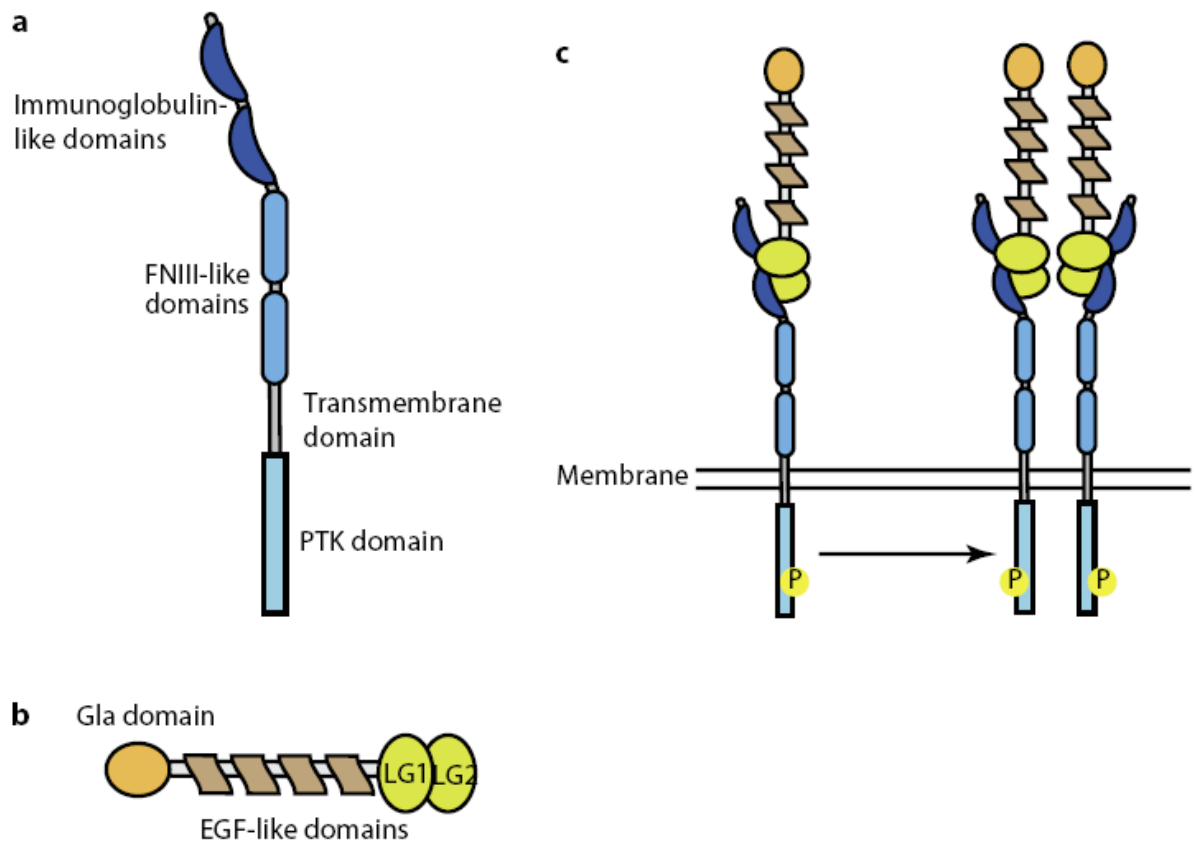


Figure 9. Schematic of TAM receptors and their ligands protein S and Gas6. a, The domain structure of TAM receptor family. b, The two TAM receptor ligands, Protein S and Gas6, also share a common domain structure. c, Binding of the ligand to the two immunoglobulin domains of the receptor is mediated via the LG1 region of the ligand. (Taken from (122)).

Table 3. TAM receptors expression in human cancers

Cancer	Axl	Mer	Tyro3
Myeloid leukemias (AML, CML)	(71-74)		(75)
Lymphoid leukemias (ALL)		(76-78)	
Erythroid leukemia	(72)		
Megakaryocytic leukemia	(72)		
Mantle cell lymphoma		(79)	
Multiple Myeloma			(80)
Uterine endometrial cancer	(81)		(81)
Gastric cancer	(82, 83)	(83)	
Colon cancer	(84)		
Prostate cancer	(85-87)	(88)	
Thyroid cancer	(89-91)		(91)
Lung cancer	(92, 93)		
Breast cancer	(94, 95)	(96)	
Ovarian cancer	(97-99)		
Liver cancer	(100)		
Renal cell carcinoma	(101)		
Astrocytoma/Glioblastoma	(102-104)	(5, 104)	
Pituitary adenoma		(105)	
Melanoma	(106-108)	(108, 109)	(108)
Osteosarcoma	(110)		
Rhabdomyosarcoma		(111)	
Pancreatic cancer	(112, 113)		
Bladder cancer	(114, 115)		
Hepatocellular carcinoma	(116, 117)		
Oral squamous cell carcinoma	(118)		

Regulation of TAM-TK activity

The reported biological ligands of TAM receptors are vitamin K-dependent Gas6, Protein S, Tubby and Tubby-like protein 1 (Tulp1) (119-121). Gas6 and protein S share 43% protein

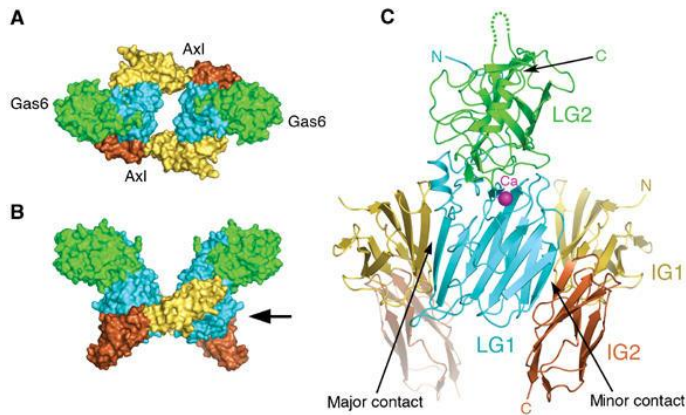


Figure 10. Overall architecture of the Gas6-LG/Axl-IG complex. Shown are three orthogonal views. A. Top view, towards the cell membrane harboring the receptor. B. Side view, with the cell membrane at the bottom. C. Front view, in the direction indicated by the arrow in (B). Surface representations are shown in (A) and (B), while a cartoon representation is shown in (C). Gas6-LG is in cyan (N-terminal segment and LG1) and green (LG2), Axl-IG is in yellow (IG1) and brown (IG2). In (C), the Gas6-LG molecule at the back has been removed for clarity, a calcium ion in the LG1-LG2 interface is shown as a pink sphere, and the Gas6/Axl contact sites are labeled. (Taken from (124)).

sequence identity and have the same structure with an N-terminal Gla domain (a region which is γ -carboxylated in a vitamin-D-dependent posttranslational modification), four epidermal growth factor (EGF)-like domains and two laminin-G (LG) domains. Thrombin cleavage sites are present in Protein S but not in Gas6 (122) (Fig. 10B). Although Gas6 binds to and activates all TAM receptors, MerTK has the lowest binding

affinity for Gas6 (120). The newly identified ligand Tup11 can bind to all three TAM members, while Tubby binds only to MerTK (121). Protein S was first described as a ligand of Tyro3 (123). Nevertheless, the validity of Protein S as a ligand of all TAM receptors requires further investigation (66). The crystal structure of the Gas6/Axl complex reveals an assembly of 2:2 stoichiometry, in which the two Ig-like domains of the Axl are crosslinked by the LG1 domain of Gas6, with no direct Axl/Axl or Gas6/Gas6 contacts (124) (Fig. 10). There are two distinctive Gas6/Axl binding sites that are required for Axl activation. However, only the minor Gas6 binding site is conserved in MerTK and Tyro3, indicating that the structures of the Gas6/MerTK and Gas6/Tyro3 complexes may be very different (124).

Conventional RTK activation is believed to be initiated by ligand binding to the extracellular domain, which leads to the trans-autophosphorylation of multiple tyrosine residues within the kinase domain and further to downstream signaling (125). In relation to this, five possible means of TAM receptor activation have been proposed: 1. ligand-independent dimerization; 2. ligand-dependent dimerization; 3. heteromeric dimerization of two different TAM receptors; 4. heterotypic dimerization with a non-TAM receptor; 5. trans-cellular binding of extracellular domains (66).

Full activation of MerTK requires the autophosphorylation of Y749, Y753 and Y754 in the activation loop of the kinase domain (126). Further *in vitro* kinase assays have identified tyrosine 749 as the preferred site of autophosphorylation, and single mutations of the three residues to phenylalanine reduced MerTK kinase activity to 39%, 10% and <6%, respectively (126). These three tyrosine residues are conserved in TAM receptors and correspond to residues Y681, Y685 and Y686 in human Tyro3 and residues Y698, Y702 and Y703 in human Axl. Interestingly, autophosphorylation of Tyro3 and Axl at these sites has not been reported (66).

The tight control of protein kinases maintains normal cellular functions, and aberrant expression or dysfunction of tyrosine kinases is responsible for many diseases, including cancers. In this connection, several counter-reactions have developed that attenuate or terminate tyrosine kinase activities induced by the stimulation of ligands, including antagonistic ligands, hetero-oligomerization with receptor inactive mutants, phosphorylation of inhibitory residues by other kinases, dephosphorylation of activating residues by phosphatases and receptor endocytosis, and degradation (125). Only a few of these mechanisms have been reported in the case of TAM receptor deactivation. Although the phosphatase C1-TEN was shown to bind Axl, neither enzymatic activity of C1-TEN nor direct dephosphorylation of Axl have been demonstrated

(127). Soluble forms of Axl and MerTK, produced by proteolytic cleavage were detected in murine and human plasma (70, 128-130). Binding of soluble Axl or MerTK to Gas6 can block the normal cellular functions of full-length kinases (70, 128).

Cellular functions of TAM-TKs

The activation of TAM receptors has diverse cellular effects depending on cell type and the microenvironment. Mice with single, double or even triple TAM member knockout are viable (68, 131, 132). However, TAM adult knockout mice develop autoimmune diseases, including rheumatoid arthritis and lupus (131, 133). The phenotype is more pronounced in double than single knockouts and most severe in triple knockouts, suggesting overlapping or cooperative roles of TAM receptors (131). Further investigation found these symptoms to be associated with a deficiency of apoptotic cell clearance by macrophage and dendritic cells (132).

Clearance of apoptotic cells plays an important role in the maintenance of normal cell function. Progressive accumulation of cell debris increases tissue necrosis, leading to inflammation and autoimmune diseases. Phosphatidylserine (PS) receptors expressed on the surface of apoptotic cells were shown to bind directly to phagocytes or indirectly to soluble proteins, including Gas6 and Protein S, which suggests that TAM receptors recognize apoptotic cells through their ligands (134, 135). The newly identified TAM receptor ligands Tubby and Tulp1 are bridging molecules, with their N-terminal regions binding to MerTK and the C-terminal regions interacting with apoptotic cells (121). Further study showed MerTK to be involved mainly in macrophage-mediated clearance while dendrite clearance of apoptotic cells was mostly regulated by Axl and Tyro3 (136). TAM receptors have also been shown to regulate mammalian spermatogenesis (68). Male animals lacking all three TAM receptors are infertile

and have smaller testes than wild-type males (68). About 1 week after the onset of sperm production, the seminiferous tubes of the testes of TAM^{-/-} mice are full of apoptotic cell debris, resulting in the death of nearly all germ cells. This degenerative phenotype is due to the lack of functional TAM receptors in Sertoli cells, which express all three TAM receptors and their ligands (68). Without TAM signaling, clearance of apoptotic germ cells in the testes is almost completely abolished (68, 137-139).

A remarkably similar phenotype is observed in the retina of TAM knockouts. In this situation, MerTK is seemed to make the major contribution (140). Adult MerTK knockouts are blind due to the rapid and progressive degeneration of photoreceptors (PRs) (141). This is a degenerative rather than a developmental phenotype as the retina of MerTK knockouts develop normally and at 2 weeks after birth are still histologically indistinguishable from wide-type. However, around 3 weeks after birth, apoptotic cells are seen specifically in the PR layer of MerTK knockouts, and by 10 weeks nearly all the PR cells have died (141). In agreement with this, mutation of MerTK was found in retinal dystrophic Royal College of Surgeons (RCS) rats and in patients with retinitis pigmentosa (142, 143). Later, co-immunoprecipitation identified an interaction between MerTK and myosin IIA heavy chain. Treating MerTK^{+/+} retinal pigment epithelial cells (RPEs) with photoreceptor outer segment (OS) tips led to the redistribution of myosin IIA and IIB from the cell periphery to co-localize with ingested OS, which consequently facilitated phagocytosis. In contrast, MerTK^{-/-} RPEs failed to regulate myosin II redistribution and exhibited a severe phagocytic defect (144). Consistently, MerTK^{-/-} mice have considerably more antibody-forming cells (AFCs) and germinal centers (GCs) than wild type, as well as Th1-skewed IgG2 antibody responses against the T cell-dependent antigen (145). MerTK is expressed by tangible body macrophages (TBM Φ s) in GCs, which contain many phagocytized apoptotic cells in various

states of degradation. MerTK^{-/-} mice have more apoptotic cells in GCs than MerTK^{+/+} mice, whereas the number of TBM Φ s is similar, suggesting an important role for MerTK in GC apoptotic cell clearance by TBM Φ s, as well as in the regulation of B cell tolerance operative in the AFC and GC pathways (145).

In addition to playing a crucial role in apoptotic cell clearance, TAM receptors have been shown to regulate innate immune responses. MerTK knockout mice produce TNF- α in excess upon lipopolysaccharide (LPS) administration with an associated increased sensitivity to LPS-induced endotoxic shock (146). Moreover, TAM receptors were shown to be negative regulators of both Toll-like receptor (TLR) and TLR-induced cytokine receptor cascades through the type I interferon receptor (IFNAR) and its associated transcription factor STAT1(147). TLR induction of IFNAR-STAT1 signaling upregulates TAM signaling and hijacks this pro-inflammatory pathway by inducing the cytokine and TLR suppressors SOCS1 and SOCS3 (147). MerTK can also prevent autoimmune diseases by negatively regulating hematopoietic cell migration into the peritoneal cavity, whilst cells lacking other TAM members, Axl or Tyro3, do not show aberrant regulation in peritoneal cell numbers or the autoimmune phenotype (148). Further study identified elevated expression of CXCL9, its receptor CXCR3, and IL-7R on MerTK^{-/-} peritoneal cells. Deletion of CXCR3 donor cells decreased the number of adoptively transferred cells that entered into the peritoneum of MerTK^{-/-} mice (148).

Furthermore, MerTK knockout mice are more vulnerable to Nephrotoxic serum (NTS) treatment, with a decreased survival rate and significantly increased proteinuria and serum urea levels compared with wild type at day 3 post-injection (149). Upon NTS treatment, MerTK expression is significantly increased in glomeruli in WT mice, whilst MerTK^{-/-} glomeruli are

hyperplastic and later become necrotic (149). The protective role of MerTK seen in NTS-induced nephritis may arise through its activity in apoptotic cell clearance and anti-inflammation.

In addition, *Gas6*^{-/-} mice and TAM single knockouts display platelet dysfunction, predicting that all TAM members are required for platelet aggregation (134, 150). Not surprisingly, TAM double or triple knockouts exhibit a more severe phenotype than single knockouts, with impaired hemostasis and mild thrombocytopenia (151).

In summary, TAM members and their ligands play essential roles in apoptotic cell clearance and innate immune response. However, it is not yet known whether the specificity of TAM signaling in phagocytosis is associated with other factors, such as the specific process leading to the death of the apoptotic cells.

1.3.1 Tyro3 signaling

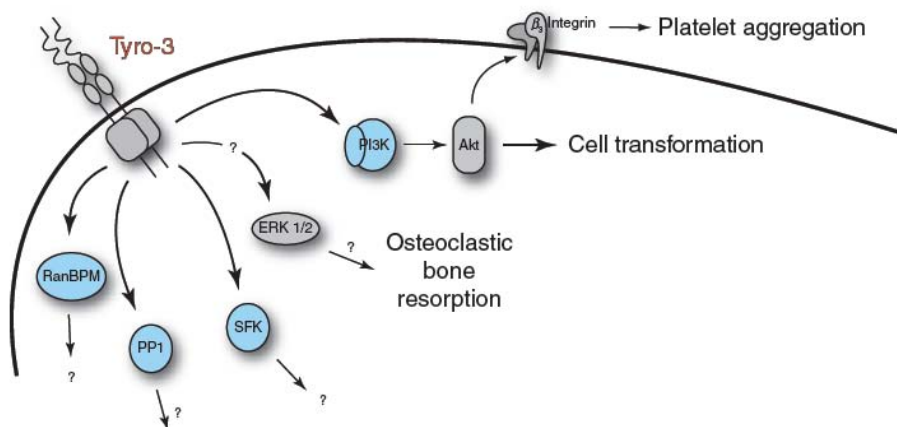


Figure 11. Tyro-3 signaling pathways mediate platelet aggregation, cell transformation, and osteoclastic bone resorption. Molecules in blue have been shown to associate with Tyro-3 through either a direct or indirect interaction. Phosphorylation of Tyro-3 at specific residues remains uncharacterized. (Taken from (66)).

Tyro3 is the least-studied of the TAM receptors and the downstream signaling pathways of Tyro3 are poorly characterized. The molecules known to be involved in

Tyro3 signaling are illustrated in Figure 11. Co-immunoprecipitation of Tyro3 transiently expressed in COS-7 cells revealed a potential interaction with Src kinase family members (152).

Due to the cross-reactivity of the Src antibody used, it is still not clear with which Src kinase member the Tyro3 interacts: Src, Fyn or Yes. It is very interesting that all Src family members are highly expressed in the central nervous system, where Tyro3 is also expressed. Ran-binding protein in the microtubulin organizing center (RanBPM) and PI3K subunit p85 were identified as interaction partners of Tyro3 by yeast two-hybrid studies (153, 154). The expression of EGFR/Tyro3 (a fusion receptor with the extracellular domain of EGFR and the transmembrane and intracellular domains of Tyro3) transformed NIH3T3 cells upon EGF treatment through the activation of PKB. Treatment with the PI3K inhibitor Wortmannin effectively diminished PKB phosphorylation and inhibited anchorage-independent colony formation, indicating that the oncogenic function of Tyro3 is to some extent mediated by the PI3K/PKB signaling cascade (153). Phosphorylation of MAPK was upregulated in parental 293 cells in response to Gas6 treatment, which linked Tyro3 to MAPK signaling pathways (119). Gas6-induced Tyro3 phosphorylation was enough to activate MAPK signaling in mouse osteoclasts, resulting in bone resorption (155). Protein S/Tyro3 inhibits oxygen/glucose deprivation-induced BBB breakdown through the activation of sphingosine 1-phosphate receptor (S1P1), leading to Rac1-dependent BBB protection (156). RNA interference studies have excluded the involvement of Axl or MerTK in the maintenance of BBB integrity, revealing the distinctive function of TAM receptors in this physiological context. Therefore, the role of Tyro3 and the mechanism of Tyro3 activation need to be defined further.

1.3.2 Axl signaling

Axl was the most intensively studied TAM receptor of the past few years. Overexpression of a chimeric receptor EGFR/Axl with the extracellular domain of EGFR and the transmembrane

and intracellular domains of Axl promoted 32D cell survival and mitogenesis by activating MAPK signaling pathways upon EGF treatment (157). In this situation, EGFR/Axl chimeric receptor associated with adaptor proteins Grb2 and Shc as well as PI3K subunit p85 in a ligand-dependent manner (157). Furthermore, tyrosine 821 was identified as the docking site for multiple effectors, including not only p85 and Grb2, but also PLC- γ , c-src and lck (158). Tyrosine 779 exhibited a lower binding affinity for p85 than tyrosine 821, and tyrosine 866 was an additional docking site for PLC- γ (158). Surprisingly, Gas6-stimulated cells did not exhibit inhibition of apoptosis or a mitogenic response, which is correlated with the absence of Ras/ERK

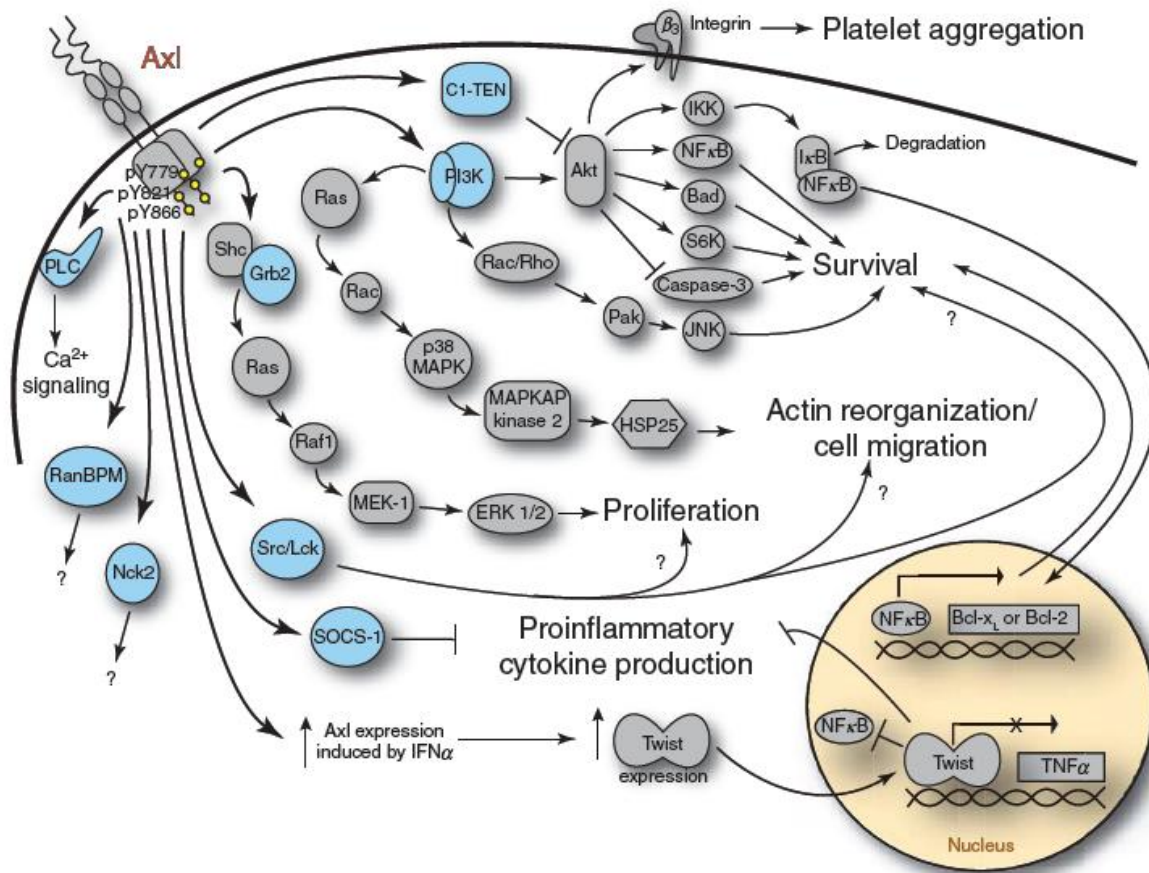


Figure 12. Axl signaling pathways. Molecules in blue have been shown to associate with Axl through either a direct or indirect interaction. Tyrosines 779, 821, and 866 of Axl are phosphorylated (yellow circles) and mediate interactions with a number of signaling molecules. Amino acid designations are from the human sequences. (Taken from (66)).

activation. This suggests that different extracellular domains substantially altered the intracellular response of Axl kinase (157).

It is also very clear that Axl binding to and activation of PI3K are important events linked to multiple downstream pathways, including survival, proliferation and migration. In NIH3T3 cells, activation of Axl upon Gas6 treatment prevents apoptosis of cells after complete growth factor removal via the recruitment of p85 and subsequent activation of PI3K downstream targets PKB and S6K (159). In addition, Src kinase activity was also shown to be required for the survival effect of Gas6 (159). Gas6 stimulation protects cells from apoptosis through PKB-mediated BAD phosphorylation in serum-starved NIH3T3 cells (160). Nuclear NF- κ B binding activity is increased upon Gas6 treatment associated with upregulation of Bcl-xL, thus promoting cell survival. In this study, p105 was identified as a substrate of GSK3 β , which is phosphorylated upon Gas6 treatment leading to its downregulation (161). In endothelial cells, Gas6 treatment promotes another Gas6/Axl-induced survival pathway involved in PI3K-mediated activation of the Rho family, Rac and Rho, as well as downstream kinases Pak, JNK/SAPK and p38 MAPK (162). While many early experiments were conducted in NIH3T3 cells expressing all three TAM receptors, Axl^{-/-} fibroblasts show high levels of serum-deprivation-induced apoptosis that cannot be rescued by addition of Gas6, indicating that Axl is the main factor in Gas6/PI3K/PKB-mediated survival (163). Constitutively activated Axl is found in lymphocytic leukemia and correlates with the activation of PI3K, Lyn, and ZAP70, as well as PLC γ 2 (164).

Gas6/Axl signaling is also involved in many other cellular functions, such as migration, cytokine production and proliferation. Axl is expressed by migratory but not post-migratory Gonadotropin-releasing hormone (GnRH) neurons. Binding to Gas6 promotes cytoskeletal remodeling and migration through the Rho family GTPase Rac and p38MAPK (165). In these

cells, Gas6-induced lamellipodia formation and motility is through the association of Axl with PI3K subunit p85, and this phenomenon is blocked after PI3K inhibition. In addition, PI3K suppression in GnRH neurons mitigated Gas6-induced Rac activation, suggesting that the PI3K pathway is the major mediator of Axl action upstream of Rac, promoting GnRH neuronal cell migration (166). In addition, Axl plays a role in the anti-inflammatory effects of type I IFNs. Activation of Axl leads to increased Twist expression and decreased TNF α production (167). Twist proteins (Twist1 and Twist2) are basic helix-loop-helix (bHLH) transcriptional repressors that bind to E boxes within the TNF α gene promoter and repress NF- κ B-mediated TNF α transcription (167). Given that Protein S stimulation also induces Twist upregulation as well as TNF α reduction, MerTK and Tyro3 may also be implicated in the regulation of Twist expression and TNF α production. Moreover, Gas6/Axl has been shown to promote Mesangial cell proliferation through the positive regulation of STAT3 phosphorylation and transcriptional activity (168).

1.3.3 MerTK signaling

MerTK was first identified in the form of the chicken proto-oncogene *c-eyk* expressed in embryonic chicken brain, which was derived from the chicken retrovirus RLP30 (169, 170). Human MerTK was cloned from a human B-lymphoblastoid Agt11 expression library and named after its predominant expression in monocytes, epithelial and reproductive tissues (76). Early studies using a chimeric receptor composed of the extracellular domain of the human colony-stimulating factor 1 receptor (Fms) and the transmembrane and cytoplasmic domains of human MerTK showed that MerTK is linked to PI3K/PKB, PLC γ , and MAPK/ERK signaling (Figure 13). Ligand stimulation of Fms-MerTK-expressing NIH3T3 cells led to cellular

transformation and increased proliferation (171). Gas6 was later identified as a ligand for MerTK that could rapidly induce MerTK phosphorylation and consequently activate the MAPK signaling pathway (119). In addition, clearance of apoptotic lymphocytes by macrophage requires the activation of MerTK, in part via association of PLC γ 2 with MerTK, and tyrosine phosphorylation of PLC γ 2 (172). Further studies revealed that the tolerogenic phenotype

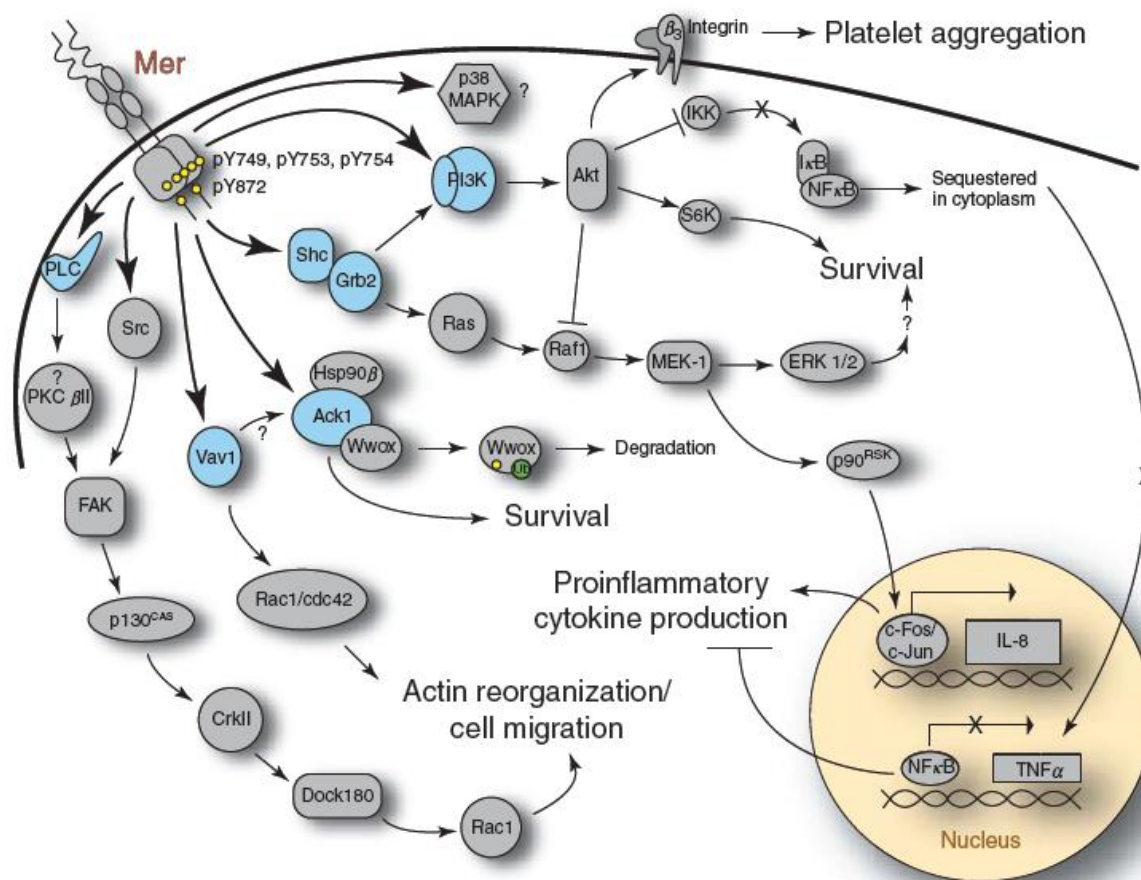


Figure 13. Mer signaling pathways lead to platelet aggregation, cell survival, regulation of proinflammatory cytokine production, and regulation of the actin cytoskeleton. Molecules in blue have been shown to associate with Mer through either a direct or indirect interaction. Tyrosines 749, 753, and 754 (yellow circles) within the Mer kinase domain are sites of autophosphorylation. Ub: ubiquitin. (Taken from (66)).

displayed by dendritic cells or macrophages upon exposure to immunogens, such as apoptotic cells and LPS, is mainly due to inhibition of NF- κ B mediated by the MerTK/PI3K/PKB pathway

(173, 174). The multiple MerTK downstream targets may act independently or in parallel according to cell type and tissue microenvironment. Convergent activation of different downstream signaling components by an EGFR-Mer chimeric receptor, including PKB, ERK1/2, and p38 MAPK, resulted in reduced apoptosis without affecting proliferation (175). Nevertheless, PI3K/PKB and MAPK/ERK are reported to be counteractive when Fms-MerTK is overexpressed in prostate cancer cell lines. Activation of MerTK leads to the upregulation of IL-8 through the nuclear accumulation of transcriptional factors c-Jun and c-Fos that bind to the AP-1 promoter region. Inhibition of MEK attenuated ERK activity and reduced IL-8 production, whilst treatment with a PI3K inhibitor did not, indicating that MerTK-induced IL-8 expression is mainly via the MEK/ERK pathway (88). However, in human macrophages, Protein S-induced MerTK activation suppressed the expression of macrophage scavenger receptor A (SR-A) at both the mRNA and protein levels by preventing binding of transcriptional factors to the AP-1 promoter element (176). Collectively, further work is needed to elucidate the myriad signaling pathways regulated by MerTK.

MerTK has also been reported to promote cell survival via atypical signaling pathways. Activated Cdc42-associated kinase (Ack1), an intracellular tyrosine kinase, was identified as a phosphoprotein that responded to MerTK activation upon Gas6 treatment (177). Association of MerTK and Ack1 was detected by co-immunoprecipitation of the endogenous proteins in a phosphotyrosine-dependent manner following Gas6 stimulation. Expression of wild-type, kinase dead and constitutively active Ack1 demonstrated that Ack1 is not a direct substrate of MerTK. However, autophosphorylation of Ack1 is significantly increased by activation of MerTK. The maintenance of Ack1 activity requires an interaction with heat shock protein 90 β (Hsp90 β). Furthermore, mass spectrometry analysis of constitutively active Ack1 immunoprecipitates also

identified the tumor suppressor Wwox as an interaction partner. Ack1 tyrosine phosphorylates Wwox predominantly at Y287 and induces its ubiquitination and degradation, demonstrating that MerTK-mediated Ack1 activation promotes anchorage-independent growth, and tumor growth *in vivo* may be due to the downregulation of pro-apoptotic tumor suppressor Wwox.

In addition to its involvement in proliferation and survival regulated by well-known signaling pathways like PI3K/PKB, MAPK/ERK, and PLC γ , MerTK has been studied in the regulation of the actin cytoskeleton. In yeast two-hybrid assays, the guanine nucleotide-exchange factor (GEF) VAV1 was found to interact with MerTK through its SH2 domain (178). Activation of MerTK resulted in tyrosine phosphorylation of Vav1 and release from MerTK, followed by GDP/GTP exchange on Rac1 and cdc42. Further study using Gas6 to stimulate primary monocytes/macrophages disclosed Rac1 and cdc42 activation and this potentially explains how MerTK precisely coordinates cytoskeletal changes that govern the ingestion of apoptotic material by macrophages and pigmented retinal epithelial cells. Furthermore, activation of MerTK induced Src-mediated tyrosine phosphorylation of FAK on Tyr⁸⁶¹, recruitment of FAK to the $\alpha\beta 5$ integrin, and formation of a p130^{CAS}/CrkII/Dock180 complex, and consequently activated Rac1 (179). The expression of phosphatidylserine (PS) on the outer surface of the apoptotic cell provides an “eat-me” signal recognized by phagocytes either directly via PS receptor (PS-R) or indirectly via $\alpha\beta 5(3)$ integrin or TAM kinases (180, 181). Co-expression of MerTK with $\alpha\beta 5$ integrin led to Rac1 activation, lamellipodial formation and the phagocytosis of apoptotic cells. Interestingly, treatment with Gas6 or the expression of constitutively active MerTK failed to stimulate p130^{CAS} tyrosine phosphorylation or phagocytosis in $\beta 5$ -deficient or in mutant $\beta 5\Delta C$ -expressing cells, indicating that functional MerTK is linked to the integrin pathway (179).

MerTK has been shown to cross-talk with other receptor tyrosine kinase pathways. A431 cells were employed to perform a large-scale functional analysis of EGF-induced pathway activation. RNA interference targeting MerTK in EGF-treated cells mitigated ERK and STAT3 phosphorylation. Notably, MerTK was found to be required for surface accumulation of EGFR and subsequent pathway activation (182).

1.3.4 Dysregulation of TAM-TKs in cancers

As shown in Table 3, overexpression of TAM receptors is associated with the development of many cancers, being involved in migration and invasion, angiogenesis, cell survival and tumor growth. Each known TAM family member was cloned originally from cancer cells and early studies demonstrated that these RTKs were able to transform 32D and NIH3T3 cells as well as BaF3 lymphocytes (69, 153, 171, 183, 184).

Malignant gliomas

The TAM receptor tyrosine kinases have recently been implicated in glioma cell growth, invasion, and chemoresistance. Upregulation of Axl and Gas6 is found in GBM cell lines and gliomas of malignancy grades WHO III and IV (102, 103). Overexpression of a dominant-negative Axl mutant was shown to suppress brain tumor growth and resulted in long-term survival of mice after intracerebral glioma cell implantation, in contrast to cells expressing Axl wild type (102). Detailed functional analysis revealed that inhibition of Axl signaling interferes with tumor cell proliferation, migration and invasion (102). Comparative immunohistological studies have demonstrated that Axl staining is most pronounced in glioma cells of pseudopalisades and reactive astrocytes. In addition, co-expression of Axl and Gas6 was

observed in glioma cells and tumor vessels, predicting a potential activity of Gas6/Axl signaling in tumor angiogenesis. Interestingly, Axl was not detected in non-neoplastic brain tissue, while Gas6 is highly expressed in neurons. GBM patients with either high expression of Axl or co-expression of Axl and Gas6 exhibited a substantially shorter lag to tumor progression and a poorer overall survival (103). More recent investigations show that knockdown of either Axl or MerTK leads to increased apoptosis of astrocytoma cells and a substantial decrease in cell proliferation in soft agar. Moreover, suppression of Axl and MerTK significantly improved chemosensitivity in astrocytoma cells upon temozolomide, carboplatin, and vincristine treatment (185). Overall, continuing investigation of the function and mechanism of TAM kinases in gliomas will be valuable, not only helping with the deciphering of gliomagenesis but also potentially providing novel targets for drug discovery.

Hematopoietic cancers

Blood cancer, including lymphoma, leukemia and myeloma, is one of the most life-threatening diseases. The molecular characterization of normal and malignant blood cells and their genetic and molecular abnormalities in particular blood cancers has led to new targeted drugs that selectively kill cancer cells, generally sparing normal cells and causing fewer side-effects than previous standard therapies. High expression and phosphorylation of Axl and MerTK were first identified in blood cancers (69, 76). The expression of Axl in a 32D myeloid cell line resulted in aggregation dependent on Gas6 treatment, suggesting an important function for Gas6/Axl signaling in the mediation of cell-cell binding and cell adhesion (186). Axl expression was further investigated in patients with acute myeloid leukemia (AML) and found to be associated with very poor overall survival (71). Further studies found that Axl is induced by

chemotherapy drugs and overexpression of Axl in myeloid leukemia cells confers drug resistance in AML. Treatment of Axl-expressing U937 cells with Gas6 not only led to activation of survival signaling pathways but also increased the expression of Bcl-2 and Twist (187). MerTK is not expressed in normal lymphocytes or thymocytes; however, aberrant MerTK mRNA transcripts and protein expression are found in acute lymphoblastic leukemia (ALL) cell lines and patients (188). MerTK transgenic mice were generated by expressing MerTK in the hematopoietic lineage under control of the Vav promoter. At ages of 12-24 months, over 55% of MerTK transgenic mice developed adenopathy, hepatosplenomegaly, and circulating lymphoblasts compared with 12% of the wild type. A significant survival improvement was observed in MerTK transgenic lymphocytes compared with wild-type lymphocytes upon dexamethasone treatment, indicating that MerTK plays a role in leukemogenesis (188). Inhibition of MerTK sensitizes B-ALL cells to apoptosis induced by cytotoxic reagents *in vitro* and delays disease onset in a mouse model of leukemia (189). Given the fact that leukemia cells can spread to all organs via the bloodstream and lymph vessels, radio/chemotherapy instead of surgery is commonly used to destroy cancer cells, concomitant with the known severe side-effects. In this situation, a comprehensive understanding of the genetic alterations and the identification of more-specific therapeutic targets are desperately needed. Taken together, ongoing research to dissect the mechanisms of TAM receptors in blood cancers may provide attractive targets for biologically based leukemia/lymphoma treatment.

Melanoma

Melanoma is a form of cancer that begins in melanocytes and it is the leading cause of death from skin disease. The National Cancer Institute at the National Institutes of Health has

estimated that the new cases from melanoma will rise to 70,230 and cause 8,790 deaths in 2011 in the USA. The standard treatment for melanoma is surgical removal of the cancerous cells and some normal tissue surrounding the neoplastic area, followed by radio/chemotherapy. In recent decades, targeted cancer therapies based on studies of molecular and cellular changes specific to cancer are becoming more effective than conventional treatments, and less harmful to normal cells. A series of microarray analyses has identified upregulation of all three TAM receptors in different subtypes of melanomas (109, 190, 191). Although the role of MerTK in melanoma oncogenesis is still poorly understood, Tyro3 is reported to be an upstream regulator of Microphthalmia-associated transcription factor (MITF) (191). MITF is a master gene mediating melanoma development and acts as a “lineage addiction” oncogene in malignant melanoma. *MITF* expression is induced upon activation of Tyro3 in a SOX10-dependent manner. In human primary melanoma tissues, high expression of Tyro3 is correlated with *MITF* mRNA levels. Depletion of Tyro3 inhibits cell proliferation and colony formation in melanoma cells and increases chemotherapeutic agent-induced apoptosis. *In vivo*, knockdown of Tyro3 in melanoma cells also prevented tumorigenesis (191). Interestingly, Axl has been shown to be highly expressed in MITF-negative melanoma tissues, demonstrating the diversity of TAM receptor-mediated signaling pathways in melanoma (192). In addition, melanoma cell motility is significantly inhibited *in vitro* by Axl knockdown. Expression of an antisense construct of Axl in Mel 290 melanoma cells resulted in downregulation of Cyr61, a member of the CCN (cyr61, ctgf, nov) proteins involved in tumor progression (107). Axl is also known to be positively correlated to PKB phosphorylation accompanied by weak TUNEL staining in squamous cell carcinoma tumors. Whilst knockdown of Axl did not affect cell proliferation, it sensitized cells to UV-induced apoptosis through activation of Bad, a change in the conformation of the Bax and Bak,

release of cytochrome *c* into the cytosol, and activation of caspases (193). Altogether, exploring the distinctive activity of TAM receptors in melanoma oncogenesis opens up an interesting research area, and selectively targeting TAM members may be an effective therapeutic strategy for specific types of skin cancers.

Breast cancer

Breast cancer starts most commonly from the ducts that transport milk from the breast to the nipple or from the lobules that produce milk. While it occurs in both men and women, the overwhelming majority of cases in humans occur in women. Standard treatments for breast cancer include surgery, radio/chemotherapy and endocrine therapy. The receptor status, such as the presence or absence of estrogen receptor (ER), progesterone receptor (PR) and HER2 within the tumor cells, is commonly used to guide treatment selection. Tumors positive for hormone receptors respond to endocrine therapy with a good prognosis. The outcome of another 20% of HER2 positive tumors significantly improves on receipt of the anti-HER2 monoclonal antibody Trastuzumab or the HER2 small-molecule inhibitor Lapatinib. Nevertheless, subsets of breast cancer are quite resistant to treatment options and prognosis is discouraging. For example, as many as 11-20% of breast cancers are negative for ER, PR or HER2 (194). Despite an increased sensitivity to standard cytotoxic chemotherapy reagents, triple-negative breast cancers carry an unfavorable prognosis. Thus, there is a pressing need to identify the mechanisms of resistance and those driving kinases in these tumors in order to develop more efficient therapeutic interventions.

High expression of Axl is positively correlated with advanced tumor stages in breast cancer patients (94, 95). Silencing Axl completely prevents the metastasis of breast carcinoma cells

from the mammary gland to lymph nodes and several organs, which substantially improves overall survival (195). Axl is strongly induced by overexpression of vimentin, an important EMT marker facilitating mesenchymal cell migration. Activated Axl elicits a positive feedback loop that further promotes vimentin-mediated cell migration. *In vivo*, Axl actively contributes to lung extravasation of breast cancer cells in mice (196). In solid cancer cell lines, including breast cancer, NSCLC (non-small cell lung cancer) and colorectal cancer (CRC), Axl expression is also shown to be regulated by miR-34a and miR-199a/b by targeting its 3'-UTR (196). In breast cancer cells, activation of Axl enhances the expression of MMP-9, facilitating Axl-mediated invasion both *in vitro* and *in vivo* (197). Overexpression of Axl leads to NF- κ B transactivation and brahma-related gene-1 (Brg-1) translocation through activation of ERK signaling. MMP-9 activation was strikingly blocked by the inhibition of ERK signaling or overexpression of the dominant negative mutant I κ B and Brg-1 (197). Additionally, Axl has been identified as a novel regulator of endothelial cell migration towards the matrix factor vitronectin. Knockdown of Axl in metastatic breast cancer cell line MDA-MB-231 significantly impeded angiogenesis *in vivo* (198, 199). Interestingly, expression of Axl and ER are positively associated and the Gas6 promoter is directly regulated by ER, suggesting a potential role for Gas6/Axl signaling in ER⁺ breast cancer progression (94, 200). Gas6 has also been shown to be highly expressed in PR-B-positive breast cancer tissues and upregulation of Gas6 mRNA was observed in PR-B- but not in PR-A expressing cells (201, 202). Notably, MerTK is highly expressed in lung metastatic MDA-MB-231 cells inversely regulated by miR-335. Inhibition of miR335 in parental MDA-MB-231 cells enhances MerTK expression and may further promote metastasis (96). Undoubtedly, the activity of MerTK in breast cancer metastasis requires further investigation. Nevertheless, these findings already suggest a novel route for metastatic breast cancer treatment.

TAM receptor inhibition in cancer treatment

Targeted therapy using specific protein kinase inhibitors is generally considered to be a less toxic intervention than traditional pan-cytotoxic chemotherapeutic agents and has been received with enthusiasm in the field of cancer therapy research. The effectiveness, for example, of Gleevec (Imatinib) in many malignancies serves as a role-model for further targeted therapy modalities through tyrosine kinase inhibition. Several clinically feasible strategies exist that can block RTK signaling (Fig. 14). The most common approach is via small-molecule compounds that compete with ATP for binding in the kinase catalytic domain. Alternatively, monoclonal antibodies that specifically bind to the receptor extracellular domain impair RTK signaling by various mechanisms, for example by the prevention of ligand binding, receptor endocytosis or receptor degradation. Furthermore, monoclonal antibodies, peptides or fusion proteins that bind the ligand can be employed to preclude ligand-dependent RTK activation. Although the latter approach would be ineffective against RTKs with constitutively active forms, the fact that activating TAM mutations have not been described has led to all three strategies being investigated and employed as methods of TAM receptor inhibition (203).

So far, several small-molecule TKIs have been described in the literature that exhibit activity against Axl. Due to high identity in the kinase domains of TAM receptors, these inhibitors may also show some degree of activity against MerTK and Tyro3. The c-Kit/Axl inhibitor Amuvatinib (MP-470, SuperGen) was the first compound reported to have Axl inhibitory activity (204). Initially designed as a c-Kit inhibitor, this TKI is more selective for c-Kit and Met than for Axl. In gastrointestinal stromal tumors (GIST), Axl and Gas6 are upregulated in Imatinib-resistant GIST cells, indicating autocrine activation. More importantly, Amuvatinib in synergy with docetaxel is cytotoxic to GIST cells (204). It is also active against PDGFR and the

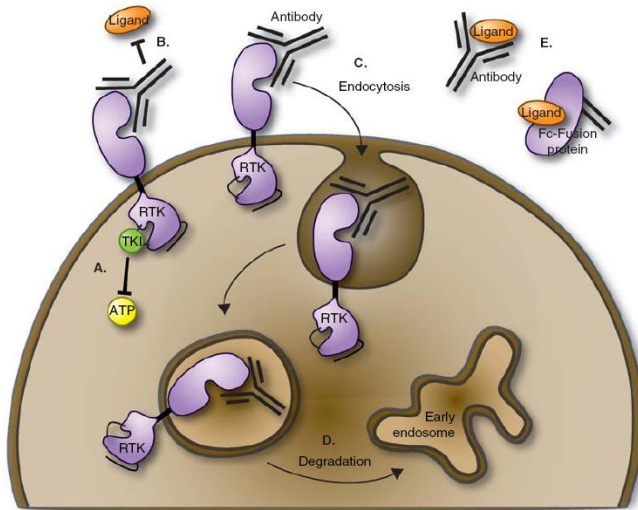


Figure 14. Molecular strategies for therapeutic inhibition of RTKs. A. Low molecular weight tyrosine kinase inhibitors (TKIs) compete with ATP for binding to the activation loop of the RTK. B-D. Anti-RTK monoclonal antibodies can prevent binding of ligand (B) and/or cause endocytosis of the RTK (C) that may result in RTK degradation (D). E. Ligand sequestration via anti-ligand monoclonal antibodies or recombinant fusion proteins such as the extracellular RTK domain fused to the Fc region of human IgG. (Taken from (203)).

DNA repair protein RAD51 and has demonstrated a clinical benefit in Phase I trials against NSCLC, neuroendocrine and endometrial tumors.

Bosutinib (SKI-606, Wyeth now PF5208763, Pfizer) was developed initially as a more potent derivative of the dual Src/Abl kinase inhibitor than Imatinib. In breast cancer cell lines, Bosutinib shows a strong inhibitory action against Axl and results in a decrease in cell motility and invasion

(205). Bosutinib is currently in Phase II trials for breast cancer and Phase III trials for CML (203).

Foretinib (GSK1363089) is a multi-kinase inhibitor against Axl, MET, and VEGFR and is currently in Phase II clinical trials. In Lapatinib-resistant, HER2-positive, ER-positive breast cancer cells, overexpression of Axl has been reported as a novel mechanism of acquired resistance to HER2-targeted drugs (206). In Lapatinib-resistant cells, inhibition or down-regulation of Axl restores cell sensitivity to the drug. Additionally, Foretinib acts synergistically with Lapatinib to inhibit PKB and ERK phosphorylation and leads to a decrease in cell growth and viability (206). Foretinib itself has shown benefit in renal cell carcinoma and hepatocellular carcinoma and is being tested in Phase II trials of metastatic gastric cancer and head and neck squamous cell carcinoma (203).

BMS-777607 (Bristol-Myers Squibb) was initially developed as a Met inhibitor. Interestingly, it is more selective for Axl ($IC_{50} = 1.1$ nM) than its intended target, Met ($IC_{50} = 3.9$ nM). Given the high identity of sequence homology in the kinase domain, BMS-777607 also inhibits MerTK ($IC_{50} = 16$ nM) and Tyro3 ($IC_{50} = 4.3$ nM) (207). This agent has proved of benefit in a xenograft model of human gastric carcinoma and was studied in a Phase I/II trial for advanced or metastatic gastroesophageal cancer, hormone refractory prostate cancer, head and neck squamous cell carcinoma and type I papillary renal cell carcinoma (203).

R428, a selective small-molecule inhibitor of Axl discovered and synthesized by Rigel, exhibits potent activity against Axl ($IC_{50} = 14$ nM) (208). The molecule effectively inhibits Axl phosphorylation and Axl-dependent breast cancer cell invasion, as well as pro-inflammatory cytokine production. It reduced metastatic burden and extended survival in two different mouse models of breast cancer and has exhibited favorable pharmacokinetic and toxicity profiles in preclinical studies. Additionally, this inhibitor synergizes with cisplatin to suppress liver metastasis (208). Selective Axl inhibition by R428 may be a promising strategy for metastatic tumor treatment. In addition, aberrant activation of Axl is observed in mesotheliomas. Suppression of Axl activity using another Axl inhibitor DP-3975 reduces cell migration and proliferation by interfering with the PI3K/PKB/mTOR and RAF/MAPK signaling pathways (209).

Inhibitory monoclonal antibodies blocking Axl have also been reported. An antibody against the extracellular domain of Axl decreased motility and invasiveness of breast cancer cell lines (199). Another Axl monoclonal antibody, MAb173, was shown to induce receptor degradation and inhibit Kaposi sarcoma cell invasion. MAb173 also reduced tumor growth, increased tumor cell apoptosis and decreased Axl protein levels in *in vivo* xenografts with Kaposi sarcoma cells

(210). In an NSCLC xenograft mouse model, Axl monoclonal antibodies attenuated tumor cell proliferation and induced apoptosis by down-regulation of receptor expression. The authors assumed that therapeutic antibodies targeting Axl may block Axl activity not only in malignant tumor cells but also in the tumor stroma (199). YW327.6S2, a phage-derived monoclonal antibody against both human and mouse Axl, blocks Gas6 binding to the receptor, mitigates receptor expression and activation, and also inhibits downstream signaling. In the A549 NSCLC model, YW327.6S2 enhanced the effect of erlotinib and chemotherapy, and significantly suppressed xenograft tumor growth. It also reduced tumor-associated vascular density and potentiated anti-VEGF treatment. Moreover, this antibody attenuated the metastasis of tumor cells to distant organs and inhibited the secretion of inflammatory cytokines and chemokines from tumor-associated macrophages in an MDA-MB-231 breast cancer model (211). While these data may be of value in the identification of novel therapeutic targets, further preclinical testing of these antibodies is required before they reach clinical trials.

2. Scope of this thesis

In our laboratory, microarray analysis has been performed on 30 brain tumor samples using non-neoplastic brain tissue and normal human astrocytes as controls (212). MerTK was one of the identified kinases that were substantially up-regulated in GBM tumors. The results were further validated by quantitative RT-PCR analysis on brain tumor samples (Morin P, unpublished data).

Aberrant expression of MerTK has been reported in several human cancer types, including breast and prostate cancer, melanoma and leukemia. GBM is the most malignant and lethal brain tumor, with only 14 months median survival after diagnosis. Importantly, how MerTK contributes to elevated tumor malignancy in GBM remains to be elucidated. The general aim of this thesis was to identify the function of MerTK in GBM.

In this study, overexpression of MerTK was found in ~90% of GBM tumors. Upregulation of MerTK not only protected cells from DNA damage-induced apoptosis, but also significantly increased cell invasion in 3D culture. MerTK-promoted tumor cell invasion is strongly dependent on its autophosphorylation-induced activity, as illustrated by dramatically suppressed pro-invasive and anti-apoptotic potentials upon knockdown of MerTK or expression of an unphosphorylatable mutant. In conclusion, the data reveal a novel function for MerTK in GBM cell survival and invasion, providing a promising target against malignant gliomas.

3. Results and discussion

Mer receptor tyrosine kinase promotes invasion and survival in glioblastoma multiforme

3.1 Abstract

The infiltration of glioma cells into adjacent tissue is one of the major obstacles in the therapeutic management of malignant brain tumors, in most cases precluding complete surgical resection. Consequently, malignant glioma patients almost invariably experience tumor recurrences. Within the brain, glioma cells migrate rapidly either amoeboidly or mesenchymally to invade surrounding structures, in dependence on the extracellular environment. In addition, radiotherapy, frequently applied as adjuvant therapeutic modality, may enhance tumor cell mobility. Here we show that the receptor tyrosine kinase Mer (MerTK) is overexpressed in glioblastoma multiforme (GBM) and that this is accompanied with increased invasive potential. MerTK expression is maintained in primary GBM-derived tumor spheres under stem cell culture conditions but diminishes significantly in serum-containing cultures with concomitant down-regulation of Nestin and Sox2. Depletion of MerTK disrupts the rounded morphology of glioma cells and decreases their invasive capacity. Furthermore, the expression and phosphorylation of myosin light chain 2 (P-MLC2) are strongly associated with MerTK activity, indicating that the effect of MerTK on glioma cell invasion is mediated by actomyosin contractility. Finally, DNA damage robustly triggers the upregulation and phosphorylation of MerTK, which protects cells from apoptosis. This effect is strongly impaired upon MerTK depletion or overexpression of an inactive MerTK mutant. Collectively, our data suggests that MerTK is a novel therapeutic target in the treatment of the malignant gliomas.

3.2 Introduction

Glioblastoma multiforme (GBM) is the most common malignant brain tumor in adults, characterized by rapid growth, high degree of invasiveness and resistance to standard adjuvant treatments. GBMs have been subdivided into “primary” and “secondary” on the basis of molecular signatures and clinical characteristics. Secondary GBMs derive from the progressive transformation from a preexisting lower grade astrocytic tumors, while primary GBMs have no evidence of prior symptoms or antecedent lower grade pathology (1). Although the median survival after diagnosis of GBM patients has improved from 10 to 14 months in the last 5 years, there is still no effective treatment for this malignant cancer (2). Thus, the demand remains for therapies improving survival and maintaining quality of life.

The infiltrative growth behavior of GBM is a major therapeutic challenge. Clinical treatments that include radio/chemotherapy after surgery enrich CD133⁺ cells and increase tumor aggressiveness (3, 4). The neural extracellular matrix (ECM) lacks typical proteins of other tissues, such as collagen, fibronectin and type-I laminin, and instead expresses hyaluronic acid and associated glycoproteins as well as proteoglycan fibers (5). Migrating glioma cells *in vivo* have a rounded, amoeboid morphology and invade adjacent brain tissue by gliding through the limited extracellular space (6). In addition, coordinated cross-bridging between non-muscle myosin II and actin is shown to be crucial for glioma cell invasion *in vivo* (6).

MerTK, which is named after its predominant expression in monocytes, cells of epithelial, and reproductive origin (7), belongs to the Tyro3, Axl and Mer (TAM) receptor tyrosine kinase family. The ligands of TAM receptors are protein S and growth arrest specific gene 6 (Gas6) (8). As MerTK has a low binding affinity for these ligands, other unknown ligand(s) or conditions may be required for MerTK activation (9). Full activation of MerTK requires the autophosphorylation of tyrosine 749, 753 and 754 within the kinase domain (10). MerTK knockout mice are fertile and viable but gradually develop lupus-like autoimmune disease as well as retinal dystrophy due to

reduced efficiency of apoptotic cell clearance (11, 12). Dysregulated MerTK plays important roles in tumorigenesis (13). A chimeric receptor with a substitution of the MerTK extracellular domain by macrophage colony-stimulating factor receptor (FMS) is able to transform NIH3T3 cells (14). MerTK is overexpressed in several cancer types, including mantle cell lymphomas (15), prostate cancer (16), breast cancer (17) and melanoma (18). In addition, MerTK knock-in mice with ectopic expression in thymocytes and lymphocytes develops T-cell lymphoblastic leukemia/lymphoma (19). Recently, MerTK was found to be upregulated in the mesenchymal subtype of primary GBMs (20). Nevertheless, the mechanisms of MerTK activation and its activity in brain tumor progression remain unclear.

We have found that MerTK is overexpressed in GBM and GBM-derived spheres compared with non-neoplastic brain tissue and normal human astrocytes, and is mitigated upon differentiation. MerTK maintains the rounded morphology of GBM cells under stem cell culture conditions. Knockdown of MerTK decreases cell infiltrative capacity and increases cell sensitivity to Etoposide-induced apoptosis. We further show that MerTK autophosphorylation is essential for its anti-apoptotic and pro-invasive activities. Depletion of MerTK attenuates the expression and phosphorylation of myosin light chain 2 (MLC2). These results identify novel activities of MerTK in glioma cell invasion and survival.

3.3 Materials and methods

Patients

Tissue samples of primary GBM were processed as described previously (21) in accordance with the guidelines of the Ethical Committee of the University Hospital of Basel and the University Hospital of Düsseldorf. Tumors were diagnosed and graded according to the World Health Organization (WHO) Classification of Tumors of the Nervous System (22).

Construction of plasmids

The inactive MerTK autophosphorylation mutant MerTKY749FY753FY754F (MerTK-mut) (10) was generated by site-directed mutagenesis according to the manufacturer's instructions (Stratagene). Short hairpin RNA pairs 5'-GATCCCGGATGAACTGTATGAAATATTCAAGAGATATTTTCATACAGTTCATCC TTTTGGAAA-3' and 5'-AGCTTTTCCAAAAAGGATGAACTGTATGAAATA TCTCTTGAA TATTTTCATACAGTTCATCC GG-3' (targeting sequence was underlined) targeting human MerTK were inserted into the pSuper.retro.puro vector and pSuper.retro.puro-shLuc was used as a control (23).

Cell culture and retroviral infection

Human GBM cell lines BS125, BS149, LN229, LN319 and U373 were cultured in DMEM supplemented with 10% FBS [the “BS” series was generated at the University of Basel, while the “LN” series was the gift of Erwin Van Meir in Lausanne, Switzerland (24)]. The GBM-derived spheres GBM-7S (25), GBM-21S and GBM-22S were obtained from Virginie Clément (University Hospitals and University of Geneva). These spheres were maintained in serum-free NeuralBasal Medium (NBM) (NBM, Invitrogen) supplemented with B27 (Invitrogen), N2 (Invitrogen), antibiotics (Invitrogen) and Glutamax (Invitrogen), plus 20 ng/ml EGF and 20 ng/ml bFGF from Peprotech. U373 GBM cells transfected with pcDNA3.1(-) (vector), pcDNA3.1(-)-MerTK (MerTK-wt) or pcDNA3.1(-)-MerTK-mut (MerTK-mut) were selected in the presence of 1 mg/ml G418 (Gibco). To produce recombinant retrovirus, 10 µg of DNA was transfected into 5x10⁶ packaging cells in a 10-cm dish. After 24 h, the medium was replaced and incubated further at 32°C for 48 h. For GBM-7S sphere infection, the cells were washed with PBS to fully remove FBS and refreshed with NBM. To infect targeting cells, the supernatant containing recombinant retroviruses was filtered (0.45 µm, Millipore) and incubated with the cells for 24 h in DMEM or

NBM at 37°C. Infected U373 cells and GBM-7S spheres were selected in the presence of 1 µg/ml and 4 µg/ml of puromycin, respectively.

Antibodies

MerCT was raised against the C-terminus of human MerTK (amino acids 856-999). Antisera were purified by affinity purification and characterized by western blotting, immunoprecipitation and immunohistochemistry (Supplementary Fig. S1A-C). The anti-MerTK mouse monoclonal antibodies 15R and 49S were raised against human MerTK (amino acids 536-999) and characterized by ELISA, dot-blot and western blotting (Supplementary Fig. S1D). MerTK mouse monoclonal antibody CVO-311 was from Caveo Therapeutics, Inc., MerTK rabbit monoclonal Y323 from Abcam, and P-MerTK antibody from FabGennix Inc.. P-MLC2 Ser19 and cleaved Caspase-3 antibodies were from Cell Signaling, cleaved PARP antibody from BD Transduction Laboratories, GFAP and total MLC2 antibodies (MY21) from Sigma, and Nestin and Actin antibodies from Santa Cruz. Alexa Fluor 647 phalloidin, goat anti-rabbit Alexa 488, goat anti-mouse Alexa 568 and goat anti-rabbit Alexa 647 were from Invitrogen and the Sox2 antibody from R&D Systems.

Immunofluorescence microscopy

Cells were processed for immunofluorescence as described previously (26). To avoid morphological disruption by centrifugation, GBM spheres were precipitated by gravity. The medium was aspirated and the spheres were fixed with 4% PFA for 30 min and then permeabilized and blocked in 0.3% Triton X-100, 2% FBS and 1% BSA for 1 h. Incubation with primary antibodies was performed overnight at 4°C, followed by incubation with the secondary antibody for 1 h. DNA was counterstained with DAPI in VECTASHIELD mounting medium

(Vectorlabs). Photographic images were obtained with a Zeiss Z1 wide-field microscope and processed in Photoshop 6.0 (Adobe Systems Inc.).

Immunohistochemistry

Staining was performed with an automated instrument-reagent system (Discovery XT, Ventana Medical Systems Inc.). Hematoxylin-counterstained sections were photographed (Nikon, YTHM) and analyzed using ImageAccess Enterprise7 software.

Immunoblotting and immunoprecipitation

Protein extracts from tissues and cells were homogenized in immunoprecipitation (IP) buffer (20 mM Tris, 150 mM NaCl, 10% glycerol, 1% Triton X-100, 5 mM EDTA, 0.5 mM EGTA, 20 mM β -glycerophosphate, 50 mM NaF, 1 mM Na_3VO_4 , 1 mM benzamidine, 4 μM leupeptin, 0.5 mM phenylmethylsulfonyl fluoride [PMSF], 1 μM microcystine, and 1 mM dithiothreitol [DTT] at pH 8.0) and subjected to western blotting. For IP, the supernatant was incubated with anti-MerTK antibody MerCT overnight and incubated subsequently with protein A-Sepharose (GE healthcare) for 3 h at 4°C before the beads were washed four times in IP buffer and analyzed by SDS-PAGE.

Quantitative real-time PCR analysis

RT-PCR reactions on DNAase-treated RNA were performed using 2X SYBR Green mix (Applied Biosystems) and an ABI Prism 7000 sequence detection system (Applied Biosystems). Relative expression of MerTK was normalized to the amount of eukaryotic translation elongation factor 1 alpha 1 (EEF1A1), a transcript that showed little variation in our microarray data (27). MerTK was detected using forward and reverse primers 5'-ACTTCAGCCACCCAAATGTC-3' and 5'-GGGCAATATCCACCATGAAC - 3'.

Cell detachment assay

Dissociated GBM-7S spheres expressing shLuc or shMerTK were seeded in triplicate onto 12-well plates (0.3×10^6 / well) and incubated for 2 h. For U373 stable cell lines, cells were trypsinized and washed with PBS to fully remove FBS. Cells were then seeded in triplicate onto 6-well plates (0.8×10^6 / well) in NBM and cultured for 48 h. The adherent and suspended cells were sorted and counted with Vi-Cell (Beckman Coulter).

3D cultures

Growth factor reduced-Matrigel (GFR-Matrigel, BD Biosciences) (100 μ l) was pipetted into BD Falcon 8-well CultureSlides. Single-cell suspensions (~500 cells in 100 μ l NBM) were loaded into each well. After 24 h, a further 200 μ l of NBM was added and replaced every 2 to 3 days.

γ -IR treatments

Cells were plated at consistent densities 24 h prior to treatment. Following a single-dose γ -IR treatment in a TORREX 120D (Astrophysics Research Corp.) instrument at 5 mA/120 kV and 0.13 Gy/s, cells were left to recover at 37°C for the indicated times before analysis.

Invasion assay

The invasive capacity of U373 cells expressing empty vector, MerTK-wt, or MerTK-mut and U373 cells infected with pSuper-retro carrying control or MerTK shRNA were evaluated by Boyden Chamber Assay (BD BioCoat Tumor Invasion Assay System, BD Biosciences) with minor modifications. Briefly, 5×10^4 serum-starved cells were seeded into the upper chamber and the bottom wells filled with NBM. After a 22-h incubation, cells that had invaded the Matrigel

matrix membrane were counterstained with DAPI. The number of invading cells was counted under a fluorescent microscope.

Apoptosis measurement

Cells undergoing apoptosis were harvested, washed with PBS and subdivided into two fractions. One fraction was stained with JC-1 (5,5',6,6'-tetrachloro-1,1',3,3'-tetraethylbenzimidazolylcarbocyanine iodide, Molecular Probes) and subjected to flow cytometry for detection of mitochondrial depolarization ($\Delta\Psi_m$). Red fluorescence (FL-2 channel) of JC-1 (J-aggregates) indicated intact mitochondria, whereas green fluorescence (FL-1 channel) showed monomeric JC-1 produced by the breakdown of $\Delta\Psi_m$ during apoptosis. The remaining cells were lysed for western blotting.

3.4 Results

MerTK is overexpressed in malignant gliomas

In previous study, we analyzed 30 glioma samples by microarray analysis (27). Consequent bioinformatics analysis identified MerTK as one of the candidate genes significantly upregulated in GBMs compared with non-neoplastic brain tissue and normal human astrocytes (data not shown). Elevated expression of MerTK in GBM samples was further validated by quantitative RT-PCR and western blotting (Fig. 1A and B). The variation in molecular weight observed was due to differential glycosylation on the extracellular domain of MerTK, as confirmed by treatment of whole U937 cell lysates with the deglycosylation enzyme PNGase F, which significantly decreased the molecular weight of MerTK (Supplementary Fig. S2) (7, 28). To further analyze MerTK expression histologically, we generated MerTK antibodies and confirmed its specificity through western blot, immunoprecipitation and immunohistochemistry (Supplementary Fig. S1). Immunohistochemical staining of human GBM samples showed that MerTK localized

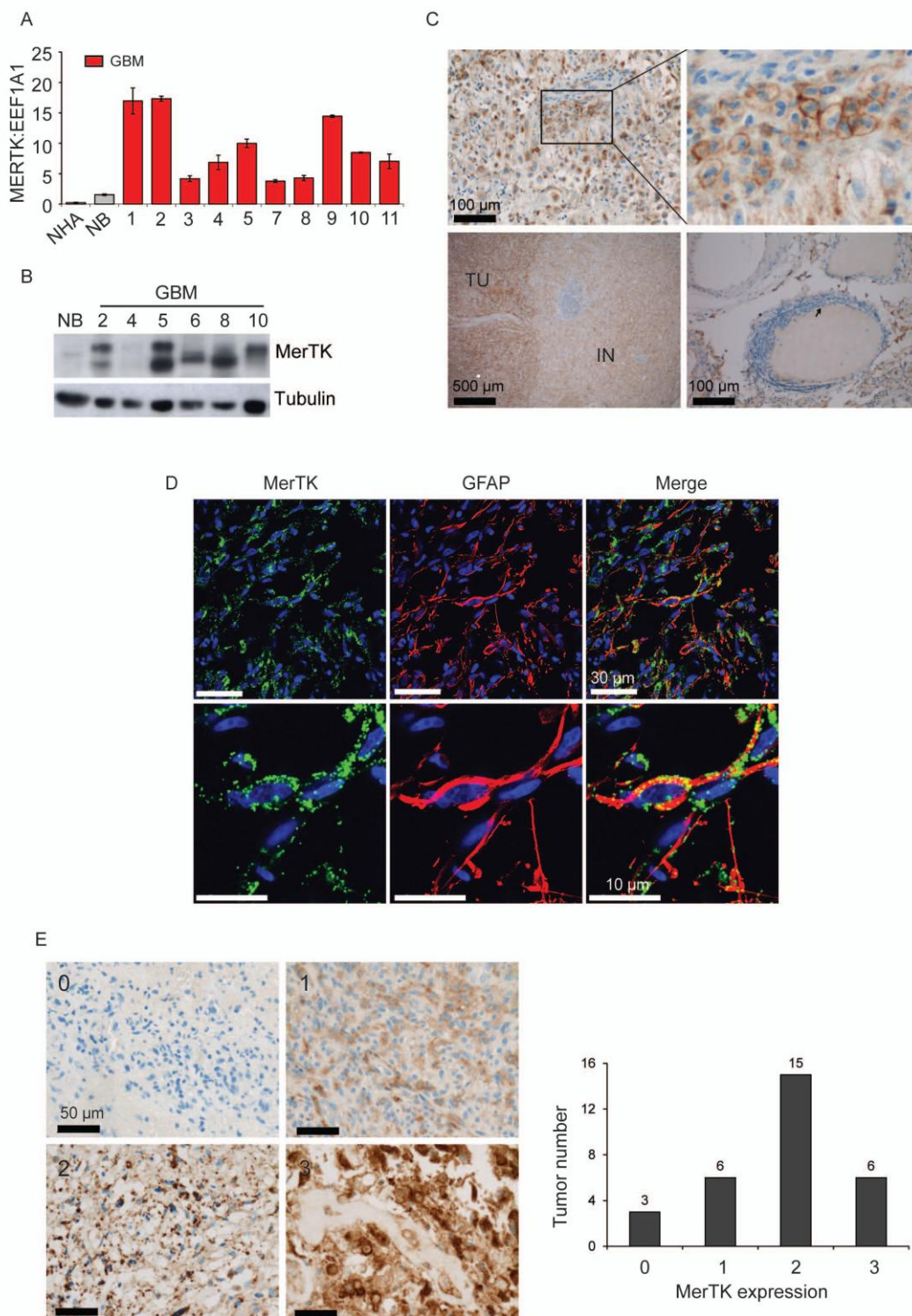


Figure 1. MerTK is overexpressed in malignant gliomas. A, The endogenous MerTK mRNA level was normalized to EEF1A1 expression on total RNA isolated from 10 GBM samples, one sample of non-neoplastic brain tissue (NB) and normal human astrocytes (NHA). B, Western blotting of MerTK expression in human GBM and non-neoplastic brain tissue (NB). C, Immunohistochemical analysis of MerTK expression in GBM samples. TU: tumor mass; IN: infiltrating zone. D, Immunofluorescent staining of MerTK and GFAP in primary GBM samples. E, Pathological scoring of MerTK expression in 30 primary GBM samples: “0” no, “1” low, “2” medium, “3” high.

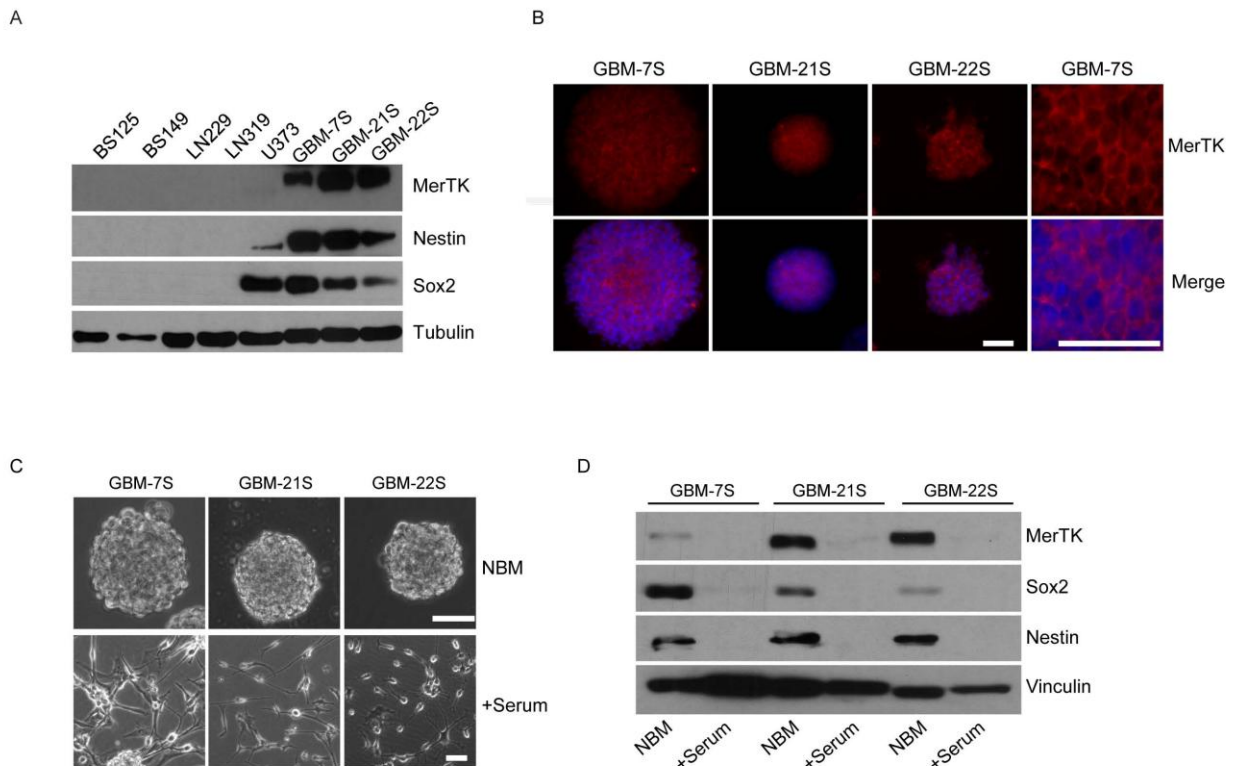


Figure 2. MerTK is highly expressed in GBM-derived spheres. A, Western blotting of MerTK, Nestin and Sox2 expression in immortalized GBM cell lines and GBM-derived spheres. B, Immunofluorescent staining of MerTK expression in three GBM-derived spheres. Nuclei were counterstained by DAPI. Scale bar 50 μ m. C, Morphology of three GBM-derived spheres cultured in NBM or DMEM+10% FBS for 10 days. Scale bar 50 μ m. D, Western blotting of MerTK, Nestin and Sox2 expression in three GBM-derived spheres cultured in NBM or in DMEM+10% FBS for 10 days.

predominantly to the cell membrane (Fig. 1C, upper images) and was expressed by cells within the solid tumor mass as well as in the infiltration zone (Fig. 1C, lower left), but not in endothelial cells (Fig. 1C, lower right). Fluorescence co-immunostaining demonstrated that MerTK was expressed by GFAP⁺ cells of the astrocytic lineage (Fig. 1D). MerTK expression was further scored in 30 primary GBM samples and found to be overexpressed in 90% of tumors (27/30) (Fig. 1E, in collaboration with Stephan Frank, Basel University Hospital).

MerTK is highly expressed in GBM-derived spheres

Due to the failure of established GBM cell lines to accurately model the human disease, long-term expansion of neurospheres from primary GBMs in serum-free medium was used to more precisely reflect tumor phenotypes (29). We analyzed the expression levels of MerTK and neural

stem cell markers Sox2 and Nestin in immortalized GBM cell lines cultured in serum-containing medium and in GBM spheres growing in NBM. Remarkably, in contrast to GBM cell lines, MerTK was highly expressed in all three GBM sphere cultures (Fig. 2A), distributed specifically to the cell membrane (Fig. 2B). Compared with other GBM cell lines, U373 cells had a relatively high level of endogenous MerTK (Supplementary Fig. S3), Sox2 and Nestin (Fig. 2A). GBM spheres GBM-7S, GBM-21S and GBM-22S growing under differentiation culture conditions showed stellate cell morphology (Fig. 2C) and loss of Nestin, Sox2 and MerTK expression (Fig. 2D). This discrepancy between MerTK expression in GBM spheres and immortalized GBM cell lines implies that MerTK is expressed under conditions that more precisely mimic the *in vivo* tumor microenvironment.

Knockdown of MerTK disrupts the morphology of GBM spheres

Unlike GBM-21S and GBM-22S, GBM-7S spheres showed both adherent and suspended phenotypes during maintenance (Fig. 3A). The differences between adherent and suspended spheres have been studied both *in vitro* and *in vivo* (30). To examine MerTK expression in this situation, we sorted suspended spheres into fresh cultures. As shown in Figure 3A, whilst attachment to the substrates did not affect expression of Nestin and Sox2, MerTK was significantly downregulated. Depletion of MerTK led to cell attachment (Fig. 3B and C), impaired the spherical form of GBM-7S spheres in NBM as revealed by F-Actin staining (Fig. 3D), and increased branchy cell cluster formation in Matrigel in the presence of NBM (Fig. 3E). In fact, over 90% of cell clusters showed a spiky phenotype upon depletion of MerTK (Fig. 3F). This suggests that MerTK is involved in regulation of cytoskeletal dynamics.

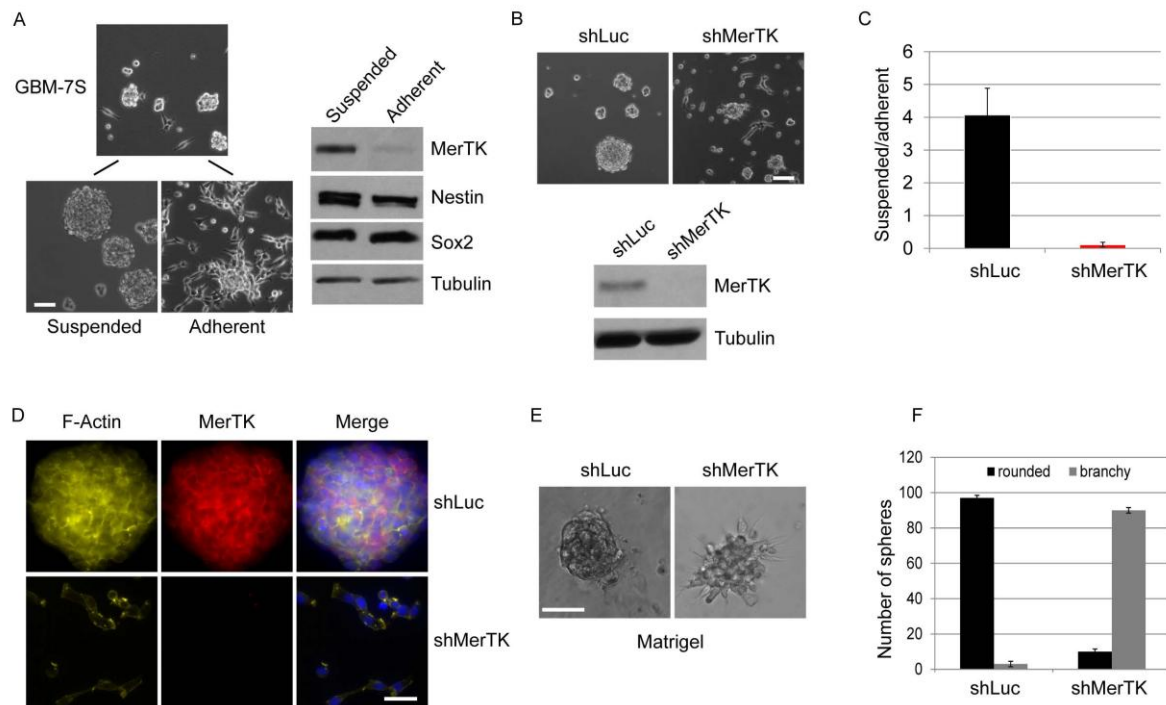


Figure 3. Knockdown of MerTK disrupts the spherical morphology of GBM spheres. A, GBM-7S spheres maintained in NBM show both adherent and suspended phenotypes. Sorted adherent and suspended GBM-7S spheres were cultured in NBM for 1 week and cell lysates subjected to western blotting for Sox2, Nestin and MerTK. Scale bar 50 μ m. B, Phase contrast images of GBM-7S spheres expressing shLuc or shMerTK. Western blotting showed MerTK knockdown efficiency in GBM-7S spheres. Scale bar 50 μ m. C, Detachment assay of GBM-7S spheres expressing shLuc or shMerTK. Data are shown as the ratio of suspended and adherent cells after being dissociated and seeded in NBM for 2 h. Data are representative of experiments in triplicate and are shown as means \pm s.d. D, GBM-7S spheres expressing shLuc or shMerTK were stained for MerTK and F-Actin. Nuclei were counterstained by DAPI. Scale bar 20 μ m. E, GBM-7S spheres expressing shLuc or shMerTK were cultured in Matrigel in the presence of NBM. Scale bar 50 μ m. F, Morphology quantification of GBM-7S spheres expressing shLuc or shMerTK cultured in Matrigel in the presence of NBM. Results are shown as means \pm s.d. of 100 spheres from three independent experiments.

Active MerTK maintains rounded cell morphology and invasive capacity

U373 cells were grown under stem cell culture conditions as reported previously (31). In these conditions, cells adopted a round morphology and formed spheres after several days, in parallel to increased MerTK expression (Fig. 4A). Interestingly, other GBM cell lines growing under stem cell culture conditions either died (data not shown) or showed adherent features with an elongated morphology (Supplementary Fig. S4A).

In order to gain insights into the biological significance of MerTK upregulation, we depleted endogenous MerTK in U373 cells by RNA interference. Knockdown of MerTK not only induced a distinct morphological change from rounded to elongated and subsequently in a more compact and organized sphere formation in NBM (Fig. 4B), but also increased cell attachment

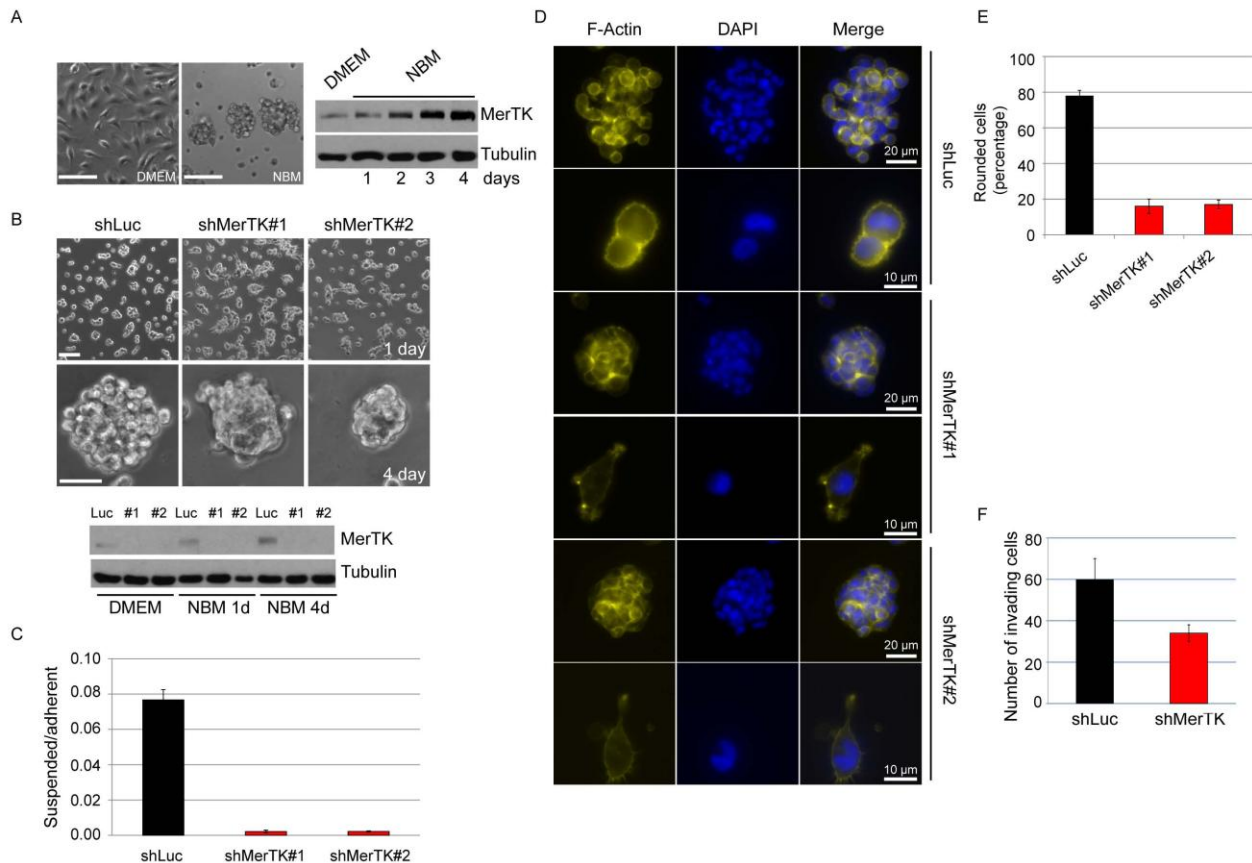


Figure 4. MerTK maintains rounded cell morphology and invasive potential. **A**, U373 cells were grown in serum-containing DMEM or NBM for 4 days. Cell morphology was captured and cells were harvested and lysed at indicated time points for analysis of MerTK expression by western blotting. Scale bar 50 μ m. **B**, MerTK was knocked down in U373 cells by shRNA (two different clones are shown as #1 and #2). U373shLuc and U373shMerTK#1 and #2 cells were cultured in NBM and cell morphology photographed after 1 day and 4 days. Knockdown efficiency of MerTK was validated by western blotting. Scale bar 50 μ m. **C**, Detachment assay of U373shLuc, U373shMerTK#1 and #2 cells. Data are shown as the ratio of suspended and adherent cells after being dissociated and cultured in NBM for 48 h. Data are representative of experiments in triplicate and are shown as means \pm s.d. **D**, U373shLuc and U373shMerTK#1 and #2 cells were cultured in NBM for 3 days and stained for F-Actin. Nuclei were counterstained by DAPI. **E**, Quantification of rounded cells stained by F-Actin. Results are means \pm s.d. of 150 cells from three independent experiments. **F**, Analysis of the invasive potential of U373shLuc and U373shMerTK cells. Cells were seeded in Boyden chambers for 22 h and the cells invading the membrane revealed by DAPI staining and counted under the microscope. Data are representative of experiments in triplicate and are shown as means \pm s.d.

(Fig. 4C). Cells expressing shMerTK had a spindle mesenchymal morphology, whilst cells expressing shLuc were rounded and amoeboid in shape in Matrigel in the presence of NBM (Supplementary Fig. S4B). Interestingly, cells lacking MerTK exhibited multiple membrane protrusions, whereas cells expressing shLuc displayed marked cortical F-Actin staining and extensive membrane blebbings (Fig. 4D); ~80% of cells lost their rounded morphology upon MerTK depletion (Fig. 4E). To test whether knockdown of MerTK impairs cell infiltrative potential, we measured the invasive capacity of U373 cells in the presence and absence of MerTK

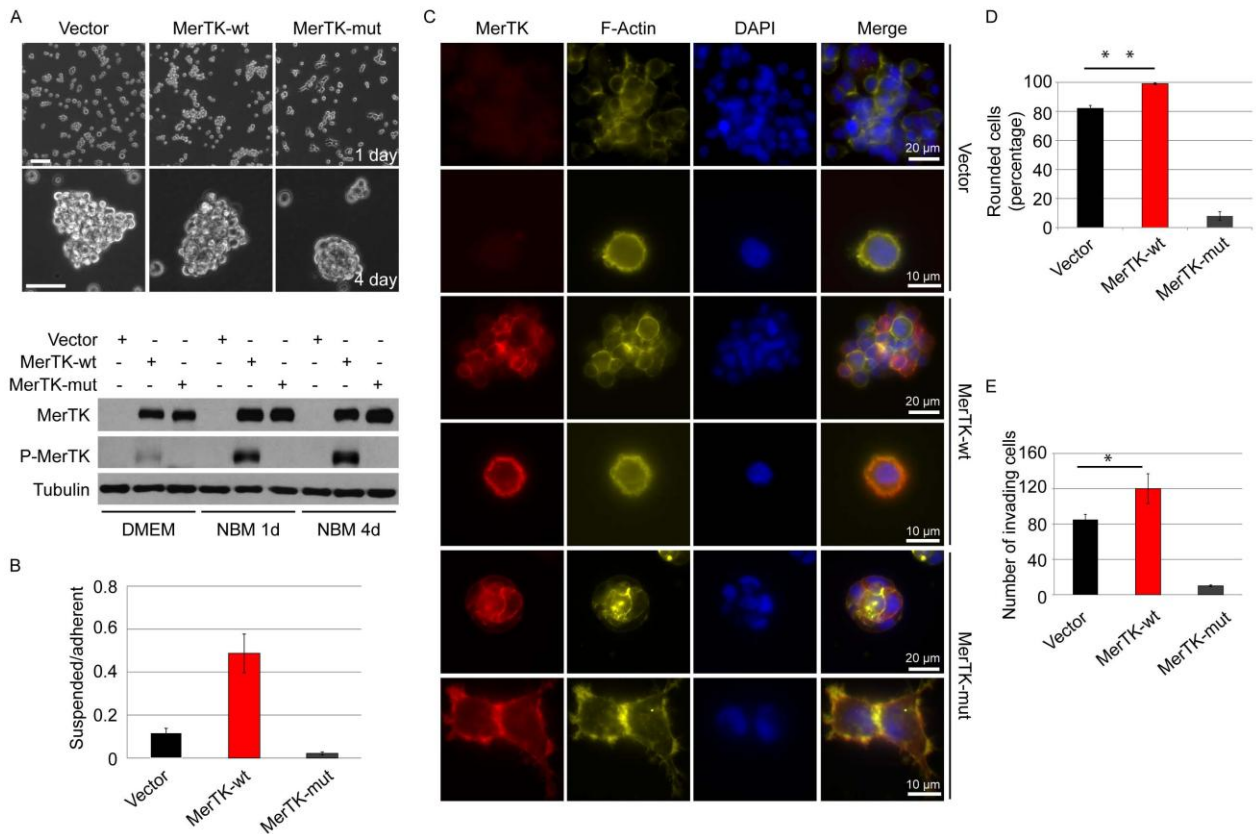


Figure 5. Autophosphorylation of MerTK is required for maintenance of rounded morphology and cell invasive capacity. A, U373 cells stably expressing empty vector, MerTK-wt, or MerTK-mut were cultured in NBM and cell morphology photographed after 1 and 4 days. P-MerTK and total MerTK were assayed by western blotting. Scale bar 50 μ m. B, Detachment assay of U373 cells expressing empty vector, MerTK-wt or MerTK-mut. Data are shown as the ratio of suspended and adherent cells after being dissociated and cultured in NBM for 48 h. Data are representative of experiments in triplicate and are shown as means \pm s.d. C, Immunofluorescent staining of F-Actin and MerTK in U373 cells expressing empty vector, MerTK-wt or MerTK-mut and cultured in NBM for 24 h. Nuclei were counterstained by DAPI. D, Quantification of rounded cells revealed by F-Actin staining. Results are means \pm s.d. of 150 cells from three independent experiments (** $P=0.004$). E, The invasive potential of U373 cells expressing empty vector, MerTK-wt or MerTK-mut was analyzed by Boyden chamber assay. The cells were seeded in the upper chamber for 22 h and invading cells stained with DAPI and counted under the microscope. Data are representative of experiments in triplicate and are shown as means \pm s.d. The differences between empty vector- and MerTK-wt-expressing cells are statistically significant (* $P=0.018$).

expression. As shown in Figure 4F, MerTK depletion strongly suppressed U373 cell invasion through the Matrigel.

In order to investigate further whether MerTK activity helps maintain rounded morphology, U373 cells stably expressing empty vector, MerTK-wt or MerTK-mut were cultured in NBM. Strikingly, wild-type MerTK was rapidly phosphorylated and cells displayed a spherical morphology after 4 days in NBM. In contrast, cells expressing MerTK-mut were elongated and showed higher adherence, similar to MerTK-depleted U373 cells (Fig. 5A and B). In fact, MerTK-mut expression was associated with changes in cellular cytoskeletal organization and

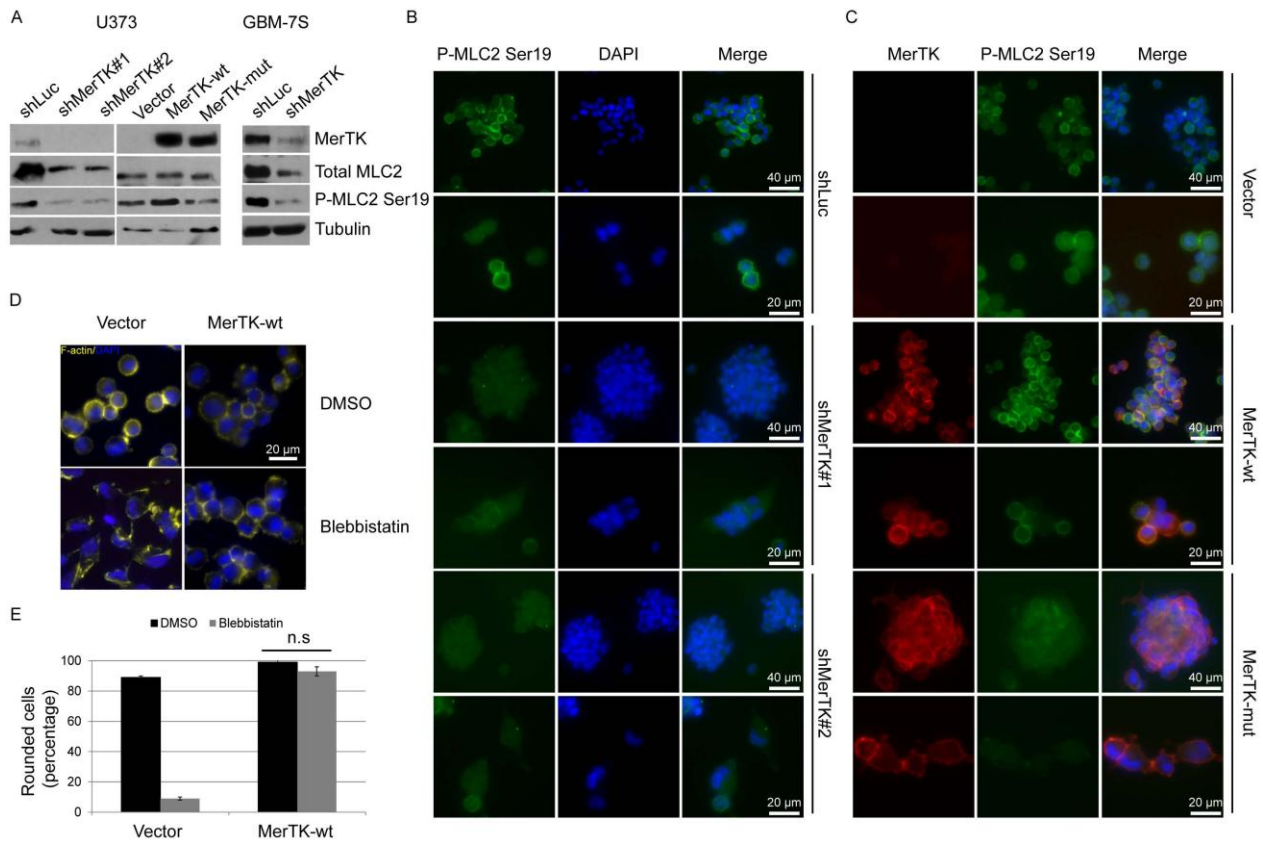


Figure 6. MerTK promotes GBM cell invasion by regulating actomyosin contractility. A, Western blotting of total MerTK, total MLC2 and P-MLC2 Ser19 in U373 and GBM-7S stable cell lines. U373shLuc, U373shMerTK#1 and #2 cells were cultured in NBM for 3 days. U373 cells stably expressing empty vector, MerTK-wt or MerTK-mut were cultured in NBM for 24 h. B, Immunofluorescent staining of P-MLC2 Ser19 in U373shLuc, U373shMerTK#1 and #2 cells cultured in NBM for 3 days. Nuclei were counterstained by DAPI. C, Immunofluorescent staining of P-MLC2 Ser19 and MerTK in U373 cells expressing empty vector, MerTK-wt or MerTK-mut cultured in NBM for 24 h. Nuclei were counterstained by DAPI. D, F-Actin staining of U373 cells expressing empty vector or MerTK-wt seeded in NBM and treated with 10 μ M Blebbistatin (Sigma) for 90 min. E, Quantification of rounded cells stained by F-Actin. Results are means \pm s.d. of 150 cells from three independent experiments.

resulted in compact sphere structures (Fig. 5C). However, when MerTK-wt was expressed and phosphorylated, more cells became rounded in shape with extensive blebbings and showed cortical F-Actin localization (Fig. 5C and D). In contrast to cells expressing empty vector or MerTK-mut, MerTK-wt-expressing U373 cells possessed an enhanced invasive potential, implying an important role for MerTK phosphorylation in cell infiltration (Fig. 5E).

MerTK promotes GBM cell invasion by regulating actomyosin contractility

Glioma cells migrate as mesenchymal cells in 2D but invade as neural progenitor cells in an amoeboid mode *in vivo* (6). Without degrading ECM, changes in glioma cell shape allow passage

of cells through gaps in the tissue environment driven by cortical actomyosin contractility (6). Although several proteins, including kinases, have been shown to be involved in cross-bridging between actin and myosin, phosphorylation at serine 19 of MLC2 is a prerequisite for actomyosin ATPase activity (32). Morphological differences in 3D culture are commonly used to distinguish mesenchymally or amoeboidly migrating cells. Since MerTK-depleted cells displayed an elongated mesenchymal phenotype, we analyzed MLC2 expression and phosphorylation in U373 cells and GBM-7S spheres. Knockdown of MerTK or overexpression of MerTK-mut significantly decreased MLC2 expression and phosphorylation (Fig. 6A-C). Treating U373 stable cell lines with Blebbistatin, a cell-permeable molecule that specifically inhibits myosin II heavy chain ATPase activity (33), significantly disrupted rounded cell morphology. This was delayed upon expression of wild-type MerTK (Fig. 6D, Supplementary Fig. 5), which suggests that myosin II activity-controlled cell motility is dependent on active MerTK.

MerTK is induced upon DNA damage and promotes cell survival

It has been shown that inhibition of MerTK and Axl in astrocytoma cells increased chemosensitivity under differentiation culture condition (34). In this present study, we observed that Etoposide treatment substantially induced MerTK expression in adherent GBM-7S cells and led to cell detachment (Fig. 7A). Knockdown of MerTK sensitized GBM-7S cells to Etoposide-induced apoptosis (Fig. 7B). Elevated MerTK expression was detected in U373 cells after DNA damage treatment (Fig. 7C). To further dissect the activity of MerTK in GBM, U373 cells stably expressing empty vector, MerTK-wt or MerTK-mut were treated with γ -irradiation or Etoposide. Interestingly, MerTK phosphorylation was significantly increased, and protected cells from apoptosis, as shown by diminished cleaved-PARP and cleaved-Caspase 3 levels (Fig. 7D, Supplementary Fig. S6).

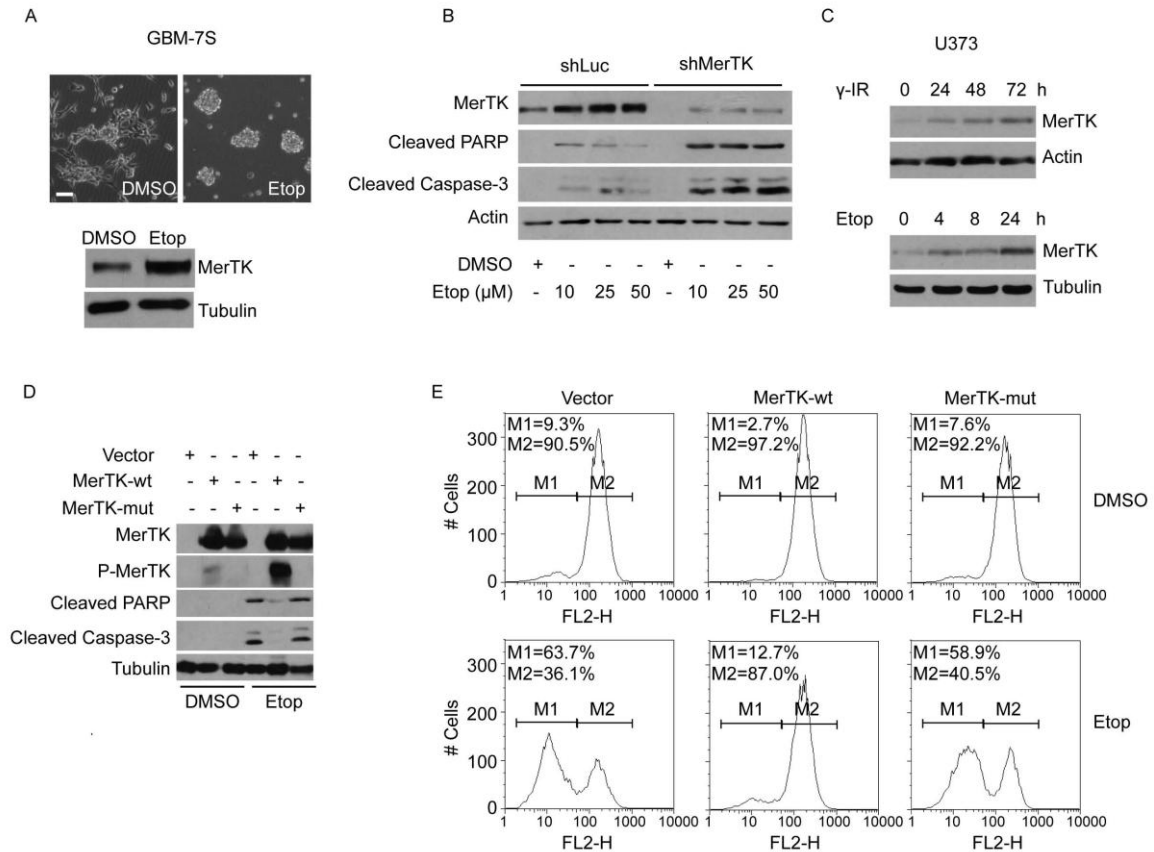


Figure 7. MerTK is induced upon DNA damage and promotes cell survival. A, Adherent GBM-7S cells were treated with 50 μ M Etoposide (Etop, Sigma) for 48 h and expression of MerTK analyzed by western blotting. Scale bar 50 μ m. B, Western blotting for cleaved PARP and cleaved Caspase-3 in MerTK-knockdown or shLuc-expressing GBM-7S spheres treated with Etoposide at different doses for 40 h. DMSO was used as control. C, U373 cells were γ -irradiated with 10 Gy or treated with 5 μ M Etoposide and cells lysed at the indicated time points. MerTK expression was analyzed by western blotting. D, U373 cells expressing empty vector, MerTK-wt or MerTK-mut were treated with DMSO or 50 μ M Etop for 20 h. Half of the cells were lysed and analyzed by western blotting with the antibodies against total MerTK, P-MerTK, cleaved PARP, and cleaved Caspase-3. E, The second half of the cells from (D) were analyzed by flow cytometry for depolarization of mitochondrial membrane potential using JC-1: M1 apoptotic cells, M2 viable cells.

An early event initiating DNA damage-induced apoptosis is loss of mitochondrial membrane potential, $\Delta\Psi$ m (35). Assessing the apoptotic fraction of cells by measuring $\Delta\Psi$ m after Etoposide treatment, we recorded increases in this fraction from 9.3% to 63.7% and from 7.6% to 58.9% in empty vector- and MerTK-mut-expressing U373 cells, respectively, but only a 10% increase in MerTK-wt-expressing cells (Fig. 7E), demonstrating that MerTK kinase activity is crucial for its anti-apoptotic function.

3.5 Discussion

Current standard GBM therapy is restricted to tumor resection and subsequent radio/chemotherapy. In the clinic, the majority of patients with primary GBM experience disease recurrence within a few months due to the high infiltrative capacity of residual GBM cells (2). Although the mechanism is still elusive, radio-resistance and enhanced invasive potential of glioma cells after radiotherapy have been reported (4, 36, 37). Upregulation and phosphorylation of MerTK upon DNA damage implicates MerTK activity in glioma cell survival and invasion after ionizing radiation therapy.

GBM-derived spheres show highly heterogeneous features as primary tumors including extensive infiltration *in vivo* and resistance to traditional therapies (4, 29). *In vitro* analyses of spheres maintained in suspension, as well as adherent and semi-adherent spheres showed no differences in proliferation rate (30). However, the latter displayed either reduced tumor size or a well-delineated tumor border *in vivo*, whilst the suspended spheres always formed infiltrative tumors (30). Interestingly, we found that MerTK is strongly suppressed in adherent/semi-adherent GBM-7S cells (Fig. 3A). Knockdown of MerTK significantly interfered with cell invasion (Fig. 4F) without affecting cell proliferation (data not shown). Invasion is initiated when tumor cells become detached from the growing tumor mass and enter into the surrounding parenchyma (38). Cells lacking MerTK or MerTK activity showed elevated adherent capacity (Figs. 3C, 4C and 5B), possibly reflecting the involvement of MerTK activity in the establishment of signaling networks between tumor cells and the microenvironment *in vivo* and, thus, in an early step of tumor cell dissemination (39-41).

Interestingly, MerTK expression and phosphorylation in U373 cells is substantially upregulated during culture in NBM (Figs. 4A and 5A). Inactivation of MerTK by mutation of all three autophosphorylation sites hampered MerTK pro-invasive and anti-apoptotic activities (Figs. 5E and 7E), indicating that its kinase activity is crucial for MerTK involvement. Notably,

overexpression of inactive MerTK in U373 cells severely decreased cell infiltration capacity (Fig. 5E), possibly due to its competitive binding to signaling transducer(s), thus negatively influencing cell invasion.

Amoeboid mesenchymal and mesenchymal amoeboid transitions (AMT/MAT) are not rigid processes and the actual transition of tumor cells is strongly influenced by the extracellular environment (42). Conversion between two different migration patterns is commonly observed in cancer cells, including glioma cells (6, 42). The force leading to penetration of amoeboidly migrating cells through the extracellular matrix is sustained by cortical actomyosin contractility, which results in plasma membrane blebbing (43). As we found that MerTK was required for the maintenance of rounded cell morphology and invasive capacity, it was hypothesized that MerTK positively regulates blebbing-associated MAT. Amoeboid migration depends largely on myosin activity regulated by the RhoA-ROCK signaling pathway via activation of MLC2 (44). Our data demonstrate that knockdown of MerTK significantly attenuates the level of total MLC2 and P-MLC2 Ser19 (Fig. 6A-C). Unlike U373 cells with a rounded amoeboid morphology under stem cell culture conditions, BS125, BS149 and U87MG cells survived but displayed elongated mesenchymal patterns (Supplementary Fig. S4A). We did not detect upregulation of MerTK in such cells cultured in NBM (data not shown), suggesting that such GBM cell lines may not be amoeboidly mobile. MerTK was reported to regulate myosin II distribution during retinal pigment epithelial phagocytosis through association with the heavy chain of myosin IIA (40). U373 cells expressing MerTK not only showed increased P-MLC2 Ser19 but were also more resistant to Blebbistatin treatment (Fig. 6A and D, Supplementary Fig. S5). These data suggest that MerTK may promote cell invasion by the regulation of myosin II activity.

Mesenchymally migrating cancer cells secrete MMPs, which facilitates metastasis or invasion (45). Although invasive glioma cells migrate *in vitro* by degrading the pericellular matrix, *in vivo* studies suggest that Matrix Metalloproteinase (MMP)-dependent proteolysis in gliomas does not

play a significant role (6). Clinical trials of MMP inhibitors did not reveal evident benefits in the case of GBM or other cancer types (46). Previous studies have demonstrated that cancer cells are able to invade in 3D after treatment with an MMP inhibitor cocktail, whilst showing the typical features of amoeboid invasiveness during migration; this indicates that blocking ECM proteolysis promotes MAT (42, 47). Inhibition of the ATPase activity of actin and myosin could reduce cell motility (48), but targeting such fundamental cytoskeleton components might have severe side-effects. A further attractive therapeutic strategy for GBM treatment has been to target cell surface growth factor receptors such as EGFR, PDGFR and VEGFR. However, due probably to the unique biology of each glioblastoma and the redundant nature of signaling pathways, the overall clinical outcome has proven unsatisfactory (2). As a receptor tyrosine kinase, MerTK is not expressed in normal brain. DNA damage-induced/activated MerTK may not only promote GBM cell survival, but may also engage in tumor cell invasion. Thus, combinatory targeting MerTK together with other “switches” of signaling pathways may be of future therapeutic value in GBM treatment.

Acknowledgements

The authors thank Sandrine Bichet and Hubertus Kohler for helping with immunohistochemistry and FACS experiments, respectively, Susanne Schenk for the generation of the MerTK monoclonal antibody, Douglass Vollrath for the pcDNA3.1(-)-MerTK construct, Janis Liebetanz and Dorian Fabbro for the GST-hMerTK (amino acids 536-999) construct, and Patrick King for editing the manuscript.

Grant Support

The FMI is part of the Novartis Research Foundation. This research was also funded by Oncosuisse CCRP grant KFP OCS-01613-12-2004. G.X. is supported by the Swiss National Science Foundation SNF 31003A_130838.

Footnotes

The current affiliation of P. Morin Jr is Université de Moncton, Moncton, Canada; Adrian Merlo is Buchserstrasse 20, CH-3006, Bern, Switzerland.

References

1. Furnari FB, Fenton T, Bachoo RM, et al. Malignant astrocytic glioma: genetics, biology, and paths to treatment. *Genes Dev* 2007; 21: 2683-710.
2. Van Meir EG, Hadjipanayis CG, Norden AD, Shu HK, Wen PY, Olson JJ. Exciting new advances in neuro-oncology: the avenue to a cure for malignant glioma. *CA Cancer J Clin* 2010; 60: 166-93.
3. Zhai GG, Malhotra R, Delaney M, et al. Radiation enhances the invasive potential of primary glioblastoma cells via activation of the Rho signaling pathway. *J Neurooncol* 2006; 76: 227-37.
4. Bao S, Wu Q, McLendon RE, et al. Glioma stem cells promote radioresistance by preferential activation of the DNA damage response. *Nature* 2006; 444: 756-60.
5. Bellail AC, Hunter SB, Brat DJ, Tan C, Van Meir EG. Microregional extracellular matrix heterogeneity in brain modulates glioma cell invasion. *Int J Biochem Cell Biol* 2004; 36: 1046-69.
6. Beadle C, Assanah MC, Monzo P, Vallee R, Rosenfeld SS, Canoll P. The role of myosin II in glioma invasion of the brain. *Mol Biol Cell* 2008; 19: 3357-68.
7. Graham DK, Dawson TL, Mullaney DL, Snodgrass HR, Earp HS. Cloning and mRNA expression analysis of a novel human protooncogene, c-mer. *Cell Growth Differ* 1994; 5: 647-57.

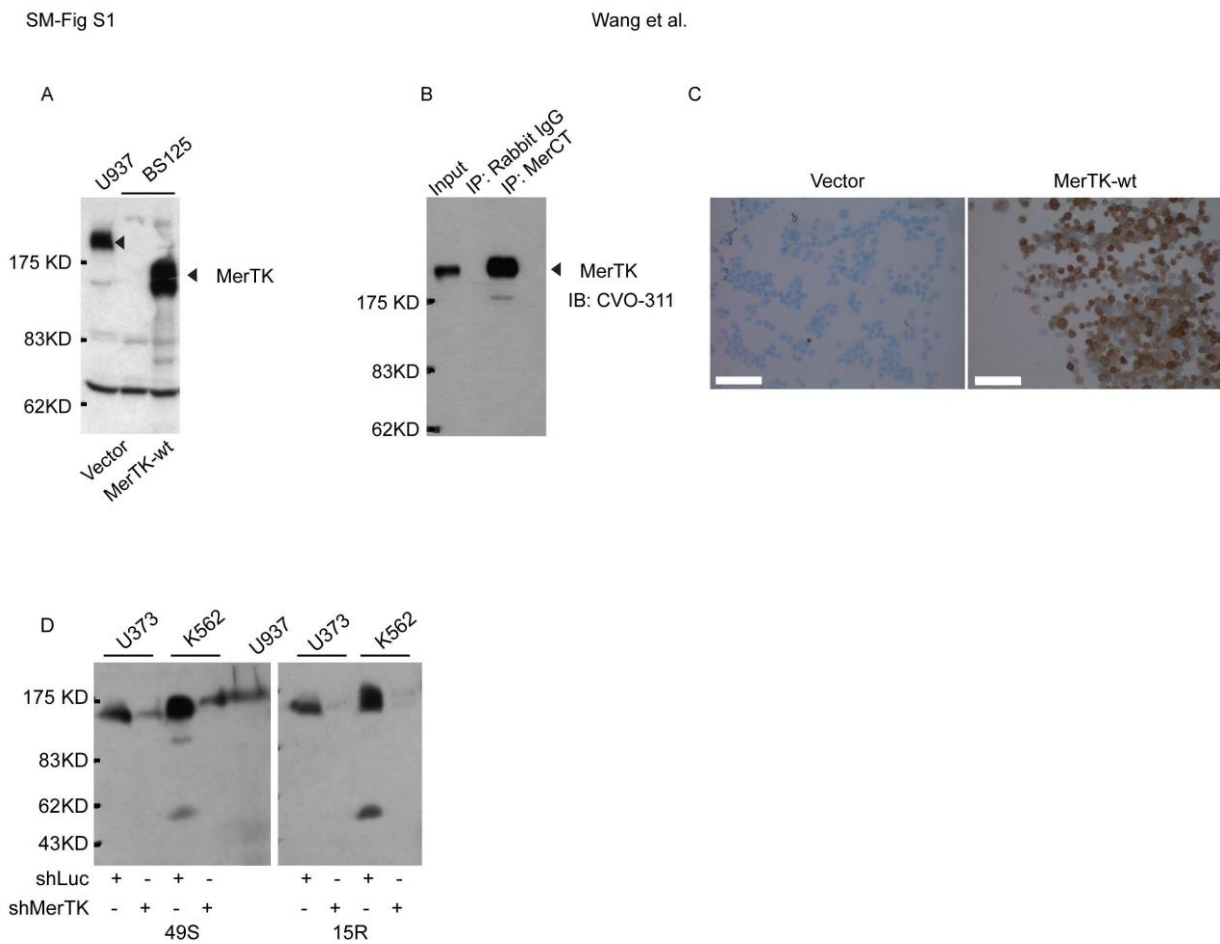
8. Linger RM, Keating AK, Earp HS, Graham DK. TAM receptor tyrosine kinases: biologic functions, signaling, and potential therapeutic targeting in human cancer. *Adv Cancer Res* 2008; 100: 35-83.
9. Nagata K, Ohashi K, Nakano T, et al. Identification of the product of growth arrest-specific gene 6 as a common ligand for Axl, Sky, and Mer receptor tyrosine kinases. *J Biol Chem* 1996; 271: 30022-7.
10. Ling L, Templeton D, Kung HJ. Identification of the major autophosphorylation sites of Nyk/Mer, an NCAM-related receptor tyrosine kinase. *J Biol Chem* 1996; 271: 18355-62.
11. Duncan JL, Yang H, Vollrath D, et al. Inherited retinal dystrophy in Mer knockout mice. *Adv Exp Med Biol* 2003; 533: 165-72.
12. Cohen PL, Caricchio R, Abraham V, et al. Delayed apoptotic cell clearance and lupus-like autoimmunity in mice lacking the c-mer membrane tyrosine kinase. *J Exp Med* 2002; 196: 135-40.
13. Hafizi S, Dahlback B. Signalling and functional diversity within the Axl subfamily of receptor tyrosine kinases. *Cytokine Growth Factor Rev* 2006; 17: 295-304.
14. Ling L, Kung HJ. Mitogenic signals and transforming potential of Nyk, a newly identified neural cell adhesion molecule-related receptor tyrosine kinase. *Mol Cell Biol* 1995; 15: 6582-92.
15. Ek S, Hogerkorp CM, Dictor M, Ehinger M, Borrebaeck CA. Mantle cell lymphomas express a distinct genetic signature affecting lymphocyte trafficking and growth regulation as compared with subpopulations of normal human B cells. *Cancer Res* 2002; 62: 4398-405.
16. Wu YM, Robinson DR, Kung HJ. Signal pathways in up-regulation of chemokines by tyrosine kinase MER/NYK in prostate cancer cells. *Cancer Res* 2004; 64: 7311-20.
17. Tavazoie SF, Alarcon C, Oskarsson T, et al. Endogenous human microRNAs that suppress breast cancer metastasis. *Nature* 2008; 451: 147-52.
18. Gyorffy B, Lage H. A Web-based data warehouse on gene expression in human malignant melanoma. *J Invest Dermatol* 2007; 127: 394-9.

19. Graham DK, Salzberg DB, Kurtzberg J, et al. Ectopic expression of the proto-oncogene Mer in pediatric T-cell acute lymphoblastic leukemia. *Clin Cancer Res* 2006; 12: 2662-9.
20. Verhaak RG, Hoadley KA, Purdom E, et al. Integrated genomic analysis identifies clinically relevant subtypes of glioblastoma characterized by abnormalities in PDGFRA, IDH1, EGFR, and NF1. *Cancer Cell* 2010; 17: 98-110.
21. Maier D, Comparone D, Taylor E, et al. New deletion in low-grade oligodendroglioma at the glioblastoma suppressor locus on chromosome 10q25-26. *Oncogene* 1997; 15: 997-1000.
22. Kleihues P, Sobin LH. World Health Organization classification of tumors. *Cancer* 2000; 88: 2887.
23. Hergovich A, Lamla S, Nigg EA, Hemmings BA. Centrosome-associated NDR kinase regulates centrosome duplication. *Mol Cell* 2007; 25: 625-34.
24. Ishii N, Maier D, Merlo A, et al. Frequent co-alterations of TP53, p16/CDKN2A, p14ARF, PTEN tumor suppressor genes in human glioma cell lines. *Brain Pathol* 1999; 9: 469-79.
25. Clement V, Marino D, Cudalbu C, et al. Marker-independent identification of glioma-initiating cells. *Nat Methods* 2010; 7: 224-8.
26. Hergovich A, Lisztwan J, Barry R, Ballschmieter P, Krek W. Regulation of microtubule stability by the von Hippel-Lindau tumour suppressor protein pVHL. *Nat Cell Biol* 2003; 5: 64-70.
27. Grzmil M, Morin P, Jr., Lino MM, et al. MAP Kinase-Interacting Kinase 1 Regulates SMAD2-Dependent TGF- β Signaling Pathway in Human Glioblastoma. *Cancer Res* 2011; 71: 2392-402.
28. Sather S, Kenyon KD, Lefkowitz JB, et al. A soluble form of the Mer receptor tyrosine kinase inhibits macrophage clearance of apoptotic cells and platelet aggregation. *Blood* 2007; 109: 1026-33.

29. Lee J, Kotliarova S, Kotliarov Y, et al. Tumor stem cells derived from glioblastomas cultured in bFGF and EGF more closely mirror the phenotype and genotype of primary tumors than do serum-cultured cell lines. *Cancer Cell* 2006; 9: 391-403.
30. Gunther HS, Schmidt NO, Phillips HS, et al. Glioblastoma-derived stem cell-enriched cultures form distinct subgroups according to molecular and phenotypic criteria. *Oncogene* 2008; 27: 2897-909.
31. Ropolo M, Daga A, Griffiero F, et al. Comparative analysis of DNA repair in stem and nonstem glioma cell cultures. *Mol Cancer Res* 2009; 7: 383-92.
32. Pankova K, Rosel D, Novotny M, Brabek J. The molecular mechanisms of transition between mesenchymal and amoeboid invasiveness in tumor cells. *Cell Mol Life Sci* 2010; 67: 63-71.
33. Zhang M, Rao PV. Blebbistatin, a novel inhibitor of myosin II ATPase activity, increases aqueous humor outflow facility in perfused enucleated porcine eyes. *Invest Ophthalmol Vis Sci* 2005; 46: 4130-8.
34. Keating AK, Kim GK, Jones AE, et al. Inhibition of Mer and Axl receptor tyrosine kinases in astrocytoma cells leads to increased apoptosis and improved chemosensitivity. *Mol Cancer Ther* 2010; 9: 1298-307.
35. Vichalkovski A, Gresko E, Cornils H, Hergovich A, Schmitz D, Hemmings BA. NDR kinase is activated by RASSF1A/MST1 in response to Fas receptor stimulation and promotes apoptosis. *Curr Biol* 2008; 18: 1889-95.
36. Hambardzumyan D, Squatrito M, Holland EC. Radiation resistance and stem-like cells in brain tumors. *Cancer Cell* 2006; 10: 454-6.
37. McCord AM, Jamal M, Williams ES, Camphausen K, Tofilon PJ. CD133+ glioblastoma stem-like cells are radiosensitive with a defective DNA damage response compared with established cell lines. *Clin Cancer Res* 2009; 15: 5145-53.

38. Nakada M, Nakada S, Demuth T, Tran NL, Hoelzinger DB, Berens ME. Molecular targets of glioma invasion. *Cell Mol Life Sci* 2007; 64: 458-78.
39. Wu Y, Singh S, Georgescu MM, Birge RB. A role for Mer tyrosine kinase in alphavbeta5 integrin-mediated phagocytosis of apoptotic cells. *J Cell Sci* 2005; 118: 539-53.
40. Strick DJ, Feng W, Vollrath D. MerTK drives myosin II redistribution during retinal pigment epithelial phagocytosis. *Invest Ophthalmol Vis Sci* 2009; 50: 2427-35.
41. Guttridge KL, Luft JC, Dawson TL, et al. Mer receptor tyrosine kinase signaling: prevention of apoptosis and alteration of cytoskeletal architecture without stimulation or proliferation. *J Biol Chem* 2002; 277: 24057-66.
42. Wolf K, Mazo I, Leung H, et al. Compensation mechanism in tumor cell migration: mesenchymal-amoeboid transition after blocking of pericellular proteolysis. *J Cell Biol* 2003; 160: 267-77.
43. Fackler OT, Grosse R. Cell motility through plasma membrane blebbing. *J Cell Biol* 2008; 181: 879-84.
44. Parri M, Chiarugi P. Rac and Rho GTPases in cancer cell motility control. *Cell Commun Signal* 2010; 8: 23.
45. Cukierman E, Pankov R, Yamada KM. Cell interactions with three-dimensional matrices. *Curr Opin Cell Biol* 2002; 14: 633-9.
46. Coussens LM, Fingleton B, Matrisian LM. Matrix metalloproteinase inhibitors and cancer: trials and tribulations. *Science* 2002; 295: 2387-92.
47. Wyckoff JB, Pinner SE, Gschmeissner S, Condeelis JS, Sahai E. ROCK- and myosin-dependent matrix deformation enables protease-independent tumor-cell invasion in vivo. *Curr Biol* 2006; 16: 1515-23.
48. Rao J, Li N. Microfilament actin remodeling as a potential target for cancer drug development. *Curr Cancer Drug Targets* 2004; 4: 345-54.

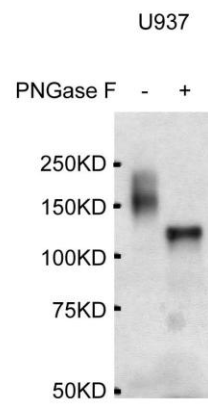
3.6 Supplementary data



Supplemental Figure S1. Characterization of MerTK antibodies. A, Raw serum from an immunized rabbit was diluted 1:5000 in 5% non-fat milk in TBS and characterized by western blotting. Protein (50 μ g) was loaded from whole cell lysates of U937 cells and BS125 GBM cells transfected with empty vector or MerTK-wt. B, Raw serum was purified by affinity purification and used to immunoprecipitate endogenous MerTK from U937 cells. Immunoprecipitation efficiency was analyzed by western blotting using the MerTK monoclonal antibody CVO-311. C, U373 cells expressing empty vector or MerTK-wt were spun down by Cytospin and immunohistochemistry was performed using MerTK at 1:100 dilution. Staining was carried out using an automated instrument-reagent system (Discovery XT, Ventana Medical Systems Inc.). Scale bar 50 μ m. D, Whole cell extracts from U373 and K562 transfected with shRNA against MerTK or luciferase and from U937 cells were used to examine the specificity of MerTK monoclonal antibodies 15R and 49S by western blotting.

SM-FigS2

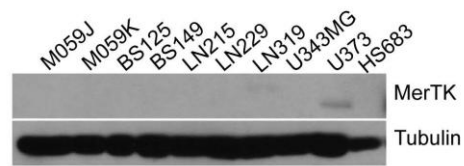
Wang et al.



Supplemental Figure S2. Deglycosylation of MerTK in U937 cells. U937 human monocytic cell lysates were deglycosylated with PNGase F (NEB) according to the user manual. MerTK expression was analyzed by western blotting.

SM-FigS3

Wang et al.

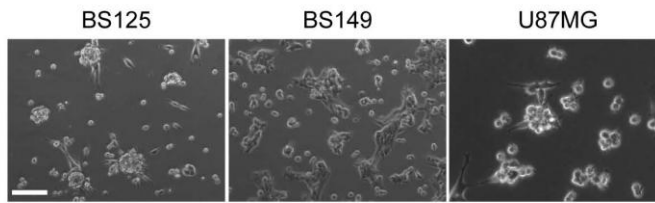


Supplemental Figure S3. Western blotting using MerTK polyclonal antibody MerCT on whole cell extracts of immortalized GBM cell lines.

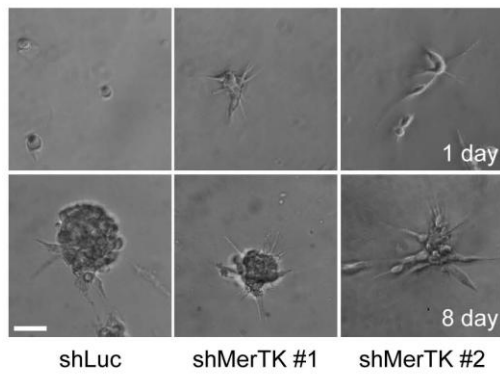
SM-FigS4

Wang et al.

A



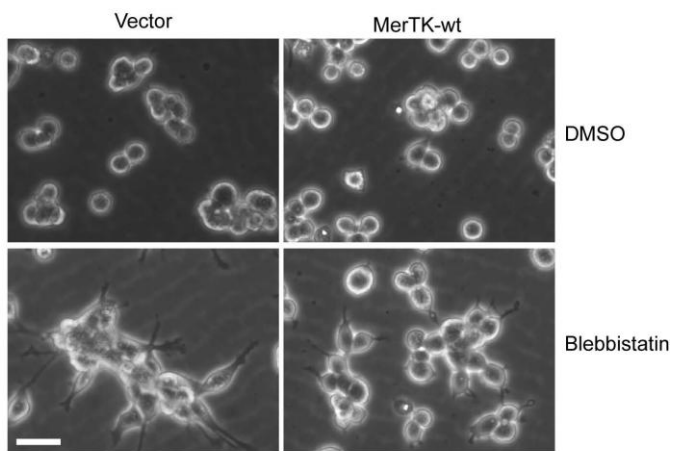
B



Supplemental Figure S4. A, BS125, BS149 and U87MG GBM cell lines were cultured in NBM for 5 days and cell morphologies photographed. Scale bar 50 μm . B, Morphology of U373shLuc, U373shMerTK#1 and #2 cells cultured in Matrigel in the presence of NBM. Images were captured after 1 and 8 days. Scale bar 50 μm .

SM-FigS5

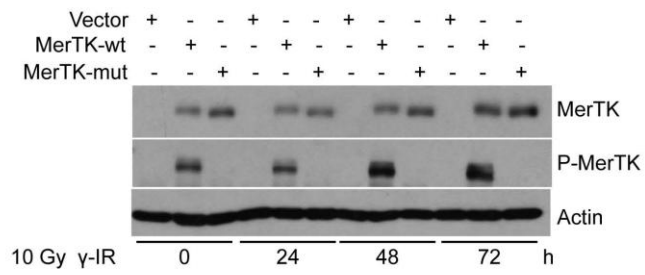
Wang et al.



Supplemental Figure S5. Phase contrast images of U373 cells expressing empty vector or MerTK-wt growing in NBM treated with 10 μ M Blebbistatin or DMSO for 16 h. Scale bar 25 μ m.

SM-FigS6

Wang et al.



Supplemental Figure S6. U373 cells stably expressing empty vector, MerTK-wt and MerTK-mut were γ irradiated with 10 Gy and cells lysed at the indicated time points. Total MerTK and P-MerTK were analyzed by western blotting.

4. General discussion

Radiotherapy is the most effective therapeutic modality for glioblastomas, significantly contributing to the prolongation of patient life expectancy. However, although many glioblastomas respond initially, they invariably all recur, even in combination with surgery and chemotherapy. The mechanisms underlying tumor radioresistance have remained poorly understood and in recent years intensive studies have been conducted to investigate the determinants of radiosensitivity and to evaluate radiosensitizers. Recent evidence suggests that a small population of clonogenic cells, known as tumor stem-like cells (TSC), contributes to glioma radioresistance through preferential activation of the DNA damage checkpoint response and an increase in DNA repair capacity (7). Stratification of glioma cells with or without a stem-like character has been based on the expression of the stem cell-associated protein CD133. The fraction of CD133-expressing cells was shown to be enriched and to survive radiotherapy, suggesting that this cellular population may potentially confer glioma radioresistance and could be the source of tumor recurrence and invasion after radiation.

The vast catalog of cancer cell genotypes has been proposed to be a manifestation of six primary cellular functions that normal cells acquire during oncogenesis: self-sufficiency in growth signals, insensitivity to anti-growth signals, evasion of apoptosis, limitless replicative potential, sustained angiogenesis, and tissue invasion and metastasis (213). As in most cancers, the major pathways contributing to these changes are related to inactivation of key molecules, such as PTEN, p53, p16^{INK4a} or p14^{ARF} or to upregulated EGFR or PDGFR autocrine/paracrine signaling cascades in GBM (214, 215). However, the first generation of molecular agents targeting tumor growth pathways in GBM have been disappointing. One explanation for the failure of targeted molecular agent monotherapy comes from the coactivation of multiple

receptor tyrosine kinases in GBM cell lines and primary cultures. Another major hindrance to the use of chemotherapy agents for GBM is that the brain is well protected behind the BBB, which effectively excludes targeted molecular drugs from the central nervous system (216). Thereby, successful strategies against GBM will have to include the induction of GBM cell destruction, and not merely anti-proliferative or anti-angiogenic effects, since invasive tumor cells infiltrate normal brain tissue independently of neo-vascularization. Meanwhile, systemically administered drugs must be able to penetrate the BBB and to target invasive GBM cells beyond the areas of the visible main tumor mass.

In this study, MerTK was found to be overexpressed in GBM tumors but is negative in normal brain tissues, suggesting that inhibition of MerTK may have maximal effects on the disease state but with minimal toxicity. Interestingly, expression of MerTK is upregulated upon DNA damage and this promotes tumor cell survival and invasion. The pro-invasive potential of MerTK has also been reported in breast cancer. Lung metastatic MDA-MB-231 (LM2) cells exceptionally express MerTK and this is inversely regulated by miR-335. Depletion of miR-335 in LM2 cells substantially increases expression of MerTK and to some extent other genes involved in tumor progression, such as Tenascin C, which suggests strongly that MerTK is an active factor in breast cancer invasion/metastasis (96). However, an improved understanding of MerTK signaling is a prerequisite for the efficient development as well as implementation of a targeting strategy. As MerTK is a receptor tyrosine kinase, small-molecule tyrosine kinase inhibitors or monoclonal antibody blockage of ligand-binding induced activation may improve the efficacy of current treatments for malignant gliomas and for other cancers.

In recent decades, immortalized cancer cell lines have been widely used as models to explore the biology of human cancers and to screen for potential therapeutic agents. However, it becomes

increasingly clear that cancer cell lines repeatedly passaged *in vitro* often reflect inadequately the phenotype of the corresponding primary human tumors (217). In contrast, brain tumor stem cells isolated from glioblastoma specimens harbor characteristics of continuous self-renewal, extensive brain parenchymal migration/infiltration, and the potential for full or partial differentiation properties not found in conventional glioma cell lines cultured in serum-rich medium. In addition, brain tumor stem cells also express neural stem cell markers and are able to grow as nonadherent spheres when maintained in the presence of EGF and bFGF under serum-free conditions. In contrast to primary GBM samples and GBM-derived spheres, MerTK expression is extremely low in immortalized GBM cell lines. Interestingly, the expression of MerTK is substantially upregulated in U373 cells grown under stem cell culture conditions. Depletion of MerTK in U373 cells and GBM-derived spheres not only disrupts cell morphology but also impairs tumor cell invasion. This discrepancy between MerTK expression in GBM tumors and cell lines suggests that expression of MerTK requires conditions that reflect more the tumor microenvironment. It would be very exciting to design *in vivo* experiments to test whether inactivation of MerTK in GBM cells can attenuate gliomagenesis or synergize with chemotherapy or radiotherapy. It would also be interesting to verify whether overexpression of MerTK in glia cells is tumorigenic *per se* and/or cooperates with established tumor pathways in the development of glioblastomas. This type of data could be of value in understanding MerTK signaling in GBM, as well as its possible contribution to therapy resistance and recurrent cancers *in vivo*. In the long term, such findings could be useful for designing future therapies.

Aberrant expression/activation of TAM receptors, especially Axl, has been studied in many cancers. Axl was shown to promote cancer cell proliferation, survival and invasion in different contexts (66). In glioblastoma, overexpression of Axl and Gas6 predicts poor prognosis for GBM

patients (103). Although Gas6 is generally seen as the ligand of TAM members, MerTK has the lowest affinity, suggesting that further factors or conditions are involved in MerTK activation in GBM. Recently, Tubby and Tulp1 have been identified as new MerTK ligands for phagocytosis, further supporting this hypothesis (218). In the future, it will be very important to work out the mechanism of MerTK activation in GBM, and another question that arises immediately is that of the downstream signaling targets of MerTK. Previous studies have shown that tyrosine 872 of MerTK can bind to Grb2, recruit PI3K subunit p85 and transcriptionally activate NF- κ B (183). MerTK is also reported to interact with VAV1 and govern the ingestion of apoptotic cells by precisely coordinating cytoskeleton changes in macrophages (178). To dissect MerTK signaling pathways, in this present study MerTK-expressing U373 GBM cells were treated with the PI3K/mTOR dual inhibitor NVP-BEZ235 and/or the MEK1/2 inhibitor U0126. Surprisingly, either individually or in combination, the two inhibitors did not interfere with MerTK anti-apoptotic activity (Yuhua Wang, unpublished data), further demonstrating that, in addition to the key cellular pathways around PI3K/PTEN/PKB, RAS/RAF/ERK and mTOR/S6K/S6, the targeting of other accessory and complementary genes and pathways that are aberrantly expressed, such as MerTK signaling, may represent excellent therapeutic interventions.

Surgical removal of the GBM tumor mass temporarily improves the patient's condition, but the capacity of GBM cells to infiltrate adjacent brain tissue and extend beyond the visible borders of the tumor invariably leads to tumor recurrence (219). The migration of tumor cells is a prerequisite for tumor cell invasion and metastasis development. Although inhibiting migration of GBM cells alone will not be sufficient to control tumor development, understanding the key molecular mechanisms necessary for cell invasion should help in the design of highly potent drug combinations with anti-migratory as well as pro-apoptotic properties. The unique

composition and properties of the neural parenchyma are believed to be refractory to cell motility and axonal extension. However, distinct mechanisms may be present in glioma cells that promote their interaction with a variety of substrates with different topography and molecular composition. This would, unfortunately, potentiate reactions to a changing microenvironment through matrix remodeling, cytoskeletal reorganization, and phenotype transition from highly proliferative to migratory. Although GBM cells secrete MMPs, which facilitates migration, MMP inhibition brought no survival benefit in glioblastoma patients (220, 221). Interestingly, glioma cells in the living brain migrate like nontransformed, neural progenitor cells that require myosin II activity. In contrast, on a 2D surface, glioma cells move more like fibroblasts independent of myosin II activity (15). PDK1 has been shown to maintain the rounded morphology and affect cancer cell motility by antagonizing inhibition of ROCK1 by RhoE (222). In this study, PDK1-mediated cortical actomyosin contractility is particularly important for cell migration in the 3D environment, but often not prominent on rigid 2D substrates. Consistent with the observation in this study that MerTK is not induced in all GBM cells lines under stem cell culture conditions, tumor cell lines that do not exhibit rounded or amoeboid motility did not require PDK1 for invasion (222). While PDK1 kinase activity is not essential for rounded cell morphology, phosphorylation of MerTK was found to be important for amoeboid invasion. There was no evidence to show that MerTK is relevant to PDK1-dependent cytoskeleton regulation, but instead the present study further demonstrated the complex and redundant signaling networks of cytoskeleton modulation and tumor cell invasion mechanisms. Notably, overexpression of an unphosphorable MerTK mutant severely reduced cell infiltration capacity, possibly due to its competitive binding to signaling transducer(s), thus negatively influencing

cell invasion. To dissect the function of the active and inactive MerTK complex opens up novel and interesting research directions.

In the physiological context, interaction between MerTK and myosin IIA is needed for retinal pigment epithelial phagocytosis in parallel with myosin IIB activation (144). However, oncogenic activity of MerTK-mediated myosin II activation has not been reported. Nonmuscle myosin II is a ubiquitous molecular motor comprising three isoforms (A, B and C). All vertebrates examined to date express at least two isoforms, myosin IIA and myosin IIB. The Myosin II isoforms regulate cell polarity, adhesion and migration in a variety of cell types through binding to and contracting filamentous actin (F-actin) in an ATP-dependent manner.

A number of studies in mammalian cells have revealed that the three myosin IIs are regulated in a similar fashion, i.e., through the phosphorylation of MLC2 (223). Phosphorylation at Ser-19 of MLC2 both elevated the actin-activated ATPase activity of myosin II and promoted myosin II filament assembly. Isoform-specific RNA interference showed that depletion of myosin IIA produces a cell phenotype similar to that following ROCK inhibition. This suggests that myosin IIA is specifically required for contractile events downstream of the Rho-ROCK signaling pathway (224, 225).

In agreement with the observation in the present study that overexpression of MerTK shows little effect on U373 cell motility under differentiation culture conditions (Yuhua Wang, unpublished data), myosin IIA-depleted cells were reported to have impaired thrombin-induced cell rounding and to assume a more motile phenotype (224). Additionally, thrombin preferentially induced phosphorylation of myosin IIA-MLC2 through the Rho-ROCK signaling cascade, whilst the phosphorylation status of myosin IIB-MLC2 was not affected (224).

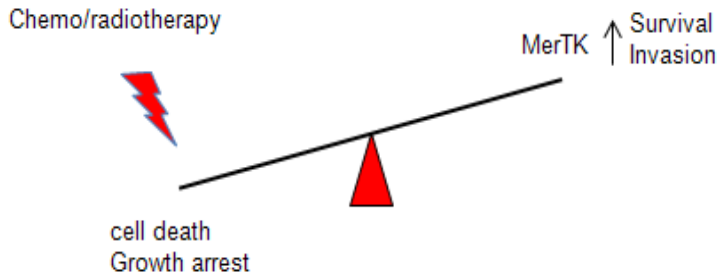


Figure 15. Model of MerTK induction and activation and functions in glioma cells. The standard therapeutic modalities are able to induce cell cycle arrest and kill tumor cells. However, under those extreme conditions, a number of proteins, including MerTK, are specifically induced and activated in certain population of cells, precluding cells from apoptosis and promoting invasion.

Mesenchymally migrating cells display an elongated cell shape and require extracellular proteolysis and integrin engagement, depending on Rac1-mediated cell polarization and lamellipodia formation. Conversely, amoeboidly moving cells have a

rounded morphology, independent of protease activity, but require high Rho GTPase activity to drive elevated levels of actomyosin contractility (226). In human monocytes, ligand-dependent MerTK activation results in tyrosine phosphorylation and the release of Vav1 from MerTK, and subsequently activates Rac1, Cdc42, and RhoA (178). Since Vav1 is specifically expressed in the hematopoietic system, MerTK likely regulates RhoA activity by binding to adaptor proteins such as Grb2 and recruiting other GEFs (183, 227). In this present study, overexpression of MerTK not only delayed a cell response to Blebbistatin treatment, but also upregulated MLC2 expression and phosphorylation, suggesting that activated MerTK maintains a rounded cell morphology, most probably by ROCK-RhoA-mediated myosin IIA activity. This hypothesis merits further investigation. We will continue this study and elucidate the complete map of the MerTK signaling network. Importantly, this work should contribute to the development of anti-invasive/pro-apoptotic therapeutic interventions.

5. references

(This section contains the references cited in the introduction and the General Discussion. References that are important for the results part can be found in the respective results section.)

1. Huse JT, Holland EC. Targeting brain cancer: advances in the molecular pathology of malignant glioma and medulloblastoma. *Nat Rev Cancer* 2010; 10: 319-31.
2. Van Meir EG, Hadjipanayis CG, Norden AD, Shu HK, Wen PY, Olson JJ. Exciting new advances in neuro-oncology: the avenue to a cure for malignant glioma. *CA Cancer J Clin* 2010; 60: 166-93.
3. Furnari FB, Fenton T, Bachoo RM, et al. Malignant astrocytic glioma: genetics, biology, and paths to treatment. *Genes Dev* 2007; 21: 2683-710.
4. Comprehensive genomic characterization defines human glioblastoma genes and core pathways. *Nature* 2008; 455: 1061-8.
5. Verhaak RG, Hoadley KA, Purdom E, et al. Integrated genomic analysis identifies clinically relevant subtypes of glioblastoma characterized by abnormalities in PDGFRA, IDH1, EGFR, and NF1. *Cancer Cell*; 17: 98-110.
6. Walker MD, Strike TA, Sheline GE. An analysis of dose-effect relationship in the radiotherapy of malignant gliomas. *Int J Radiat Oncol Biol Phys* 1979; 5: 1725-31.
7. Bao S, Wu Q, McLendon RE, et al. Glioma stem cells promote radioresistance by preferential activation of the DNA damage response. *Nature* 2006; 444: 756-60.
8. Zhai GG, Malhotra R, Delaney M, et al. Radiation enhances the invasive potential of primary glioblastoma cells via activation of the Rho signaling pathway. *J Neurooncol* 2006; 76: 227-37.

9. Drappatz J, Norden AD, Wen PY. Therapeutic strategies for inhibiting invasion in glioblastoma. *Expert Rev Neurother* 2009; 9: 519-34.
10. Joo KM, Kim SY, Jin X, et al. Clinical and biological implications of CD133-positive and CD133-negative cells in glioblastomas. *Lab Invest* 2008; 88: 808-15.
11. Wang J, Sakariassen PO, Tsinkalovsky O, et al. CD133 negative glioma cells form tumors in nude rats and give rise to CD133 positive cells. *Int J Cancer* 2008; 122: 761-8.
12. Son MJ, Woolard K, Nam DH, Lee J, Fine HA. SSEA-1 is an enrichment marker for tumor-initiating cells in human glioblastoma. *Cell Stem Cell* 2009; 4: 440-52.
13. Van Meir EG, Hadjipanayis CG, Norden AD, Shu HK, Wen PY, Olson JJ. Exciting new advances in neuro-oncology: the avenue to a cure for malignant glioma. *CA Cancer J Clin*; 60: 166-93.
14. Bellail AC, Hunter SB, Brat DJ, Tan C, Van Meir EG. Microregional extracellular matrix heterogeneity in brain modulates glioma cell invasion. *Int J Biochem Cell Biol* 2004; 36: 1046-69.
15. Beadle C, Assanah MC, Monzo P, Vallee R, Rosenfeld SS, Canoll P. The role of myosin II in glioma invasion of the brain. *Mol Biol Cell* 2008; 19: 3357-68.
16. Hoelzinger DB, Demuth T, Berens ME. Autocrine factors that sustain glioma invasion and paracrine biology in the brain microenvironment. *J Natl Cancer Inst* 2007; 99: 1583-93.
17. Oliveira R, Christov C, Guillamo JS, et al. Contribution of gap junctional communication between tumor cells and astroglia to the invasion of the brain parenchyma by human glioblastomas. *BMC Cell Biol* 2005; 6: 7.
18. Mueller MM, Werbowetski T, Del Maestro RF. Soluble factors involved in glioma invasion. *Acta Neurochir (Wien)* 2003; 145: 999-1008.

19. Kaur B, Khwaja FW, Severson EA, Matheny SL, Brat DJ, Van Meir EG. Hypoxia and the hypoxia-inducible-factor pathway in glioma growth and angiogenesis. *Neuro Oncol* 2005; 7: 134-53.
20. Tan C, de Noronha RG, Roecker AJ, et al. Identification of a novel small-molecule inhibitor of the hypoxia-inducible factor 1 pathway. *Cancer Res* 2005; 65: 605-12.
21. Fujiwara S, Nakagawa K, Harada H, et al. Silencing hypoxia-inducible factor-1alpha inhibits cell migration and invasion under hypoxic environment in malignant gliomas. *Int J Oncol* 2007; 30: 793-802.
22. Libermann TA, Nusbaum HR, Razon N, et al. Amplification, enhanced expression and possible rearrangement of EGF receptor gene in primary human brain tumours of glial origin. *Nature* 1985; 313: 144-7.
23. Wong AJ, Ruppert JM, Bigner SH, et al. Structural alterations of the epidermal growth factor receptor gene in human gliomas. *Proc Natl Acad Sci U S A* 1992; 89: 2965-9.
24. Lankiewicz S, Rother E, Zimmermann S, Hollmann C, Korangy F, Greten TF. Tumour-associated transcripts and EGFR deletion variants in colorectal cancer in primary tumour, metastases and circulating tumour cells. *Cell Oncol* 2008; 30: 463-71.
25. Gan HK, Kaye AH, Luwor RB. The EGFRvIII variant in glioblastoma multiforme. *J Clin Neurosci* 2009; 16: 748-54.
26. Wheeler SE, Suzuki S, Thomas SM, et al. Epidermal growth factor receptor variant III mediates head and neck cancer cell invasion via STAT3 activation. *Oncogene*; 29: 5135-45.
27. Lokker NA, Sullivan CM, Hollenbach SJ, Israel MA, Giese NA. Platelet-derived growth factor (PDGF) autocrine signaling regulates survival and mitogenic pathways in glioblastoma

cells: evidence that the novel PDGF-C and PDGF-D ligands may play a role in the development of brain tumors. *Cancer Res* 2002; 62: 3729-35.

28. Guo P, Hu B, Gu W, et al. Platelet-derived growth factor-B enhances glioma angiogenesis by stimulating vascular endothelial growth factor expression in tumor endothelia and by promoting pericyte recruitment. *Am J Pathol* 2003; 162: 1083-93.

29. Jain RK, di Tomaso E, Duda DG, Loeffler JS, Sorensen AG, Batchelor TT. Angiogenesis in brain tumours. *Nat Rev Neurosci* 2007; 8: 610-22.

30. Hutchinson L. Targeted therapies: the answer to individualized treatment? *Nat Clin Pract Oncol* 2007; 4: 323.

31. Wen PY, Kesari S. Malignant gliomas in adults. *N Engl J Med* 2008; 359: 492-507.

32. Pankova K, Rosel D, Novotny M, Brabek J. The molecular mechanisms of transition between mesenchymal and amoeboid invasiveness in tumor cells. *Cell Mol Life Sci*; 67: 63-71.

33. Friedl P, Wolf K. Tumour-cell invasion and migration: diversity and escape mechanisms. *Nat Rev Cancer* 2003; 3: 362-74.

34. Friedl P, Zanker KS, Brocker EB. Cell migration strategies in 3-D extracellular matrix: differences in morphology, cell matrix interactions, and integrin function. *Microsc Res Tech* 1998; 43: 369-78.

35. Miki H, Suetsugu S, Takenawa T. WAVE, a novel WASP-family protein involved in actin reorganization induced by Rac. *EMBO J* 1998; 17: 6932-41.

36. Rohatgi R, Ma L, Miki H, et al. The interaction between N-WASP and the Arp2/3 complex links Cdc42-dependent signals to actin assembly. *Cell* 1999; 97: 221-31.

37. Suetsugu S, Miki H, Yamaguchi H, Obinata T, Takenawa T. Enhancement of branching efficiency by the actin filament-binding activity of N-WASP/WAVE2. *J Cell Sci* 2001; 114: 4533-42.
38. Zaidel-Bar R, Cohen M, Addadi L, Geiger B. Hierarchical assembly of cell-matrix adhesion complexes. *Biochem Soc Trans* 2004; 32: 416-20.
39. Tester AM, Ruangpanit N, Anderson RL, Thompson EW. MMP-9 secretion and MMP-2 activation distinguish invasive and metastatic sublines of a mouse mammary carcinoma system showing epithelial-mesenchymal transition traits. *Clin Exp Metastasis* 2000; 18: 553-60.
40. Jeffers M, Rong S, Vande Woude GF. Enhanced tumorigenicity and invasion-metastasis by hepatocyte growth factor/scatter factor-met signalling in human cells concomitant with induction of the urokinase proteolysis network. *Mol Cell Biol* 1996; 16: 1115-25.
41. Pulyaeva H, Bueno J, Polette M, et al. MT1-MMP correlates with MMP-2 activation potential seen after epithelial to mesenchymal transition in human breast carcinoma cells. *Clin Exp Metastasis* 1997; 15: 111-20.
42. Sternlicht MD, Lochter A, Sympon CJ, et al. The stromal proteinase MMP3/stromelysin-1 promotes mammary carcinogenesis. *Cell* 1999; 98: 137-46.
43. Wolf K, Mazo I, Leung H, et al. Compensation mechanism in tumor cell migration: mesenchymal-amoeboid transition after blocking of pericellular proteolysis. *J Cell Biol* 2003; 160: 267-77.
44. Mandeville JT, Lawson MA, Maxfield FR. Dynamic imaging of neutrophil migration in three dimensions: mechanical interactions between cells and matrix. *J Leukoc Biol* 1997; 61: 188-200.

45. Friedl P, Borgmann S, Brocker EB. Amoeboid leukocyte crawling through extracellular matrix: lessons from the Dictyostelium paradigm of cell movement. *J Leukoc Biol* 2001; 70: 491-509.
46. Sahai E, Marshall CJ. Differing modes of tumour cell invasion have distinct requirements for Rho/ROCK signalling and extracellular proteolysis. *Nat Cell Biol* 2003; 5: 711-9.
47. Kraus AC, Ferber I, Bachmann SO, et al. In vitro chemo- and radio-resistance in small cell lung cancer correlates with cell adhesion and constitutive activation of AKT and MAP kinase pathways. *Oncogene* 2002; 21: 8683-95.
48. Rintoul RC, Sethi T. The role of extracellular matrix in small-cell lung cancer. *Lancet Oncol* 2001; 2: 437-42.
49. Falcioni R, Cimino L, Gentileschi MP, et al. Expression of beta 1, beta 3, beta 4, and beta 5 integrins by human lung carcinoma cells of different histotypes. *Exp Cell Res* 1994; 210: 113-22.
50. Jaspars LH, Bonnet P, Bloemena E, Meijer CJ. Extracellular matrix and beta 1 integrin expression in nodal and extranodal T-cell lymphomas. *J Pathol* 1996; 178: 36-43.
51. Wyckoff JB, Pinner SE, Gschmeissner S, Condeelis JS, Sahai E. ROCK- and myosin-dependent matrix deformation enables protease-independent tumor-cell invasion in vivo. *Curr Biol* 2006; 16: 1515-23.
52. Kimura K, Ito M, Amano M, et al. Regulation of myosin phosphatase by Rho and Rho-associated kinase (Rho-kinase). *Science* 1996; 273: 245-8.
53. Amano M, Ito M, Kimura K, et al. Phosphorylation and activation of myosin by Rho-associated kinase (Rho-kinase). *J Biol Chem* 1996; 271: 20246-9.

54. Mierke CT, Rosel D, Fabry B, Brabek J. Contractile forces in tumor cell migration. *Eur J Cell Biol* 2008; 87: 669-76.
55. Keller H, Eggli P. Protrusive activity, cytoplasmic compartmentalization, and restriction rings in locomoting blebbing Walker carcinosarcoma cells are related to detachment of cortical actin from the plasma membrane. *Cell Motil Cytoskeleton* 1998; 41: 181-93.
56. Simian M, Hirai Y, Navre M, Werb Z, Lochter A, Bissell MJ. The interplay of matrix metalloproteinases, morphogens and growth factors is necessary for branching of mammary epithelial cells. *Development* 2001; 128: 3117-31.
57. Davidson LA, Keller RE. Neural tube closure in *Xenopus laevis* involves medial migration, directed protrusive activity, cell intercalation and convergent extension. *Development* 1999; 126: 4547-56.
58. Klinowska TC, Soriano JV, Edwards GM, et al. Laminin and beta1 integrins are crucial for normal mammary gland development in the mouse. *Dev Biol* 1999; 215: 13-32.
59. Hegerfeldt Y, Tusch M, Brocker EB, Friedl P. Collective cell movement in primary melanoma explants: plasticity of cell-cell interaction, beta1-integrin function, and migration strategies. *Cancer Res* 2002; 62: 2125-30.
60. Sanz-Moreno V, Gadea G, Ahn J, et al. Rac activation and inactivation control plasticity of tumor cell movement. *Cell* 2008; 135: 510-23.
61. Wang HR, Ogunjimi AA, Zhang Y, Ozdamar B, Bose R, Wrana JL. Degradation of RhoA by Smurf1 ubiquitin ligase. *Methods Enzymol* 2006; 406: 437-47.
62. Sahai E, Garcia-Medina R, Pouyssegur J, Vial E. Smurf1 regulates tumor cell plasticity and motility through degradation of RhoA leading to localized inhibition of contractility. *J Cell Biol* 2007; 176: 35-42.

63. Gadea G, de Toledo M, Anguille C, Roux P. Loss of p53 promotes RhoA-ROCK-dependent cell migration and invasion in 3D matrices. *J Cell Biol* 2007; 178: 23-30.
64. Manning G, Whyte DB, Martinez R, Hunter T, Sudarsanam S. The protein kinase complement of the human genome. *Science* 2002; 298: 1912-34.
65. Robinson DR, Wu YM, Lin SF. The protein tyrosine kinase family of the human genome. *Oncogene* 2000; 19: 5548-57.
66. Linger RM, Keating AK, Earp HS, Graham DK. TAM receptor tyrosine kinases: biologic functions, signaling, and potential therapeutic targeting in human cancer. *Adv Cancer Res* 2008; 100: 35-83.
67. Graham DK, Bowman GW, Dawson TL, Stanford WL, Earp HS, Snodgrass HR. Cloning and developmental expression analysis of the murine c-mer tyrosine kinase. *Oncogene* 1995; 10: 2349-59.
68. Lu Q, Gore M, Zhang Q, et al. Tyro-3 family receptors are essential regulators of mammalian spermatogenesis. *Nature* 1999; 398: 723-8.
69. O'Bryan JP, Frye RA, Cogswell PC, et al. axl, a transforming gene isolated from primary human myeloid leukemia cells, encodes a novel receptor tyrosine kinase. *Mol Cell Biol* 1991; 11: 5016-31.
70. Sather S, Kenyon KD, Lefkowitz JB, et al. A soluble form of the Mer receptor tyrosine kinase inhibits macrophage clearance of apoptotic cells and platelet aggregation. *Blood* 2007; 109: 1026-33.
71. Rochlitz C, Lohri A, Bacchi M, et al. Axl expression is associated with adverse prognosis and with expression of Bcl-2 and CD34 in de novo acute myeloid leukemia (AML): results from

- a multicenter trial of the Swiss Group for Clinical Cancer Research (SAKK). *Leukemia* 1999; 13: 1352-8.
72. Challier C, Uphoff CC, Janssen JW, Drexler HG. Differential expression of the ufo/axl oncogene in human leukemia-lymphoma cell lines. *Leukemia* 1996; 10: 781-7.
73. Neubauer A, Fiebeler A, Graham DK, et al. Expression of axl, a transforming receptor tyrosine kinase, in normal and malignant hematopoiesis. *Blood* 1994; 84: 1931-41.
74. Gioia R, Leroy C, Drullion C, et al. Quantitative phosphoproteomics revealed interplay between Syk and Lyn in the resistance to nilotinib in chronic myeloid leukemia cells. *Blood* 2011; 118: 2211-21.
75. Crosier PS, Hall LR, Vitas MR, Lewis PM, Crosier KE. Identification of a novel receptor tyrosine kinase expressed in acute myeloid leukemic blasts. *Leuk Lymphoma* 1995; 18: 443-9.
76. Graham DK, Dawson TL, Mullaney DL, Snodgrass HR, Earp HS. Cloning and mRNA expression analysis of a novel human protooncogene, c-mer. *Cell Growth Differ* 1994; 5: 647-57.
77. Graham DK, Salzberg DB, Kurtzberg J, et al. Ectopic expression of the proto-oncogene Mer in pediatric T-cell acute lymphoblastic leukemia. *Clin Cancer Res* 2006; 12: 2662-9.
78. Yeoh EJ, Ross ME, Shurtleff SA, et al. Classification, subtype discovery, and prediction of outcome in pediatric acute lymphoblastic leukemia by gene expression profiling. *Cancer Cell* 2002; 1: 133-43.
79. Ek S, Hogerkorp CM, Dictor M, Ehinger M, Borrebaeck CA. Mantle cell lymphomas express a distinct genetic signature affecting lymphocyte trafficking and growth regulation as compared with subpopulations of normal human B cells. *Cancer Res* 2002; 62: 4398-405.
80. De Vos J, Couderc G, Tarte K, et al. Identifying intercellular signaling genes expressed in malignant plasma cells by using complementary DNA arrays. *Blood* 2001; 98: 771-80.

81. Sun WS, Fujimoto J, Tamaya T. Coexpression of growth arrest-specific gene 6 and receptor tyrosine kinases Axl and Sky in human uterine endometrial cancers. *Ann Oncol* 2003; 14: 898-906.
82. Lin WC, Li AF, Chi CW, et al. tie-1 protein tyrosine kinase: a novel independent prognostic marker for gastric cancer. *Clin Cancer Res* 1999; 5: 1745-51.
83. Wu CW, Li AF, Chi CW, et al. Clinical significance of AXL kinase family in gastric cancer. *Anticancer Res* 2002; 22: 1071-8.
84. Craven RJ, Xu LH, Weiner TM, et al. Receptor tyrosine kinases expressed in metastatic colon cancer. *Int J Cancer* 1995; 60: 791-7.
85. Jacob AN, Kalapurakal J, Davidson WR, et al. A receptor tyrosine kinase, UFO/Axl, and other genes isolated by a modified differential display PCR are overexpressed in metastatic prostatic carcinoma cell line DU145. *Cancer Detect Prev* 1999; 23: 325-32.
86. Sainaghi PP, Castello L, Bergamasco L, Galletti M, Bellosta P, Avanzi GC. Gas6 induces proliferation in prostate carcinoma cell lines expressing the Axl receptor. *J Cell Physiol* 2005; 204: 36-44.
87. Shiozawa Y, Pedersen EA, Patel LR, et al. GAS6/AXL axis regulates prostate cancer invasion, proliferation, and survival in the bone marrow niche. *Neoplasia*; 12: 116-27.
88. Wu YM, Robinson DR, Kung HJ. Signal pathways in up-regulation of chemokines by tyrosine kinase MER/NYK in prostate cancer cells. *Cancer Res* 2004; 64: 7311-20.
89. Ito M, Nakashima M, Nakayama T, et al. Expression of receptor-type tyrosine kinase, Axl, and its ligand, Gas6, in pediatric thyroid carcinomas around chernobyl. *Thyroid* 2002; 12: 971-5.

90. Ito T, Ito M, Naito S, et al. Expression of the Axl receptor tyrosine kinase in human thyroid carcinoma. *Thyroid* 1999; 9: 563-7.
91. Avilla E, Guarino V, Visciano C, et al. Activation of TYRO3/AXL tyrosine kinase receptors in thyroid cancer. *Cancer Res* 2011; 71: 1792-804.
92. Shieh YS, Lai CY, Kao YR, et al. Expression of axl in lung adenocarcinoma and correlation with tumor progression. *Neoplasia* 2005; 7: 1058-64.
93. Wimmel A, Glitz D, Kraus A, Roeder J, Schuermann M. Axl receptor tyrosine kinase expression in human lung cancer cell lines correlates with cellular adhesion. *Eur J Cancer* 2001; 37: 2264-74.
94. Berclaz G, Altermatt HJ, Rohrbach V, Kieffer I, Dreher E, Andres AC. Estrogen dependent expression of the receptor tyrosine kinase axl in normal and malignant human breast. *Ann Oncol* 2001; 12: 819-24.
95. Meric F, Lee WP, Sahin A, Zhang H, Kung HJ, Hung MC. Expression profile of tyrosine kinases in breast cancer. *Clin Cancer Res* 2002; 8: 361-7.
96. Tavazoie SF, Alarcon C, Oskarsson T, et al. Endogenous human microRNAs that suppress breast cancer metastasis. *Nature* 2008; 451: 147-52.
97. Macleod K, Mullen P, Sewell J, et al. Altered ErbB receptor signaling and gene expression in cisplatin-resistant ovarian cancer. *Cancer Res* 2005; 65: 6789-800.
98. Sun W, Fujimoto J, Tamaya T. Coexpression of Gas6/Axl in human ovarian cancers. *Oncology* 2004; 66: 450-7.
99. Rankin EB, Fuh KC, Taylor TE, et al. AXL is an essential factor and therapeutic target for metastatic ovarian cancer. *Cancer Res*; 70: 7570-9.

100. Tsou AP, Wu KM, Tsen TY, et al. Parallel hybridization analysis of multiple protein kinase genes: identification of gene expression patterns characteristic of human hepatocellular carcinoma. *Genomics* 1998; 50: 331-40.
101. Chung BI, Malkowicz SB, Nguyen TB, Libertino JA, McGarvey TW. Expression of the proto-oncogene Axl in renal cell carcinoma. *DNA Cell Biol* 2003; 22: 533-40.
102. Vajkoczy P, Knyazev P, Kunkel A, et al. Dominant-negative inhibition of the Axl receptor tyrosine kinase suppresses brain tumor cell growth and invasion and prolongs survival. *Proc Natl Acad Sci U S A* 2006; 103: 5799-804.
103. Hutterer M, Knyazev P, Abate A, et al. Axl and growth arrest-specific gene 6 are frequently overexpressed in human gliomas and predict poor prognosis in patients with glioblastoma multiforme. *Clin Cancer Res* 2008; 14: 130-8.
104. Keating AK, Kim GK, Jones AE, et al. Inhibition of Mer and Axl receptor tyrosine kinases in astrocytoma cells leads to increased apoptosis and improved chemosensitivity. *Mol Cancer Ther*; 9: 1298-307.
105. Evans CO, Young AN, Brown MR, et al. Novel patterns of gene expression in pituitary adenomas identified by complementary deoxyribonucleic acid microarrays and quantitative reverse transcription-polymerase chain reaction. *J Clin Endocrinol Metab* 2001; 86: 3097-107.
106. Quong RY, Bickford ST, Ing YL, Terman B, Herlyn M, Lassam NJ. Protein kinases in normal and transformed melanocytes. *Melanoma Res* 1994; 4: 313-9.
107. van Ginkel PR, Gee RL, Shearer RL, et al. Expression of the receptor tyrosine kinase Axl promotes ocular melanoma cell survival. *Cancer Res* 2004; 64: 128-34.
108. Tworkoski K, Singhal G, Szpakowski S, et al. Phosphoproteomic screen identifies potential therapeutic targets in melanoma. *Mol Cancer Res*; 9: 801-12.

109. Gyorffy B, Lage H. A Web-based data warehouse on gene expression in human malignant melanoma. *J Invest Dermatol* 2007; 127: 394-9.
110. Nakano T, Tani M, Ishibashi Y, et al. Biological properties and gene expression associated with metastatic potential of human osteosarcoma. *Clin Exp Metastasis* 2003; 20: 665-74.
111. Khan J, Bittner ML, Saal LH, et al. cDNA microarrays detect activation of a myogenic transcription program by the PAX3-FKHR fusion oncogene. *Proc Natl Acad Sci U S A* 1999; 96: 13264-9.
112. Koorstra JB, Karikari CA, Feldmann G, et al. The Axl receptor tyrosine kinase confers an adverse prognostic influence in pancreatic cancer and represents a new therapeutic target. *Cancer Biol Ther* 2009; 8: 618-26.
113. Song X, Wang H, Logsdon CD, et al. Overexpression of receptor tyrosine kinase Axl promotes tumor cell invasion and survival in pancreatic ductal adenocarcinoma. *Cancer* 2010; 117: 734-43.
114. Sayan AE, Stanford R, Vickery R, et al. Fra-1 controls motility of bladder cancer cells via transcriptional upregulation of the receptor tyrosine kinase AXL. *Oncogene* 2011.
115. Yeh CY, Shin SM, Yeh HH, et al. Transcriptional activation of the Axl and PDGFR-alpha by c-Met through a ras- and Src-independent mechanism in human bladder cancer. *BMC Cancer* 2011; 11: 139.
116. He L, Zhang J, Jiang L, et al. Differential expression of Axl in hepatocellular carcinoma and correlation with tumor lymphatic metastasis. *Mol Carcinog* 2010; 49: 882-91.
117. Xu MZ, Chan SW, Liu AM, et al. AXL receptor kinase is a mediator of YAP-dependent oncogenic functions in hepatocellular carcinoma. *Oncogene* 2011; 30: 1229-40.

118. Lee CH, Yen CY, Liu SY, et al. Axl Is a Prognostic Marker in Oral Squamous Cell Carcinoma. *Ann Surg Oncol* 2011.
119. Chen J, Carey K, Godowski PJ. Identification of Gas6 as a ligand for Mer, a neural cell adhesion molecule related receptor tyrosine kinase implicated in cellular transformation. *Oncogene* 1997; 14: 2033-9.
120. Nagata K, Ohashi K, Nakano T, et al. Identification of the product of growth arrest-specific gene 6 as a common ligand for Axl, Sky, and Mer receptor tyrosine kinases. *J Biol Chem* 1996; 271: 30022-7.
121. Caberoy NB, Zhou Y, Li W. Tubby and tubby-like protein 1 are new MerTK ligands for phagocytosis. *EMBO J*; 29: 3898-910.
122. Binder MD, Kilpatrick TJ. TAM receptor signalling and demyelination. *Neurosignals* 2009; 17: 277-87.
123. Stitt TN, Conn G, Gore M, et al. The anticoagulation factor protein S and its relative, Gas6, are ligands for the Tyro 3/Axl family of receptor tyrosine kinases. *Cell* 1995; 80: 661-70.
124. Sasaki T, Knyazev PG, Clout NJ, et al. Structural basis for Gas6-Axl signalling. *EMBO J* 2006; 25: 80-7.
125. Schlessinger J. Cell signaling by receptor tyrosine kinases. *Cell* 2000; 103: 211-25.
126. Ling L, Templeton D, Kung HJ. Identification of the major autophosphorylation sites of Nyk/Mer, an NCAM-related receptor tyrosine kinase. *J Biol Chem* 1996; 271: 18355-62.
127. Hafizi S, Alindri F, Karlsson R, Dahlback B. Interaction of Axl receptor tyrosine kinase with C1-TEN, a novel C1 domain-containing protein with homology to tensin. *Biochem Biophys Res Commun* 2002; 299: 793-800.

128. Budagian V, Bulanova E, Orinska Z, et al. Soluble Axl is generated by ADAM10-dependent cleavage and associates with Gas6 in mouse serum. *Mol Cell Biol* 2005; 25: 9324-39.
129. Costa M, Bellosta P, Basilico C. Cleavage and release of a soluble form of the receptor tyrosine kinase ARK in vitro and in vivo. *J Cell Physiol* 1996; 168: 737-44.
130. O'Bryan JP, Fridell YW, Koski R, Varnum B, Liu ET. The transforming receptor tyrosine kinase, Axl, is post-translationally regulated by proteolytic cleavage. *J Biol Chem* 1995; 270: 551-7.
131. Lemke G, Lu Q. Macrophage regulation by Tyro 3 family receptors. *Curr Opin Immunol* 2003; 15: 31-6.
132. Lu Q, Lemke G. Homeostatic regulation of the immune system by receptor tyrosine kinases of the Tyro 3 family. *Science* 2001; 293: 306-11.
133. Cohen PL, Caricchio R, Abraham V, et al. Delayed apoptotic cell clearance and lupus-like autoimmunity in mice lacking the c-mer membrane tyrosine kinase. *J Exp Med* 2002; 196: 135-40.
134. Angelillo-Scherrer A, de Frutos P, Aparicio C, et al. Deficiency or inhibition of Gas6 causes platelet dysfunction and protects mice against thrombosis. *Nat Med* 2001; 7: 215-21.
135. Nakano T, Ishimoto Y, Kishino J, et al. Cell adhesion to phosphatidylserine mediated by a product of growth arrest-specific gene 6. *J Biol Chem* 1997; 272: 29411-4.
136. Seitz HM, Camenisch TD, Lemke G, Earp HS, Matsushima GK. Macrophages and dendritic cells use different Axl/Mertk/Tyro3 receptors in clearance of apoptotic cells. *J Immunol* 2007; 178: 5635-42.

137. Wang H, Chen Y, Ge Y, et al. Immunoexpression of Tyro 3 family receptors--Tyro 3, Axl, and Mer--and their ligand Gas6 in postnatal developing mouse testis. *J Histochem Cytochem* 2005; 53: 1355-64.
138. Xiong W, Chen Y, Wang H, Wu H, Lu Q, Han D. Gas6 and the Tyro 3 receptor tyrosine kinase subfamily regulate the phagocytic function of Sertoli cells. *Reproduction* 2008; 135: 77-87.
139. Chen Y, Wang H, Qi N, et al. Functions of TAM RTKs in regulating spermatogenesis and male fertility in mice. *Reproduction* 2009; 138: 655-66.
140. Prasad D, Rothlin CV, Burrola P, et al. TAM receptor function in the retinal pigment epithelium. *Mol Cell Neurosci* 2006; 33: 96-108.
141. Duncan JL, LaVail MM, Yasumura D, et al. An RCS-like retinal dystrophy phenotype in mer knockout mice. *Invest Ophthalmol Vis Sci* 2003; 44: 826-38.
142. D'Cruz PM, Yasumura D, Weir J, et al. Mutation of the receptor tyrosine kinase gene *Mertk* in the retinal dystrophic RCS rat. *Hum Mol Genet* 2000; 9: 645-51.
143. Gal A, Li Y, Thompson DA, et al. Mutations in *MERTK*, the human orthologue of the RCS rat retinal dystrophy gene, cause retinitis pigmentosa. *Nat Genet* 2000; 26: 270-1.
144. Strick DJ, Feng W, Vollrath D. *Mertk* drives myosin II redistribution during retinal pigment epithelial phagocytosis. *Invest Ophthalmol Vis Sci* 2009; 50: 2427-35.
145. Rahman ZS, Shao WH, Khan TN, Zhen Y, Cohen PL. Impaired apoptotic cell clearance in the germinal center by *Mer*-deficient tingible body macrophages leads to enhanced antibody-forming cell and germinal center responses. *J Immunol*; 185: 5859-68.

146. Camenisch TD, Koller BH, Earp HS, Matsushima GK. A novel receptor tyrosine kinase, Mer, inhibits TNF- α production and lipopolysaccharide-induced endotoxic shock. *J Immunol* 1999; 162: 3498-503.
147. Rothlin CV, Ghosh S, Zuniga EI, Oldstone MB, Lemke G. TAM receptors are pleiotropic inhibitors of the innate immune response. *Cell* 2007; 131: 1124-36.
148. Williams JC, Wagner NJ, Earp HS, Vilen BJ, Matsushima GK. Increased hematopoietic cells in the *mertk*^{-/-} mouse peritoneal cavity: a result of augmented migration. *J Immunol*; 184: 6637-48.
149. Shao WH, Zhen Y, Rosenbaum J, et al. A protective role of Mer receptor tyrosine kinase in nephrotoxic serum-induced nephritis. *Clin Immunol*; 136: 236-44.
150. Angelillo-Scherrer A, Burnier L, Flores N, et al. Role of Gas6 receptors in platelet signaling during thrombus stabilization and implications for antithrombotic therapy. *J Clin Invest* 2005; 115: 237-46.
151. Wang H, Chen S, Chen Y, et al. The role of Tyro 3 subfamily receptors in the regulation of hemostasis and megakaryocytopoiesis. *Haematologica* 2007; 92: 643-50.
152. Toshima J, Ohashi K, Iwashita S, Mizuno K. Autophosphorylation activity and association with Src family kinase of Sky receptor tyrosine kinase. *Biochem Biophys Res Commun* 1995; 209: 656-63.
153. Lan Z, Wu H, Li W, et al. Transforming activity of receptor tyrosine kinase tyro3 is mediated, at least in part, by the PI3 kinase-signaling pathway. *Blood* 2000; 95: 633-8.
154. Hafizi S, Gustafsson A, Stenhoff J, Dahlback B. The Ran binding protein RanBPM interacts with Axl and Sky receptor tyrosine kinases. *Int J Biochem Cell Biol* 2005; 37: 2344-56.

155. Katagiri M, Hakeda Y, Chikazu D, et al. Mechanism of stimulation of osteoclastic bone resorption through Gas6/Tyro 3, a receptor tyrosine kinase signaling, in mouse osteoclasts. *J Biol Chem* 2001; 276: 7376-82.
156. Zhu D, Wang Y, Singh I, et al. Protein S controls hypoxic/ischemic blood-brain barrier disruption through the TAM receptor Tyro3 and sphingosine 1-phosphate receptor. *Blood*; 115: 4963-72.
157. Fridell YW, Jin Y, Quilliam LA, et al. Differential activation of the Ras/extracellular-signal-regulated protein kinase pathway is responsible for the biological consequences induced by the Axl receptor tyrosine kinase. *Mol Cell Biol* 1996; 16: 135-45.
158. Braunger J, Schleithoff L, Schulz AS, et al. Intracellular signaling of the Ufo/Axl receptor tyrosine kinase is mediated mainly by a multi-substrate docking-site. *Oncogene* 1997; 14: 2619-31.
159. Goruppi S, Ruaro E, Varnum B, Schneider C. Requirement of phosphatidylinositol 3-kinase-dependent pathway and Src for Gas6-Axl mitogenic and survival activities in NIH 3T3 fibroblasts. *Mol Cell Biol* 1997; 17: 4442-53.
160. Lee WP, Wen Y, Varnum B, Hung MC. Akt is required for Axl-Gas6 signaling to protect cells from E1A-mediated apoptosis. *Oncogene* 2002; 21: 329-36.
161. Demarchi F, Verardo R, Varnum B, Brancolini C, Schneider C. Gas6 anti-apoptotic signaling requires NF-kappa B activation. *J Biol Chem* 2001; 276: 31738-44.
162. Goruppi S, Ruaro E, Varnum B, Schneider C. Gas6-mediated survival in NIH3T3 cells activates stress signalling cascade and is independent of Ras. *Oncogene* 1999; 18: 4224-36.

163. Bellosta P, Zhang Q, Goff SP, Basilico C. Signaling through the ARK tyrosine kinase receptor protects from apoptosis in the absence of growth stimulation. *Oncogene* 1997; 15: 2387-97.
164. Ghosh AK, Secreto C, Boysen J, et al. The novel receptor tyrosine kinase Axl is constitutively active in B-cell chronic lymphocytic leukemia and acts as a docking site of nonreceptor kinases: implications for therapy. *Blood*; 117: 1928-37.
165. Allen MP, Linseman DA, Udo H, et al. Novel mechanism for gonadotropin-releasing hormone neuronal migration involving Gas6/Ark signaling to p38 mitogen-activated protein kinase. *Mol Cell Biol* 2002; 22: 599-613.
166. Nielsen-Preiss SM, Allen MP, Xu M, et al. Adhesion-related kinase induction of migration requires phosphatidylinositol-3-kinase and ras stimulation of rac activity in immortalized gonadotropin-releasing hormone neuronal cells. *Endocrinology* 2007; 148: 2806-14.
167. Sharif MN, Sosic D, Rothlin CV, et al. Twist mediates suppression of inflammation by type I IFNs and Axl. *J Exp Med* 2006; 203: 1891-901.
168. Yanagita M, Arai H, Nakano T, et al. Gas6 induces mesangial cell proliferation via latent transcription factor STAT3. *J Biol Chem* 2001; 276: 42364-9.
169. Jia R, Mayer BJ, Hanafusa T, Hanafusa H. A novel oncogene, v-ryk, encoding a truncated receptor tyrosine kinase is transduced into the RPL30 virus without loss of viral sequences. *J Virol* 1992; 66: 5975-87.
170. Jia R, Hanafusa H. The proto-oncogene of v-eyk (v-ryk) is a novel receptor-type protein tyrosine kinase with extracellular Ig/GN-III domains. *J Biol Chem* 1994; 269: 1839-44.

171. Ling L, Kung HJ. Mitogenic signals and transforming potential of Nyk, a newly identified neural cell adhesion molecule-related receptor tyrosine kinase. *Mol Cell Biol* 1995; 15: 6582-92.
172. Todt JC, Hu B, Curtis JL. The receptor tyrosine kinase MerTK activates phospholipase C gamma2 during recognition of apoptotic thymocytes by murine macrophages. *J Leukoc Biol* 2004; 75: 705-13.
173. Sen P, Wallet MA, Yi Z, et al. Apoptotic cells induce Mer tyrosine kinase-dependent blockade of NF-kappaB activation in dendritic cells. *Blood* 2007; 109: 653-60.
174. Eken C, Martin PJ, Sadallah S, Treves S, Schaller M, Schifferli JA. Ectosomes released by polymorphonuclear neutrophils induce a MerTK-dependent anti-inflammatory pathway in macrophages. *J Biol Chem*; 285: 39914-21.
175. Guttridge KL, Luft JC, Dawson TL, et al. Mer receptor tyrosine kinase signaling: prevention of apoptosis and alteration of cytoskeletal architecture without stimulation or proliferation. *J Biol Chem* 2002; 277: 24057-66.
176. Liao D, Wang X, Li M, Lin PH, Yao Q, Chen C. Human protein S inhibits the uptake of AcLDL and expression of SR-A through Mer receptor tyrosine kinase in human macrophages. *Blood* 2009; 113: 165-74.
177. Mahajan NP, Whang YE, Mohler JL, Earp HS. Activated tyrosine kinase Ack1 promotes prostate tumorigenesis: role of Ack1 in polyubiquitination of tumor suppressor Wwox. *Cancer Res* 2005; 65: 10514-23.
178. Mahajan NP, Earp HS. An SH2 domain-dependent, phosphotyrosine-independent interaction between Vav1 and the Mer receptor tyrosine kinase: a mechanism for localizing guanine nucleotide-exchange factor action. *J Biol Chem* 2003; 278: 42596-603.

179. Wu Y, Singh S, Georgescu MM, Birge RB. A role for Mer tyrosine kinase in alphavbeta5 integrin-mediated phagocytosis of apoptotic cells. *J Cell Sci* 2005; 118: 539-53.
180. Lewis JM, Cheresch DA, Schwartz MA. Protein kinase C regulates alpha v beta 5-dependent cytoskeletal associations and focal adhesion kinase phosphorylation. *J Cell Biol* 1996; 134: 1323-32.
181. Todt JC, Hu B, Punturieri A, Sonstein J, Polak T, Curtis JL. Activation of protein kinase C beta II by the stereo-specific phosphatidylserine receptor is required for phagocytosis of apoptotic thymocytes by resident murine tissue macrophages. *J Biol Chem* 2002; 277: 35906-14.
182. Komurov K, Padron D, Cheng T, Roth M, Rosenblatt KP, White MA. Comprehensive mapping of the human kinome to epidermal growth factor receptor signaling. *J Biol Chem* 2010; 285: 21134-42.
183. Georgescu MM, Kirsch KH, Shishido T, Zong C, Hanafusa H. Biological effects of c-Mer receptor tyrosine kinase in hematopoietic cells depend on the Grb2 binding site in the receptor and activation of NF-kappaB. *Mol Cell Biol* 1999; 19: 1171-81.
184. McCloskey P, Pierce J, Koski RA, Varnum B, Liu ET. Activation of the Axl receptor tyrosine kinase induces mitogenesis and transformation in 32D cells. *Cell Growth Differ* 1994; 5: 1105-17.
185. Keating AK, Kim GK, Jones AE, et al. Inhibition of Mer and Axl receptor tyrosine kinases in astrocytoma cells leads to increased apoptosis and improved chemosensitivity. *Mol Cancer Ther* 2010; 9: 1298-307.
186. McCloskey P, Fridell YW, Attar E, et al. GAS6 mediates adhesion of cells expressing the receptor tyrosine kinase Axl. *J Biol Chem* 1997; 272: 23285-91.

187. Hong CC, Lay JD, Huang JS, et al. Receptor tyrosine kinase AXL is induced by chemotherapy drugs and overexpression of AXL confers drug resistance in acute myeloid leukemia. *Cancer Lett* 2008; 268: 314-24.
188. Keating AK, Salzberg DB, Sather S, et al. Lymphoblastic leukemia/lymphoma in mice overexpressing the Mer (MerTK) receptor tyrosine kinase. *Oncogene* 2006; 25: 6092-100.
189. Linger RM, DeRyckere D, Brandao L, et al. Mer receptor tyrosine kinase is a novel therapeutic target in pediatric B-cell acute lymphoblastic leukemia. *Blood* 2009; 114: 2678-87.
190. Green J, Ikram M, Vyas J, et al. Overexpression of the Axl tyrosine kinase receptor in cutaneous SCC-derived cell lines and tumours. *Br J Cancer* 2006; 94: 1446-51.
191. Zhu S, Wurdak H, Wang Y, et al. A genomic screen identifies TYRO3 as a MITF regulator in melanoma. *Proc Natl Acad Sci U S A* 2009; 106: 17025-30.
192. Sensi M, Catani M, Castellano G, et al. Human Cutaneous Melanomas Lacking MITF and Melanocyte Differentiation Antigens Express a Functional Axl Receptor Kinase. *J Invest Dermatol* 2011.
193. Papadakis ES, Cichon MA, Vyas JJ, et al. Axl promotes cutaneous squamous cell carcinoma survival through negative regulation of pro-apoptotic Bcl-2 family members. *J Invest Dermatol* 2011; 131: 509-17.
194. Gluz O, Liedtke C, Gottschalk N, Pusztai L, Nitz U, Harbeck N. Triple-negative breast cancer--current status and future directions. *Ann Oncol* 2009; 20: 1913-27.
195. Gjerdrum C, Tiron C, Hoiby T, et al. Axl is an essential epithelial-to-mesenchymal transition-induced regulator of breast cancer metastasis and patient survival. *Proc Natl Acad Sci U S A* 2010; 107: 1124-9.

196. Vuoriluoto K, Haugen H, Kiviluoto S, et al. Vimentin regulates EMT induction by Slug and oncogenic H-Ras and migration by governing Axl expression in breast cancer. *Oncogene* 2011; 30: 1436-48.
197. Tai KY, Shieh YS, Lee CS, Shiah SG, Wu CW. Axl promotes cell invasion by inducing MMP-9 activity through activation of NF-kappaB and Brg-1. *Oncogene* 2008; 27: 4044-55.
198. Holland SJ, Powell MJ, Franci C, et al. Multiple roles for the receptor tyrosine kinase axl in tumor formation. *Cancer Res* 2005; 65: 9294-303.
199. Li Y, Ye X, Tan C, et al. Axl as a potential therapeutic target in cancer: role of Axl in tumor growth, metastasis and angiogenesis. *Oncogene* 2009; 28: 3442-55.
200. Mo R, Tony Zhu Y, Zhang Z, Rao SM, Zhu YJ. GAS6 is an estrogen-inducible gene in mammary epithelial cells. *Biochem Biophys Res Commun* 2007; 353: 189-94.
201. Mc Cormack O, Chung WY, Fitzpatrick P, et al. Growth arrest-specific gene 6 expression in human breast cancer. *Br J Cancer* 2008; 98: 1141-6.
202. Richer JK, Jacobsen BM, Manning NG, Abel MG, Wolf DM, Horwitz KB. Differential gene regulation by the two progesterone receptor isoforms in human breast cancer cells. *J Biol Chem* 2002; 277: 5209-18.
203. Linger RM, Keating AK, Earp HS, Graham DK. Taking aim at Mer and Axl receptor tyrosine kinases as novel therapeutic targets in solid tumors. *Expert Opin Ther Targets* 2010; 14: 1073-90.
204. Mahadevan D, Cooke L, Riley C, et al. A novel tyrosine kinase switch is a mechanism of imatinib resistance in gastrointestinal stromal tumors. *Oncogene* 2007; 26: 3909-19.
205. Zhang YX, Knyazev PG, Cheburkin YV, et al. AXL is a potential target for therapeutic intervention in breast cancer progression. *Cancer Res* 2008; 68: 1905-15.

206. Liu L, Greger J, Shi H, et al. Novel mechanism of lapatinib resistance in HER2-positive breast tumor cells: activation of AXL. *Cancer Res* 2009; 69: 6871-8.
207. Schroeder GM, An Y, Cai ZW, et al. Discovery of N-(4-(2-amino-3-chloropyridin-4-yloxy)-3-fluorophenyl)-4-ethoxy-1-(4-fluorophenyl)-2-oxo-1,2-dihydropyridine-3-carboxamide (BMS-777607), a selective and orally efficacious inhibitor of the Met kinase superfamily. *J Med Chem* 2009; 52: 1251-4.
208. Holland SJ, Pan A, Franci C, et al. R428, a selective small molecule inhibitor of Axl kinase, blocks tumor spread and prolongs survival in models of metastatic breast cancer. *Cancer Res* 2010; 70: 1544-54.
209. Ou WB, Corson JM, Flynn DL, et al. AXL regulates mesothelioma proliferation and invasiveness. *Oncogene* 2011; 30: 1643-52.
210. Liu R, Gong M, Li X, et al. Induction, regulation, and biologic function of Axl receptor tyrosine kinase in Kaposi sarcoma. *Blood* 2010; 116: 297-305.
211. Ye X, Li Y, Stawicki S, et al. An anti-Axl monoclonal antibody attenuates xenograft tumor growth and enhances the effect of multiple anticancer therapies. *Oncogene* 2010; 29: 5254-64.
212. Grzmil M, Morin P, Jr., Lino MM, et al. MAP Kinase-Interacting Kinase 1 Regulates SMAD2-Dependent TGF- β Signaling Pathway in Human Glioblastoma. *Cancer Res* 2011; 71: 2392-402.
213. Hanahan D, Weinberg RA. The hallmarks of cancer. *Cell* 2000; 100: 57-70.
214. Maher EA, Furnari FB, Bachoo RM, et al. Malignant glioma: genetics and biology of a grave matter. *Genes Dev* 2001; 15: 1311-33.

215. Merlo A. Genes and pathways driving glioblastomas in humans and murine disease models. *Neurosurg Rev* 2003; 26: 145-58.
216. Lampson LA. Monoclonal antibodies in neuro-oncology: Getting past the blood-brain barrier. *MAbs* 2011; 3: 153-60.
217. Gunther HS, Schmidt NO, Phillips HS, et al. Glioblastoma-derived stem cell-enriched cultures form distinct subgroups according to molecular and phenotypic criteria. *Oncogene* 2008; 27: 2897-909.
218. Caberoy NB, Zhou Y, Li W. Tubby and tubby-like protein 1 are new MerTK ligands for phagocytosis. *EMBO J* 2010; 29: 3898-910.
219. Merlo A, Bettler B. Glioblastomas on the move. *Sci STKE* 2004; 2004: pe18.
220. Coussens LM, Fingleton B, Matrisian LM. Matrix metalloproteinase inhibitors and cancer: trials and tribulations. *Science* 2002; 295: 2387-92.
221. Sarkar S, Nuttall RK, Liu S, Edwards DR, Yong VW. Tenascin-C stimulates glioma cell invasion through matrix metalloproteinase-12. *Cancer Res* 2006; 66: 11771-80.
222. Pinner S, Sahai E. PDK1 regulates cancer cell motility by antagonising inhibition of ROCK1 by RhoE. *Nat Cell Biol* 2008; 10: 127-37.
223. Conti MA, Adelstein RS. Nonmuscle myosin II moves in new directions. *J Cell Sci* 2008; 121: 11-8.
224. Sandquist JC, Swenson KI, Demali KA, Burrige K, Means AR. Rho kinase differentially regulates phosphorylation of nonmuscle myosin II isoforms A and B during cell rounding and migration. *J Biol Chem* 2006; 281: 35873-83.
225. Even-Ram S, Doyle AD, Conti MA, Matsumoto K, Adelstein RS, Yamada KM. Myosin IIA regulates cell motility and actomyosin-microtubule crosstalk. *Nat Cell Biol* 2007; 9: 299-309.

226. Parri M, Chiarugi P. Rac and Rho GTPases in cancer cell motility control. *Cell Commun Signal* 2010; 8: 23.
227. Zarich N, Oliva JL, Martinez N, et al. Grb2 is a negative modulator of the intrinsic Ras-GEF activity of hSos1. *Mol Biol Cell* 2006; 17: 3591-7.

6. Appendix

6.1 MAP Kinase-Interacting Kinase 1 Regulates SMAD2- Dependent TGF- β Signaling Pathway in Human Glioblastoma

Michal Grzmil, Pier Jr Morin, Maria Maddalena Lino, Adrian Merlo, Stephan Frank, **Yuhua Wang**, Gerald Moncayo, and Brian A. Hemmings



Cancer Research

MAP Kinase-Interacting Kinase 1 Regulates SMAD2-Dependent TGF- β Signaling Pathway in Human Glioblastoma

Michal Grzmil, Pier Morin, Jr, Maria Maddalena Lino, et al.

Cancer Res 2011;71:2392-2402. Published OnlineFirst March 14, 2011.

Updated Version Access the most recent version of this article at:
doi:[10.1158/0008-5472.CAN-10-3112](https://doi.org/10.1158/0008-5472.CAN-10-3112)

Supplementary Material Access the most recent supplemental material at:
<http://cancerres.aacrjournals.org/content/suppl/2011/03/09/71.6.2392.DC1.html>

Cited Articles This article cites 43 articles, 17 of which you can access for free at:
<http://cancerres.aacrjournals.org/content/71/6/2392.full.html#ref-list-1>

E-mail alerts [Sign up to receive free email-alerts](#) related to this article or journal.

Reprints and Subscriptions To order reprints of this article or to subscribe to the journal, contact the AACR Publications Department at pubs@aacr.org.

Permissions To request permission to re-use all or part of this article, contact the AACR Publications Department at permissions@aacr.org.

MAP Kinase-Interacting Kinase 1 Regulates SMAD2-Dependent TGF- β Signaling Pathway in Human Glioblastoma

Michal Grzmil¹, Pier Jr Morin¹, Maria Maddalena Lino², Adrian Merlo², Stephan Frank³, Yuhua Wang¹, Gerald Moncayo¹, and Brian A. Hemmings¹

Abstract

Glioblastoma multiforme (GBM) is the most common aggressive brain cancer with a median survival of approximately 1 year. In a search for novel molecular targets that could be therapeutically developed, our kinome-focused microarray analysis identified the MAP (mitogen-activated protein) kinase-interacting kinase 1 (MNK1) as an attractive theranostic candidate. MNK1 overexpression was confirmed in both primary GBMs and glioma cell lines. Inhibition of MNK1 activity in GBM cells by the small molecule CGP57380 suppressed eIF4E phosphorylation, proliferation, and colony formation whereas concomitant treatment with CGP57380 and the mTOR inhibitor rapamycin accentuated growth inhibition and cell-cycle arrest. siRNA-mediated knockdown of MNK1 expression reduced proliferation of cells incubated with rapamycin. Conversely, overexpression of full-length MNK1 reduced rapamycin-induced growth inhibition. Analysis of polysomal profiles revealed inhibition of translation in CGP57380 and rapamycin-treated cells. Microarray analysis of total and polysomal RNA from MNK1-depleted GBM cells identified mRNAs involved in regulation of TGF- β pathway. Translation of SMAD2 mRNA as well as TGF- β -induced cell motility and vimentin expression was regulated by MNK1 signaling. Tissue microarray analysis revealed a positive correlation between the immunohistochemical staining of MNK1 and SMAD2. Taken together, our findings offer insights into how MNK1 pathways control translation of cancer-related mRNAs including SMAD2, a key component of the TGF- β signaling pathway. Furthermore, they suggest MNK1-controlled translational pathways in targeted strategies to more effectively treat GBM. *Cancer Res*; 71(6); 2392–402. ©2011 AACR.

Introduction

In the last decade, genetic profiling of brain tumors has improved our understanding of gliomagenesis and led to the development of many targeted therapies based on molecular interference with deregulated signaling networks (1–3). Although many screens have characterized and proposed the targeting of deregulated signaling pathways for therapeutic interference, recent reports have identified therapy resistance based on the compensatory activation of alternative signaling pathways. Thus, effective treatment

requires combined regimens targeting the glioblastoma kinome (4–7).

The overall rate of protein synthesis is an important determinant of cancer cell metabolism (8). Many previous observations have indicated that deregulated growth pathways in human cancers are involved in the control of translation supporting cell proliferation and survival. In response to nutrients and growth factors, activated AKT/mTOR pathways enhance global protein synthesis. They phosphorylate and inactivate the eukaryotic translation initiation factor 4E-binding protein (eIF4E-BP), a repressor of mRNA translation and activate ribosomal S6 kinase 1 (S6K1) involved in ribosome biogenesis (9). Kinases associated with translation initiation complexes have a potential for regulating translation. MAP (mitogen-activated protein) kinase-interacting kinases (MNK1/2) can bind to translation initiation factor, eIF4G, and phosphorylate the cap-binding protein, the translation initiation factor eIF4E (10). The phosphorylation of eIF4E on Ser209 is increased in cancer cells and eIF4E expression levels are upregulated in many tumors (11–13). Recent findings demonstrate that eIF4E phosphorylation by MNKs is absolutely required for the eIF4E activity that opposes apoptosis and promotes tumorigenesis *in vivo* (14). In addition, MNKs can also phosphorylate RNA-binding protein, hnRNP A1, which binds AU-rich elements of messenger RNA (e.g.,

Authors' Affiliations: ¹Friedrich Miescher Institute for Biomedical Research; ²Laboratory of Molecular Neuro-oncology, Departments of Research and Surgery; and ³Department of Neuropathology, Institute of Pathology, University of Basel, Basel, Switzerland

Note: Supplementary data for this article are available at Cancer Research Online (<http://cancerres.aacrjournals.org/>).

Current affiliation for P. Jr Morin: Universite de Moncton, Moncton, Canada

Corresponding Author: Michal Grzmil or Brian A. Hemmings, Friedrich Miescher Institute for Biomedical Research, Maulbeerstrasse 66, CH-4058 Basel, Switzerland. Phone: 41-61-6974872 or 41-61-6974046; Fax: 41-61-6973976; E-mail: michal.grzmil@fmi.ch or brian.hemmings@fmi.ch

doi: 10.1158/0008-5472.CAN-10-3112

©2011 American Association for Cancer Research.

TNF- α), thereby regulating its stability and/or translation (15). Thus, MNK signaling appears to play an important role in posttranscriptional regulation of cancer-related gene expression.

Materials and Methods

Antibodies and chemicals

MNK1 (C4C1), p-MNK1 (Thr197/202), SMAD2 (86F7), p-SMAD2 (Ser245/250/255), eIF4E (C46H6), p-eIF4E (Ser209), p-S6 (Ser235/236), p38 (9212), p-p38 (Thr180/Tyr182), ERK1/2 (9102), p-ERK1/2 (Thr202/Tyr204), and p-EGFR (Tyr992) antibodies were from Cell Signaling. Actin (I-19) and EGFR (epidermal growth factor receptor; sc-03) antibodies from Santa Cruz Biotechnology, vimentin (V9) from Thermo Scientific and generated α -tubulin YL1/2 was used as hybridoma supernatant. CGP57380 and rapamycin were from Sigma, RAD001 from Novartis, SB431542 from Tocris, and TGF- β from PeproTech.

Patients

Primary glioma tissues obtained from the operating room were processed as previously described (16) in accordance with the guidelines of the Ethical Committee of the University Hospitals of Basel and Dusseldorf. Tumors were diagnosed and graded according to the current WHO Classification. The patient set is summarized in Supplementary Table 1.

Cell culture and standard techniques

Human glioma cells: BS125, LN18, LN229, BS149, LN319, LN405, LN215, LN71, U343MG, U373, U87MG, Hs683, A172, and M059K were cultured in DMEM supplemented with 10% FCS (fetal calf serum) and antibiotics at 37°C and 5% CO₂. Glioblastoma multiforme (GBM)-derived BS287 spheres were cultured as described previously (17). Clonetics normal human astrocytes (NHA) were from Cambrex and cultured according to the manufacturer's recommendations. Transfection, treatments, cellular assays, including proliferation, viability, colony formation, flow cytometry as well as RNA and protein isolation followed by quantitative real-time PCR, microarray hybridization, Western blotting, and immunohistochemistry are described in Supplementary Experimental Procedures.

Microarray data analysis

Data mining and visualization of microarray-profiled gliomas were performed using Genedata's Analyst 4.1 package. Median fold ratio values at $P < 0.05$ in the t test were used for analysis. All samples were quintile normalized and median scaled to correct for minor variations in their expression distributions. The data obtained have been deposited in the Gene Expression Omnibus (GEO) database (GSE15824). Polysomal profiles (triplicate experiment for transfection and inhibitor treatments) and RNA extraction was accomplished as previously described (18) and used for microarray hybridization described in Supplementary Material. Data analysis was carried out using R/Bioconductor (19). Signal condensation was performed using the RMA from the Bioconductor Affy package. Differentially expressed genes were identified by

the empirical Bayes method (F test) implemented in the LIMMA package and adjusted with the false discovery rate method (20). Visualization was done in R. Probe sets with a log₂ average contrast signal of at least 5, an adjusted P value of < 0.05 , and an absolute log₂ fold-change of greater than 0.585 (1.5-fold in linear space) were used.

Cell motility

Forty-eight hours after transfection or 24 hours after treatment, a scratch was made and the migration of cells was monitored using a live-imaging system Widefield TILL5, Long Run, Axiovert 200M (Carl Zeiss). Images were captured every 20 minutes over a period of 22 hours with a CCD camera using MetaMorph software (Molecular Devices) and analyzed using ImageJ software (NIH).

Results

MNK1 overexpression in human glioblastoma

Microarray analysis of 30 brain tumor samples was performed including 15 high-grade gliomas (glioblastomas) and 15 low-grade tumors (8 astrocytomas and 7 oligodendrogliomas). Kinase expression in each tumor was normalized to the expression levels in normal brain and expression values from NHAs were used as an additional control. Apart from kinases known to be associated with gliomagenesis (e.g., EGFR; data not shown), a further protein kinase was found to be upregulated in primary glioblastomas. The transcript level of MNK1 was upregulated more than 2-fold in 12 of 15 glioblastomas and in 5 of 8 astrocytomas ($P < 0.01$ for both groups, compared with expression in normal brain and human normal astrocytes) whereas 3 of 7 patients exhibited elevated MNK1 levels in oligodendroglioma (Fig. 1A). MNK2 kinase expression was not significantly altered in the human gliomas analyzed (data not shown). There was no significant correlation between MNK1 expression and survival in profiled glioma patients. Changes in MNK1 expression were further validated by real-time PCR. In 10 of 11 glioblastoma samples, MNK1 was elevated more than 2-fold (Fig. 1B). Human MNK1 arises from an alternatively spliced transcript giving rise to 2 isoforms, longer MNK1a (50 kDa) and a shorter MNK1b variant (38 kDa) that lacks 89 C-terminal amino acids (21). We determined MNK1a protein levels in GBM tumors and cell lines using an MNK1a-specific monoclonal antibody. An increase in MNK1 kinase was observed in 14 of 20 (70%) primary glioblastomas and in 11 of 13 (84%) glioma cell lines, compared with normal brain and NHAs, respectively (Fig. 1C). Immunohistochemical analysis of tumor sections from 12 GBM patients and tissue arrays containing 34 GBMs and 5 normal brains also demonstrated high MNK1 protein levels, with stronger cytoplasmic signals in GBM cells than in weakly stained normal brain (Fig. 1D). Antibody specificity was tested on whole protein cell lysates (Fig. 1C) and on formalin-fixed BS125 cells (Fig. 1D) transfected with siRNA against the *MNK1* gene or luciferase (control). MNK1 phosphorylation correlated with total level of MNK1 (correlation coefficient = 0.51) and was significantly higher in 7 of 11 (64%) GBM patients than in normal human brain and astrocytes (Fig. 1C and Supplementary Fig. S1). To

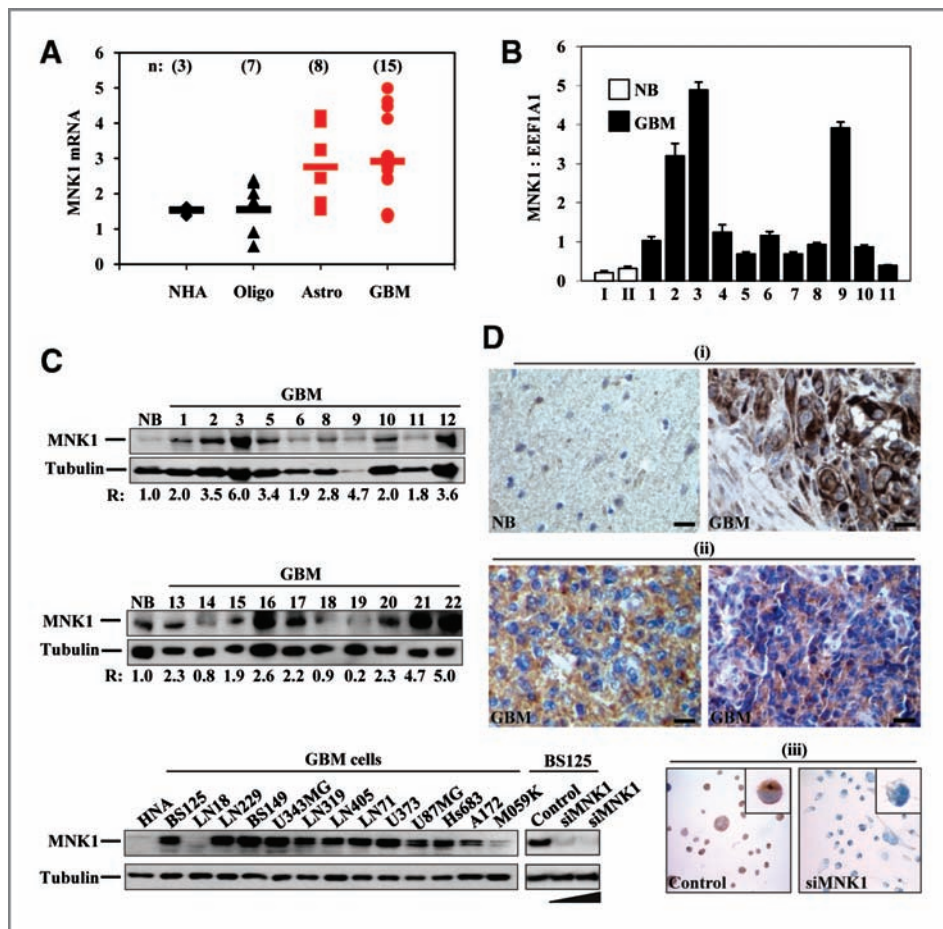


Figure 1. Expression of MNK1 in human gliomas. **A**, MNK1 transcript levels in primary brain tumors obtained from microarray analysis. NHA, Oligo (oligodendroglioma), Astro (astrocytoma), and GBM. Expression of MNK1 in normal brain (NB) was set to 1. Patient information is given in Supplementary Table 1. **B**, quantitative RT-PCR analysis of MNK1 (normalized to EEF1A1 expression) on total RNA isolated from glioblastoma and 2 NB: I and II samples. **C**, Western blot analysis using an MNK1-specific antibody on whole protein lysates obtained from human GBM (lanes 1–22), NB samples as well as from different GBM cell lines, NHA and BS125 cells at 3 days after transfection with increasing concentrations of duplex siRNA against MNK1 or against luciferase (control). Blots were stripped and reprobed with an α -tubulin antibody. Ratios (R) of MNK1-specific signals relative to tubulin expression are shown below. The MNK1/tubulin ratio for NB was set to 1. **D**, immunohistochemistry (IHC) of MNK1 in normal brain and primary GBM in tissue arrays (i), GBM paraffin sections (ii), and formalin-fixed BS125 cells 72 hours after siRNA transfection (iii); bar, 20 μ m.

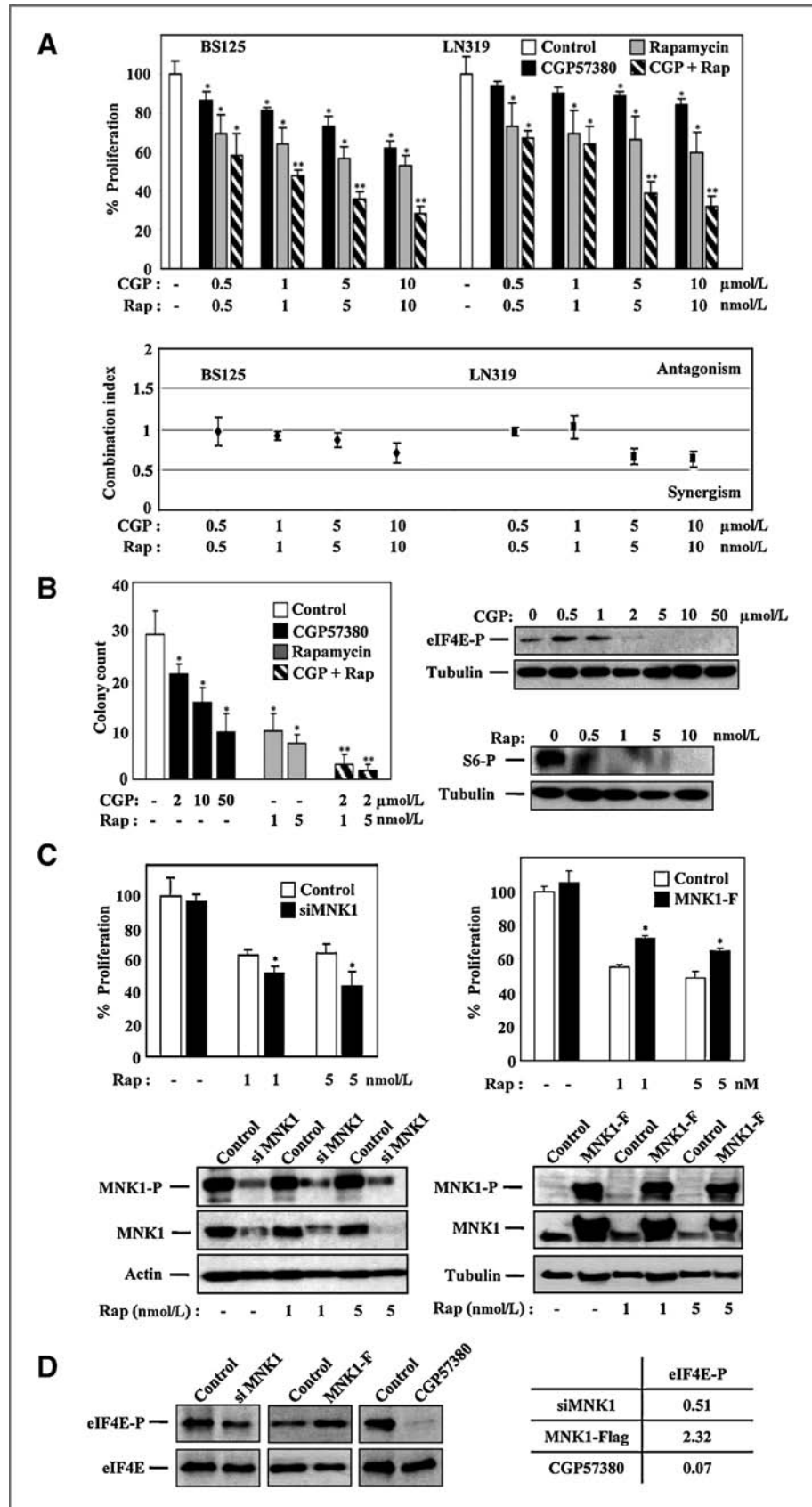
investigate whether MNK1 expression is regulated by EGFR, which is often amplified and hyperactivated in GBM, the correlation between MNK1 and EGFR was analyzed in glioma patients and in GBM cell lines. Microarray analysis showed no significant correlation between MNK1 and EGFR in human gliomas (correlation coefficient = 0.29). There was also no correlation between MNK1 and EGFR or phospho-EGFR levels in analyzed GBM cells (Fig. 1C and Supplementary Fig. S2). Likewise, treatment with the EGFR inhibitor AEE788 did not affect the MNK1 protein level indicating that MNK1 expression is not regulated by EGFR pathways.

Inhibition of MNK1 reduces GBM cell proliferation and colony formation and acts additively with rapamycin

To investigate MNK1 as a potential therapeutic target, a pharmacologic approach was first taken using an efficient inhibitor of MNK kinases, CGP57380 (22). As MNK1 signaling is involved in the regulation of translation, inhibition of MNK1 was combined with the targeting of mTOR pathways, which also act at the translational level. Treatment with either CGP57380 or rapamycin alone reduced proliferation and their combination had an additive effect on human GBM cell lines BS125, LN319, LN405, and BS287 spheres (Fig. 2A and Sup-

plementary Fig. S3). There was a synergistic effect at the highest concentrations of CGP57380 (10 μ mol/L) and rapamycin (10 nmol/L), with combination index values of 0.71 and 0.63 in BS125 and LN319 cells, respectively. Concomitant treatments with CGP57380 and rapamycin over 5 days greatly reduced BS125 and LN319 cell number (data not shown). The observed additive inhibitory effect was confirmed further using CGP57380 together with the rapamycin derivative RAD001 in BS125 cells (Supplementary Fig. S3). The effects of inhibitor treatments were monitored by immunoblotting using phospho-specific antibodies against eIF4E (treatment with CGP57380) and ribosomal protein S6 (treatment with rapamycin; Fig. 2B, right). CGP57380 at 2 μ mol/L or rapamycin at 0.5 nmol/L was sufficient to decrease significantly eIF4E and S6 phosphorylation, respectively. Furthermore, the growth of BS125 cells in soft agar at increasing concentrations of CGP57380 and rapamycin was inhibited in a dose-dependent manner (Fig. 2B, left). Concomitant treatment with CGP57380 and rapamycin amplified inhibitory effect; CGP57380 at 2 μ mol/L significantly increased the growth inhibition by rapamycin. To analyze the relationship specifically between MNK1 protein level and cell proliferation after rapamycin treatment, RNAi (RNA interference) was used to

Figure 2. Targeting MNK1 inhibited cell growth and sensitized GBM cells to rapamycin. **A**, an MTT-based assay of BS125 and LN319 cell proliferation after 3 days of incubation with CGP57380 alone or in combination with rapamycin (Rap). Results were obtained in triplicate and are shown as % proliferation compared with control cells. Bottom, corresponding combination index (CI) values greater than 1.1 indicate antagonism, between 0.9 and 1.1 additive effects, and lower than 0.9 synergism. **B**, resuspended BS125 cells in soft agar were incubated at the indicated concentrations of CGP57380 and/or rapamycin. After 16 days, colonies were photographed and analyzed as described in the Materials and Methods section. All experiments were carried out in triplicate and the results are shown as mean values \pm SD. **Right**, phosphorylation of eIF4E (Ser209) or ribosomal protein S6 (Ser235/236) in BS125 cells treated with CGP57380 or rapamycin for 24 hours was monitored by immunoblotting using phospho-specific antibodies. The blots were stripped and reprobed with antitubulin antibody to control for equal loading. **C**, BS125 cells were transfected with duplex siRNA oligonucleotides against *MNK1* (si) or with a control duplex against luciferase. For the full-length MNK1 overexpression, cells were transfected with a MNK1-Flag construct or an empty control vector. Twenty-four hours after transfection, cells were treated with rapamycin at the concentrations indicated for a further 48 hours and used for MTT-based assay as described above. Bottom, whole protein lysates isolated from transfected and rapamycin-treated cells were subjected to Western blot analysis using phospho-specific (Thr197/202) and total MNK1 antibodies. Actin- or tubulin-specific antibodies were used as loading controls. **D**, eIF4E phosphorylation in MNK1-depleted or overexpressing BS125 cells 48 hours after transfection or treatment with 10 μ M CGP57380 was analyzed by Western blot using specific antibodies against phosphorylated and total eIF4E. **Right**, changes in eIF4E phosphorylation depicted as the ratio of phospho- to total eIF4E-specific signals. Ratios in controls were normalized to 1. *, $P < 0.05$ or **, $P < 0.02$ compared with control or single drug treatment using Student's *t* test.



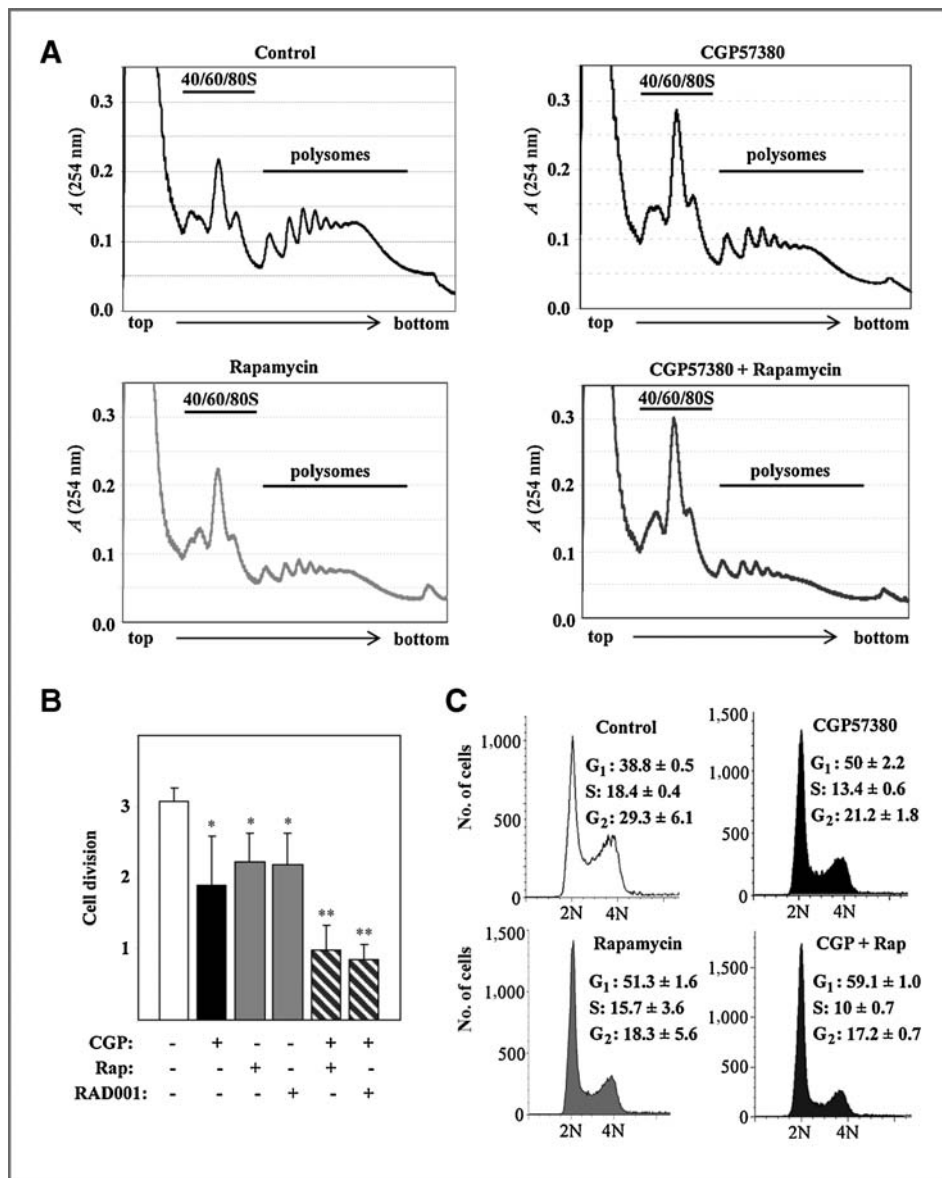


Figure 3. Inhibition of MNK1 by CGP57380 reduced global translation and induced cell-cycle arrest; combined treatment with rapamycin increased the inhibitory effect. **A**, polysome profiles from BS125 cells treated with DMSO (dimethyl sulfoxide; control), 10 μ mol/L CGP57380, and/or 10 nmol/L rapamycin for 24 hours. The A_{254} peaks corresponding to ribosomal subunits and polysomes are indicated. **B**, cell division was determined 72 hours after treatment (as described above) using the CFSE (carboxyfluorescein succinimidyl ester) cell-labeling assay followed by FACS (fluorescence-activated cell-sorting) analysis. The rapamycin derivative RAD001 was used at 10 nmol/L. *, $P < 0.05$ or **, $P < 0.01$ versus control or single treatment. **C**, cell-cycle analysis of BS125 cells treated for 24 hours as indicated above. Results are means \pm SD from 3 independent incubations.

inhibit MNK1 expression. For complete depletion of MNK1, duplex siRNA were used specific for splice variants *MNK1a* and *MNK1b*, which encode identical catalytic domains. BS125 cells transfected with an MNK1-specific siRNA duplex showed significantly reduced endogenous expression of both phospho- and total MNK1 protein and enhanced sensitivity to rapamycin (Fig. 2C). To investigate this further, a full-length MNK1-Flag fusion protein was overexpressed in BS125 cells. Ectopically expressed MNK1 protein was phosphorylated and this reduced the inhibition of BS125 cell proliferation by rapamycin (Fig. 2C, right). MNK1 overexpression increased phosphorylation of the MNK1 substrate eIF4E more than 2-fold, indicating that the MNK1-Flag-tagged kinase was fully functional whereas MNK1-specific knockdown or CGP57380 treatment reduced eIF4E phosphorylation to 51% and 7%, respectively, compared with control-treated cells (Fig. 2D).

Finally, the MNK1 protein level correlated positively (correlation coefficient = 0.7) with resistance to mTOR inhibition after 3 days treatment with 5 nmol/L rapamycin in 6 GBM cell lines: BS125, LN319, LN18, LN405, U343MG, and BS145 (Fig. 2A, Supplementary Fig. S3, and data not shown).

Targeting signaling pathways regulating translation reduces global translation and induces cell-cycle arrest

Polysome profiles obtained by sucrose gradient centrifugation revealed a substantial increase in the inhibition of global translation in BS125 cells treated simultaneously with CGP57380 and rapamycin (Fig. 3A). Comparison analysis of the areas occupied under the curves in polysomal profiles (data not shown) indicates that CGP57380 increased the relative abundance of free ribosomes (1.35 ± 0.3 -fold) and decreased polysomes (0.65 ± 0.05) whereas rapamycin alone

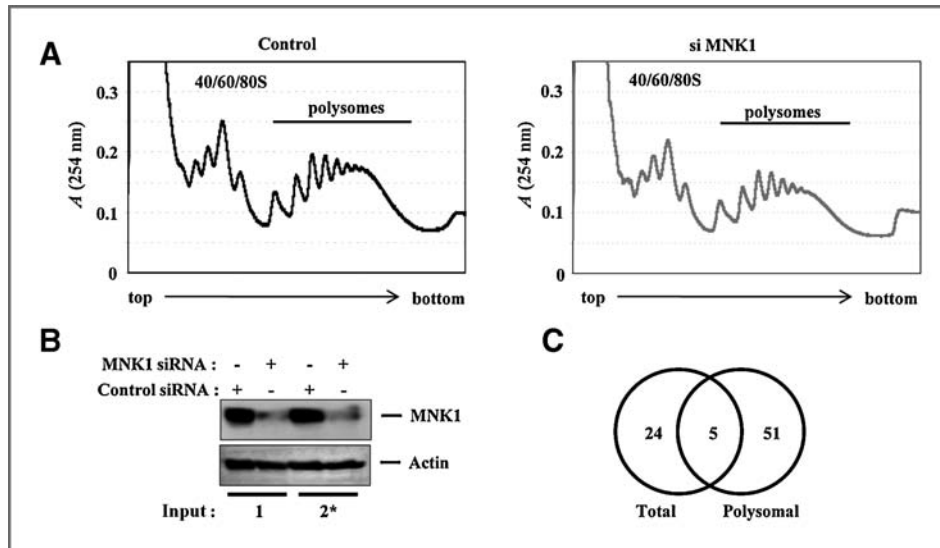


Figure 4. MNK1 knockdown had no major impact on global translation but regulated the expression of a subset of mRNAs. **A**, polysome profiles from BS125 cell lysates prepared 48 hours after transfection with duplex siRNA against *MNK1* gene (si) or with a control duplex against luciferase. The A_{254} peaks corresponding to ribosomal subunits and polysomes are indicated. **B**, the same protein lysates were subjected to Western blot analysis with MNK1- and tubulin-specific antibodies. *, profiles in **A** were obtained from the indicated lysates. **C**, results from expression profiling of total and polysome-associated mRNAs from MNK1-depleted and control-transfected BS125 cells shown as a Venn diagram representing the numbers of significantly affected RNAs.

significantly reduced the abundance of polysomes (0.43 ± 0.04) compared with control. Cotreatment with CGP57380 and rapamycin both increased free ribosomes (1.48 ± 0.23) and reduced polysomes abundance (0.31 ± 0.05). Furthermore, as shown in Figure 3B and C, the inhibition of global translation was accompanied by G₁ cell-cycle arrest. This demonstrates a major cytostatic effect in BS125 cells treated with CGP57380 together with rapamycin or RAD001.

Identification of MNK1-regulated targets

Sucrose gradient separation revealed no major differences in polysome profiles between BS125 cells transfected with siRNA against *MNK1* and the control duplex (Fig. 4A and B), suggesting that MNK1 is involved rather in the regulation of a small subset of mRNAs. To investigate this further, total and polysome-associated RNAs isolated from the same transfected cells were compared using microarray hybridization. In addition to reduced MNK1 expression, we identified 56 differentially expressed mRNAs ($P < 0.05$) using polysomal RNA and 29 using total RNA (Fig. 4C, Supplementary Tables S2 and S3). Of these, 5 targets were common to both polysomal and total RNAs. The identified MNK1 targets have been subjected to gene ontology and pathway analysis using the DAVID web-based bioinformatics tool (23, 24). These analyses indicated that MNK1 regulates a group of mRNAs encoding proteins involved in TGF- β signaling, with the highest enrichment value of 8.3 whereas mRNAs associated with signal transduction and cell communication showed 3.1- and 2.6-fold enrichment, respectively (Table 1). Of note, the SMAD2 transcript was present in all 3 identified gene groups, suggesting that SMAD2 expression plays an important role in the MNK1-regulated phenotype.

MNK1 regulates SMAD2-dependent TGF- β pathways in human GBM

The microarray data demonstrating decreased SMAD2 mRNA association with polysomes (Fig. 5A) were further validated by RT-PCR analysis of polysomal and total RNA (Fig. 5B) or at the protein level in MNK1-depleted BS125 and LN319 cells (Fig. 5C). SMAD2 protein was also reduced at the presence of RNA polymerase II inhibitor, actinomycin D, indicating posttranscriptional regulation. In addition, the SMAD2 protein level was found to be higher in MNK1-over-expressing BS125 stable clones than in control-transfected cells (Fig. 5C, bottom). To further validate the *in vitro* data, tissue arrays were used to analyze MNK1 and SMAD2 expression at the protein level in 34 GBM tumors and 5 normal brains, as described above. Strong MNK1 and SMAD2 immunostaining was recorded in comparable areas of analyzed tumors, whereas normal brain tissue showed significantly weaker expression (Fig. 5D). Comparative bioinformatics analysis of MNK1 and SMAD2 expression gave a correlation coefficient of 0.6, supporting our *in vitro* observation that MNK1 regulates SMAD2 protein levels in human GBM.

Exploring how far MNK1 may be involved in the regulation of TGF- β /SMAD-dependent phenotype, we found that TGF- β at 5 nmol/L is sufficient to increase cell motility of BS125 and Hs683 cells compared with untreated cells (data not shown). Furthermore, siRNA knockdown of MNK1 or inhibition by CGP57380 reduced total as well as TGF- β -induced phosphorylated SMAD2 levels and led to a pronounced inhibition of cellular motility (Fig. 6A). Bioinformatics analysis of microarray data from GBM patients revealed a significant correlation between MNK1 expression and TGF- β -regulated genes. For this analysis, we chose hallmarks of the epithelial to

Table 1. Bioinformatics analysis of MNK1-regulated genes identified by microarray hybridization. Enrichment was scored for terms with $P < 0.05$ for a group of at least 3 genes.

Functional annotations for MNK1-regulated genes	Enrichment
TGF- β signaling pathway (pathway: hsa04350, $P = 0.04$); <i>SMAD2</i> , <i>BMP8</i> , <i>DP1</i>	8.3
Regulation of signal transduction (GO:0009966, $P = 0.01$); regulation of cell communication (GO:0010646, $P = 0.02$); <i>CTGLF3</i> , <i>CTGLF5</i> , <i>GPR89B</i> , <i>SMAD2</i> , <i>TGIF</i> , <i>RAC1</i> , <i>SNX13</i> , <i>TLR4</i> , <i>TNFSF15</i>	3.1; 2.6

mesenchymal transition (EMT) that plays a crucial role in malignant cancer cell migration and motility (25). Expression of vimentin and fibronectin positively correlated with MNK1 expression levels (correlation coefficients = 0.74 and 0.70, respectively), whereas, E-cadherin and tight junction protein 1 showed negative correlations of -0.64 and -0.65 , respectively (Fig. 6B). Decreased vimentin expression was further confirmed at the protein level in MNK1-depleted BS125 GBM cells (Fig. 6B) whereas E-cadherin expression was not detected by Western blotting (data not shown). The lack of vimentin and other TGF- β -regulated EMT markers among the MNK1-regulated mRNAs (Supplementary Tables S2 and S3) may be explained by the fact that microarray analyses were performed 48 hours after transfection, which was sufficient for MNK1 knockdown at the protein level, whereas a significant decrease in SMAD2 protein was only observed after 72 hours (Fig. 5C). As only a marginal decrease in SMAD2 protein expression was reached 48 hours after transfection, we concluded that a significant decrease in SMAD2 protein synthesis begins after that time point resulting in alterations in TGF- β /SMAD2 signaling pathways.

In this study, we showed that SMAD2 protein synthesis depends on MNK1 and that targeting MNK1 sensitizes GBM cells to rapamycin. Therefore, we asked whether inhibition of the TGF- β /SMAD2 pathway, instead of MNK1, also has an additive effect. For this, we made use of the SB431542 compound known to inhibit SMAD2 phosphorylation (26). As demonstrated in Supplementary Figure S4, concomitant treatment with SB431542 and rapamycin (or RAD001) for 5 days had an inhibitory effect on GBM cell growth (27%–30% of control) similar to that in cells treated with CGP57380, rapamycin or RAD001 (20%–23%). Targeting all 3 pathways (mTOR, SMAD2, and MNK1) did not increase the inhibitory effect (20%–22%) and concomitant treatment with CGP57380 and SB431542 was not additive. Finally, as shown in Figure 6C, TGF- β treatment induced activation of MNK1 upstream kinases p38 and ERK1/2, and increased MNK1

phosphorylation, thus supporting our model for MNK1 and TGF- β /SMAD2 pathways convergence (Fig. 6D).

Discussion

The biological function of eIF4E phosphorylation at Ser209 by MNKs has long been controversial. Some studies have reported that eIF4E phosphorylation enhances translation in general (27), whereas others concluded that it has no effect or even reduces translation (22, 28). Our analysis of polysome profiles from MNK-depleted cells revealed that growth inhibition occurs as a result of reduced translation, arguing for positive regulation of translation via the MNK/eIF4E pathway. Although eIF4E is known to be a general translation factor, it can also preferentially enhance the translation of carcinogenesis-associated mRNAs, including regulators of the cell cycle, apoptosis, angiogenesis and invasion (29–32). Therefore, it is very likely that CGP57380-mediated reduction of translation and G₁ cell-cycle arrest results from inhibition of the selective translation of MNK-regulated, growth-promoting transcripts. Furthermore, analysis of polysomal profiles prepared from MNK1-depleted glioblastoma cells indicated that MNK1 signaling is not required for global translation. As previously reported, mice lacking both Mnk1 and Mnk2 develop normally and eIF4E phosphorylation at Ser209 does not occur, even when MNK upstream kinases are activated (33). These results demonstrate that MNK signaling is not crucial for normal growth; although, MNK activity may be necessary for growth and survival under certain conditions, for example particular stresses or cancer states. Indeed, in the same model, loss of MNK function sensitized mouse fibroblasts to apoptosis induced by serum withdrawal suggesting a function in adaptive responses to stress (34). Similarly, arsenic-induced apoptosis was enhanced in cells with targeted disruption of *MNK* genes (35). Thus, our results together with the previously published data, promote elevated MNK activity in human glioblastoma as an attractive therapeutic target for 2 reasons. First, MNK signaling is not required for normal cell growth or development. Second, its inhibition may neutralize the cellular stress responses that aid cancer cell survival and are triggered by many therapies.

The different degree of translation reduction in CGP57380-treated cells compared with MNK1-specific knockdown (Figs. 3 and 4) may be explained by the fact that CGP57380 targets all human MNKs and inhibits eIF4E phosphorylation almost completely whereas MNK1 knockdown reduces the phosphorylated form of eIF4E by 50%, presumably due to an MNK2 compensatory function. In our study, similar effects were also observed in proliferation assays, where CGP57380 had a more dramatic effect on cell phenotype than a genetic approach using MNK1-specific knockdown. We found MNK1, but not MNK2, to be overexpressed in human gliomas. Although the 2 kinases share eIF4E as a substrate, they exhibit 70% identity in their catalytic domains (36), potentially indicating regulation of different downstream pathways. An MNK1-specific role that is not compensated by MNK2 has already been proposed from the results of experiments in which reintroduction of wild-type Mnk1, but not Mnk2,

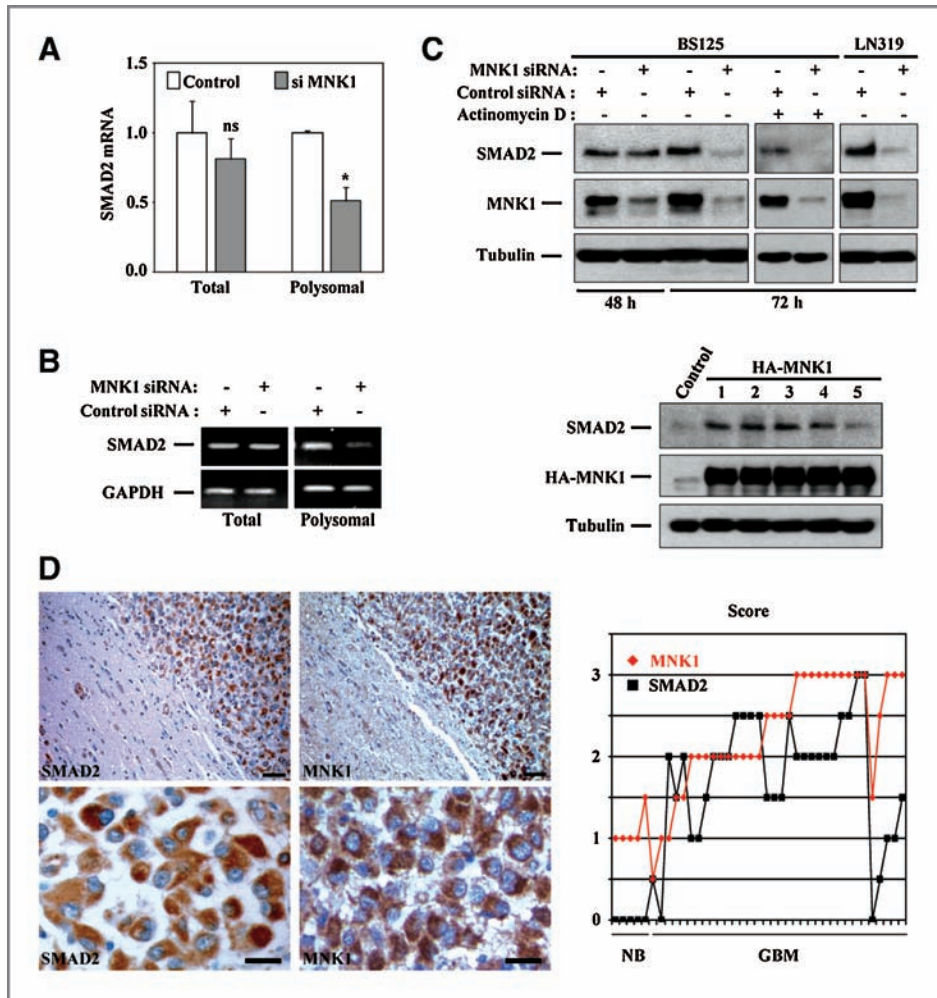


Figure 5. MNK1 regulated SMAD2 translation in human glioblastoma. **A**, SMAD2 transcript levels obtained by microarray analysis of total and polysomal RNA from MNK1-depleted and control-transfected BS125 cells. Expression of SMAD2 in controls was set to 1. *, $P < 0.05$ or nonsignificant (ns) versus controls. **B**, microarray data validation by semi-quantitative RT-PCR analysis using SMAD2 and GAPDH (control) specific primers. **C**, BS125 and LN319 whole cell protein lysates prepared 48 or 72 hours after transfection with duplex siRNA against MNK1 or with a control duplex against luciferase were subjected to Western blot analysis using antibodies specific to total SMAD2, MNK1, and tubulin, as an equal loading control. In addition, 48 hours after transfection, BS125 cells were further incubated with 1 $\mu\text{mol/L}$ of actinomycin D for the next 24 hours and the protein lysates were analyzed as described above. Bottom, SMAD2 and MNK1 expression analyzed by Western blotting in stable BS125 cell clones overexpressing the full-length HA-MNK1 fusion protein and control cells transfected with an empty vector. **D**, examples of immunostaining for MNK1 and SMAD2 in GBM tumors. Slides were stained with MNK1- or SMAD2-specific monoclonal antibodies (brown) and counterstained with hematoxylin (blue); bars, 50 and 20 μm . Right, expression of MNK1 and SMAD2 obtained by tissue array analysis in 34 GBM patients and 5 normal brains (NB).

rescued the starvation-induced apoptotic phenotype of mouse embryonic fibroblasts from *mnk1/2* double-knockout animals (34). Furthermore, in the most recent study, MNK1-specific knockdown in U87MG cells was sufficient to reduce tumor formation in mouse xenograft model (37) suggesting that MNK1 plays an essential role in gliomagenesis. Therefore, to investigate the role of MNK1 in regulation of gene expression, we used a genetic approach for specifically knocking down MNK1 expression. Our microarray analysis detected 80 MNK1-dependent mRNAs, with 56 of them using polysomal RNA, indicating that MNK1-dependent gene expression is regulated mainly at the translational level. In a previous study, translation of the antiapoptotic protein Mcl-1 was found to be

regulated by eIF4E phosphorylation, thus supporting a role for MNK1 signaling in lymphoma cell survival (14). A more recent study using CGP57380 compound and an array of 263 prostate carcinoma-related genes identified new translationally regulated MNK targets involved in the response to hypoxia-inducible factor (HIF1 α) and cell-cycle regulation (cyclin-dependent kinases and inhibitors) in prostate cancer cells (38). Our screen used a genetic approach together with a genome-wide microarray to identify MNK1-specific-regulated genes. The fact that this screen did not identify previously described MNK targets may be due to GBM cell specificity. In addition, by targeting MNK1 (but not MNK2 or eIF4E phosphorylation), we identified an MNK1-specific subset of mRNAs

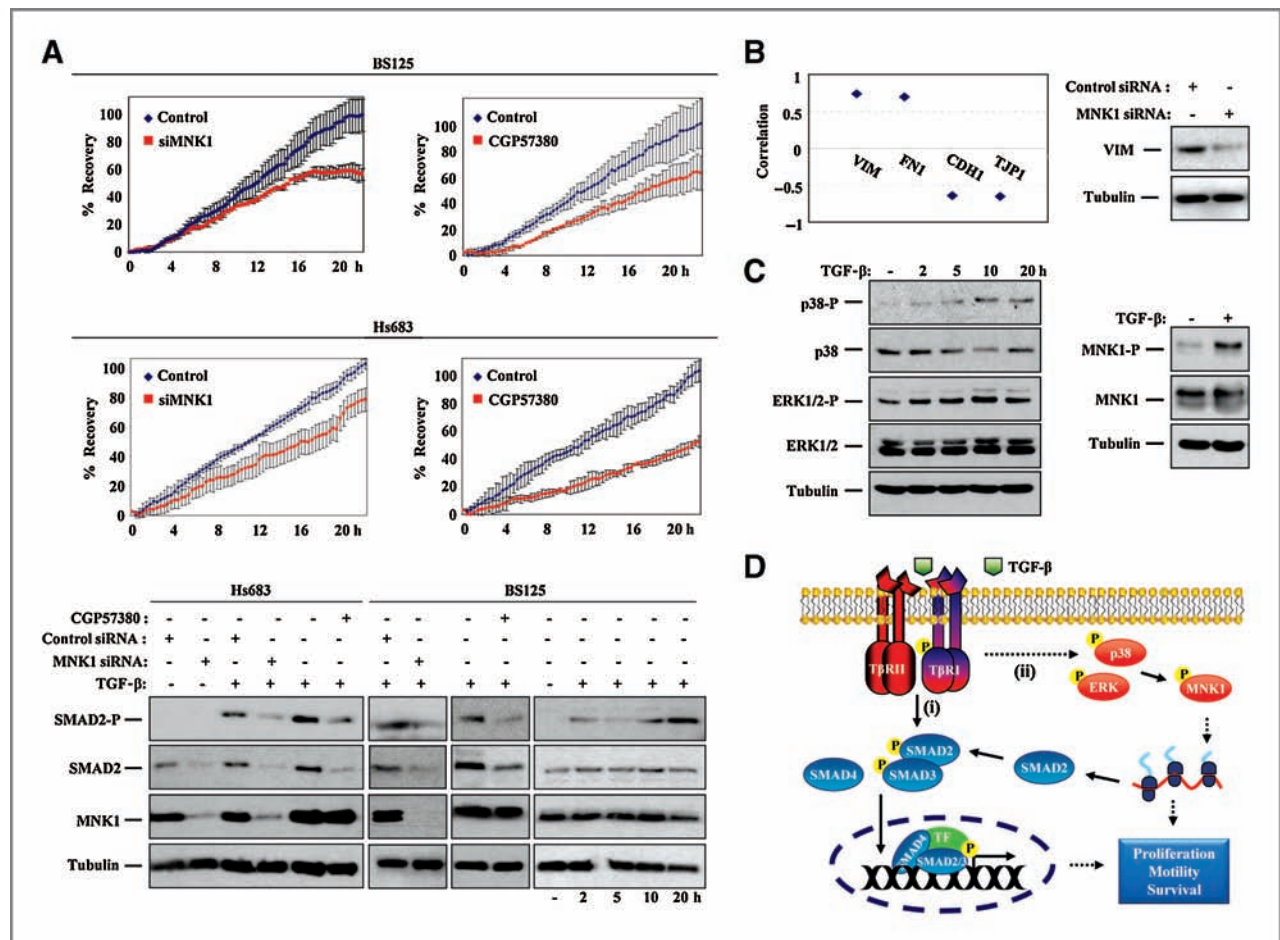


Figure 6. MNK1 signaling regulated TGF- β -induced glioma cell motility. **A**, BS125 and Hs683 cells were transfected with duplex siRNA oligonucleotides against the *MNK1* gene (si) or luciferase (control). A scratch was made 48 hours after transfection or 24 hours after treatment with 10 μ M/L CGP57380 or DMSO (control) and cellular motility was monitored in the presence of 5 nmol/L TGF- β . After 22 hours, the scratch "wound" recovery was set to 100% in control cells. All experiments were assayed in triplicate and results shown as means \pm SD. Bottom, whole protein lysates isolated from transfected and/or treated cells (as described above) were subjected to Western blot analysis using p-SMAD2 (Ser245/250/255), SMAD2, MNK1, and tubulin antibodies. **B**, correlation coefficients of the comparison of MNK1 and EMT markers in 15 GBMs and 2 normal brain samples. VIM, vimentin; FN1, fibronectin; CDH1, E-cadherin; and TJP1, tight junction protein 1. Right, MNK1-dependent expression of vimentin analyzed by Western blotting in MNK1-depleted BS125 cells after duplex siRNA transfection and TGF- β treatment as described above. **C**, expression of p-p38 (Thr180/Tyr182), p38, p-ERK1/2 (Thr202/Tyr204), ERK1/2, p-MNK1 (Thr197/202), and MNK1 was analyzed by Western blotting in BS125 cells treated with 5 nmol/L TGF- β at indicated time points or for 24 hours. **D**, model for MNK1 and TGF- β pathway convergence. Overexpressed and activated MNK1 kinase increases SMAD2 translation thereby contributing to signaling of canonical (i) TGF- β pathways via SMAD2/3/4 complexes that interact with transcription factors (TF) and induce expression of genes involved in proliferation, motility, and survival of malignant GBM cells. Hyperactivated TGF- β receptors (T β RI and T β RII) can also activate noncanonical pathways (ii) leading to phosphorylation of ERKs and p38 kinases and activation of MNK1 that can further increase translation of specific mRNAs involved in cancer progression.

that may be different to MNK2- or phospho-EIF4E-regulated target gene groups.

Genetic or pharmacologic targeting of MNK1 reduced total and phosphorylated SMAD2 levels as well as TGF- β -associated cell motility of glioma cells indicating that MNK1 regulates not only one of the main transducers of TGF- β signals but also an TGF- β /SMAD2-dependent phenotype. The correlation between EMT markers and MNK1 expression in GBM patients, and the reduced vimentin expression in MNK1-depleted GBM cells, suggest MNK1 regulation of TGF- β -induced gene expression. In addition, the correlation found between MNK1 and SMAD2 protein

expression in human GBMs further supports our model in GBM patients. SMAD2 is one of the major signal transducers during TGF- β pathway activation. Previous studies showed that high TGF- β /SMAD activity in human glioma patients correlated with poor prognosis and was dependent on platelet-derived growth factor beta (PDGFB) expression (39) and a more recent report demonstrates that TGF- β can induce the self-renewal capacity of glioma-initiating cells in a SMAD-dependent manner (40). In our study, MNK1 expression correlated with PDGFB in primary GBM patients (correlation coefficient = 0.56, data not shown) and targeting MNKs reduced GBM-derived spheres growth

suggesting that MNK1 signaling supports TGF- β activity in malignant gliomas.

In invasive cancers, TGF- β signaling has a tumor-promoting effect supporting cell motility, invasion, angiogenesis, immunosuppression, and EMT (41). Interestingly, noncanonical TGF- β signaling pathways can activate ERKs and p38 kinases (42) that phosphorylate and activate MNKs. In agreement with previous study, TGF- β induced ERK and p38 activity as well as MNK1 phosphorylation in GBM cells. Therefore, our data together with previous observations propose a model whereby activation of MNK1 and TGF- β pathways and their mutual regulation support GBM progression (Fig. 6D).

A balance between MNK activity and mTOR pathways was reported in prostate and lung cancer cells, where downregulation of one pathway was correlated with the activation of another, resulting in a defined level of translation that supported cancer cell survival (38, 43). In agreement with a recent study, simultaneous blocking of the MNK and mTOR pathways significantly blocked GBM cell proliferation, colony formation, and tumor sphere growth. We observed a marked additive effect on translation inhibition and G₁ cell-cycle arrest compared with the single treatment, thus also indicating a therapeutic potential of targeting MNK and mTOR

pathways against certain tumor entities including malignant gliomas.

Disclosure of Potential Conflicts of Interest

Part of the results of this study has been used for the patent application WO 2010/055072.

Acknowledgments

The authors thank E. Oakley and T. Roloff for microarray analysis; S. Bichet and H. Kohler for help with immunohistochemistry and FACS experiments, respectively; H. Gram for the MNK1-Flag construct; and P. King for editing the manuscript.

Grant Support

This research was funded by Oncosuisse CCRP grant KFP OCS-01613-12-2004 to B.A. Hemmings and A. Merlo and supported by a Marie Curie Fellowship (FP7-IEF-236745) to M. Grzmil. The FMI is part of the Novartis Research Foundation.

The costs of publication of this article were defrayed in part by the payment of page charges. This article must therefore be hereby marked *advertisement* in accordance with 18 U.S.C. Section 1734 solely to indicate this fact.

Received August 25, 2010; revised December 22, 2010; accepted December 22, 2010; published OnlineFirst March 15, 2011.

References

- Mischel PS, Shai R, Shi T, Horvath S, Lu KV, Choe G, et al. Identification of molecular subtypes of glioblastoma by gene expression profiling. *Oncogene* 2003;22:2361-73.
- Cancer Genome Atlas Research Network. Comprehensive genomic characterization defines human glioblastoma genes and core pathways. *Nature* 2008;455:1061-8.
- Parsons DW, Jones S, Zhang X, Lin JC, Leary RJ, Angenendt P, Mankoo P, et al. An integrated genomic analysis of human glioblastoma multiforme. *Science* 2008;321:1807-12.
- Mellinghoff IK, Wang MY, Vivanco I, Haas-Kogan DA, Zhu S, Dia EQ, et al. Molecular determinants of the response of glioblastomas to EGFR kinase inhibitors. *N Engl J Med* 2005;353:2012-24.
- Stommel JM, Kimmelman AC, Ying H, Nabioullin R, Ponugoti AH, Wiedemeyer R, et al. Coactivation of receptor tyrosine kinases affects the response of tumor cells to targeted therapies. *Science* 2007;318:287-90.
- Van Meir EG, Hadjipanayis CG, Norden AD, Shu HK, Wen PY, Olson JJ. Exciting new advances in neuro-oncology: the avenue to a cure for malignant glioma. *CA Cancer J Clin* 2010;60:166-93.
- Grzmil M, Hemmings BA. Deregulated signalling networks in human brain tumours. *Biochim Biophys Acta* 2010;1804:476-83.
- Proud CG. Signalling to translation: how signal transduction pathways control the protein synthetic machinery. *Biochem J* 2007;403:217-34.
- Hay N, Sonenberg N. Upstream and downstream of mTOR. *Genes Dev* 2004;18:1926-45.
- Buxade M, Parra-Palau JL, Proud CG. The Mnk1s: MAP kinase-interacting kinases (MAP kinase signal-integrating kinases). *Front Biosci* 2008;13:5359-73.
- De Benedetti A, Graff JR. eIF-4E expression and its role in malignancies and metastases. *Oncogene* 2004;23:3189-99.
- Fan S, Ramalingam SS, Kauh J, Xu Z, Khuri FR, Sun SY. Phosphorylated eukaryotic translation initiation factor 4 (eIF4E) is elevated in human cancer tissues. *Cancer Biol Ther* 2009;8:1463-9.
- Silvera D, Formenti SC, Schneider RJ. Translational control in cancer. *Nat Rev Cancer* 2010;10:254-66.
- Wendel HG, Silva RL, Malina A, Mills JR, Zhu H, Ueda T, et al. Dissecting eIF4E action in tumorigenesis. *Genes Dev* 2007;21:3232-7.
- Buxadé M, Parra JL, Rousseau S, Shpiro N, Marquez R, Morrice N, et al. The Mnk1s are novel components in the control of TNF alpha biosynthesis and phosphorylate and regulate hnRNP A1. *Immunity* 2005;23:177-89.
- Maier D, Comparone D, Taylor E, Zhang Z, Gratzl O, Van Meir EG, et al. New deletion in low-grade oligodendroglioma at the glioblastoma suppressor locus on chromosome 10q25-26. *Oncogene* 1997;15:997-1000.
- Korur S, Huber RM, Sivasankaran B, Petrich M, Morin P Jr, Hemmings BA, et al. GSK3beta regulates differentiation and growth arrest in glioblastoma. *PLoS One* 2009;4:e7443.
- Grzmil M, Rzymiski T, Milani M, Harris AL, Capper RG, Saunders NJ, et al. An oncogenic role of eIF3e/INT6 in human breast cancer. *Oncogene* 2010;29:4080-9.
- Gentleman RC, Carey VJ, Bates DM, Bolstad B, Dettling M, Dudoit S, et al. Bioconductor: open software development for computational biology and bioinformatics. *Genome Biol* 2004;5:R80.
- Wettenhall JM, Smyth GK. limmaGUI: a graphical user interface for linear modeling of microarray data. *Bioinformatics* 2004;20:3705-6.
- O'Loughlen A, Gonzalez VM, Pineiro D, Perez-Morgado MI, Salinas M, Martin ME. Identification and molecular characterization of Mnk1b, a splice variant of human MAP kinase-interacting kinase Mnk1. *Exp Cell Res* 2004;299:343-55.
- Knauf U, Tschopp C, Gram H. Negative regulation of protein translation by mitogen-activated protein kinase-interacting kinases 1 and 2. *Mol Cell Biol* 2001;21:5500-11.
- Dennis G Jr, Sherman BT, Hosack DA, Yang J, Gao W, Lane HC, et al. DAVID: Database for Annotation, Visualization, and Integrated Discovery. *Genome Biol* 2003;4:P3.
- Huang DW, Sherman BT, Lempicki RA. Systematic and integrative analysis of large gene lists using DAVID Bioinformatics Resources. *Nature Protoc* 2009;4:44-57.
- Micalizzi DS, Ford HL. Epithelial-mesenchymal transition in development and cancer. *Future Oncol* 2009;5:1129-43.
- Matsuyama S, Iwadate M, Kondo M, Saitoh M, Hanyu A, Shimizu K, et al. SB-431542 and Gleevec inhibit transforming growth factor-beta-induced proliferation of human osteosarcoma cells. *Cancer Res* 2003;63:7791-8.

27. Kleijn M, Scheper GC, Voorma HO, Thomas AA. Regulation of translation initiation factors by signal transduction. *Eur J Biochem* 1998;253:531–44.
28. Saghir AN, Tuxworth WJ Jr, Hagedorn CH, McDermott PJ. Modifications of eukaryotic initiation factor 4F (eIF4F) in adult cardiocytes by adenoviral gene transfer: differential effects on eIF4F activity and total protein synthesis rates. *Biochem J* 2001;356:557–66.
29. Mamane Y, Petroulakis E, Martineau Y, Sato TA, Larsson O, Rajasekhar VK, et al. Epigenetic activation of a subset of mRNAs by eIF4E explains its effects on cell proliferation. *PLoS One* 2007;2:e242.
30. Larsson O, Li S, Issaenko OA, Avdulov S, Peterson M, Smith K, et al. Eukaryotic translation initiation factor 4E induced progression of primary human mammary epithelial cells along the cancer pathway is associated with targeted translational deregulation of oncogenic drivers and inhibitors. *Cancer Res* 2007;67:6814–24.
31. Chung J, Bachelder RE, Lipscomb EA, Shaw LM, Mercurio AM. Integrin (alpha 6 beta 4) regulation of eIF-4E activity and VEGF translation: a survival mechanism for carcinoma cells. *J Cell Biol* 2002;158:165–74.
32. Furic L, Rong L, Larsson O, Koumakpayi IH, Yoshida K, Brueschke A, et al. eIF4E phosphorylation promotes tumorigenesis and is associated with prostate cancer progression. *Proc Natl Acad Sci U S A* 2010;107:14134–9.
33. Ueda T, Watanabe-Fukunaga R, Fukuyama H, Nagata S, Fukunaga R. Mnk2 and Mnk1 are essential for constitutive and inducible phosphorylation of eukaryotic initiation factor 4E but not for cell growth or development. *Mol Cell Biol* 2004;24:6539–49.
34. Chrestensen CA, Eschenroeder A, Ross WG, Ueda T, Watanabe-Fukunaga R, Fukunaga R, et al. Loss of MNK function sensitizes fibroblasts to serum-withdrawal induced apoptosis. *Genes Cells* 2007;12:1133–40.
35. Dolniak B, Katsoulidis E, Carayol N, Altman JK, Redig AJ, Tallman MS, et al. Regulation of arsenic trioxide-induced cellular responses by Mnk1 and Mnk2. *J Biol Chem* 2008;283:12034–42.
36. Roux PP, Blenis J. ERK and p38 MAPK-activated protein kinases: a family of protein kinases with diverse biological functions. *Microbiol Mol Biol Rev* 2004;68:320–44.
37. Ueda T, Sasaki M, Elia AJ, Chio II, Hamada K, Fukunaga R, et al. Combined deficiency for MAP kinase-interacting kinase 1 and 2 (Mnk1 and Mnk2) delays tumor development. *Proc Natl Acad Sci U S A* 2010;107:13984–90.
38. Bianchini A, Loiarro M, Bielli P, Busà R, Paronetto MP, Loreni F, et al. Phosphorylation of eIF4E by MNKs supports protein synthesis, cell cycle progression and proliferation in prostate cancer cells. *Carcinogenesis* 2008;29:2279–88.
39. Bruna A, Darken RS, Rojo F, Ocaña A, Peñuelas S, Arias A, et al. High TGFbeta-Smad activity confers poor prognosis in glioma patients and promotes cell proliferation depending on the methylation of the PDGF-B gene. *Cancer Cell* 2007;11:147–60.
40. Peñuelas S, Anido J, Prieto-Sánchez RM, Folch G, Barba I, Cuartas I, et al. TGF-beta increases glioma-initiating cell self-renewal through the induction of LIF in human glioblastoma. *Cancer Cell* 2009;15:315–27.
41. Leivonen SK, Kahari VM. Transforming growth factor-beta signaling in cancer invasion and metastasis. *Int J Cancer* 2007;121:2119–24.
42. Moustakas A, Heldin CH. The regulation of TGFbeta signal transduction. *Development* 2009;136:3699–714.
43. Wang X, Yue P, Chan CB, Ye K, Ueda T, Watanabe-Fukunaga R, et al. Inhibition of mammalian target of rapamycin induces phosphatidylinositol 3-kinase-dependent and Mnk-mediated eukaryotic translation initiation factor 4E phosphorylation. *Mol Cell Biol* 2007;27:7405–13.

6.2 Generation of MerTK monoclonal antibody

(In collaboration with Susanne Schenk, FMI)

The recombinant GST-tagged human MerTK (amino acids 536-999; from Janis Liebetanz, Dorian Fabbro, Novartis) was used as antigen to generate MerTK monoclonal antibody. Supernatants from hybridoma cells were screened by ELISA with MBP-tagged human MerTK (amino acids 536-999) as the antigen, and by western blotting on U373, K562 and U937 whole cell extracts. Primary hybridoma clones were subcloned by limiting dilution.

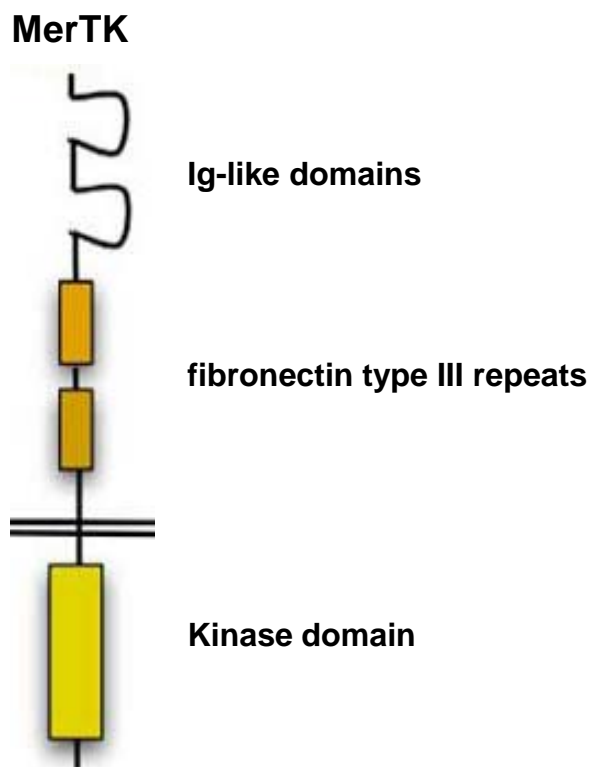
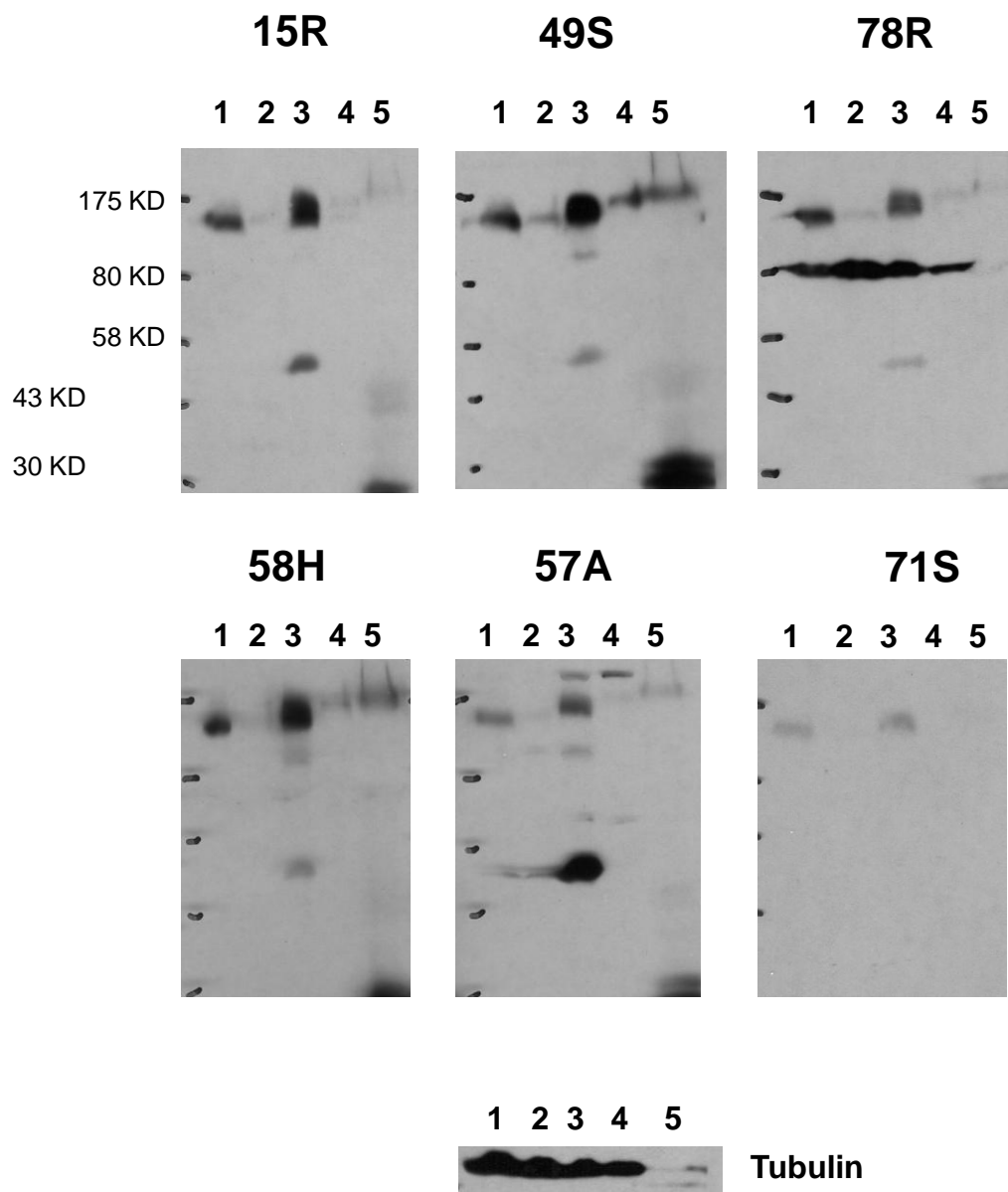


Figure 1: Schema of Mer receptor tyrosine kinase



1. U373 2. U373shMerTK 3. K562 4. K562 shMerTK 5. U937

Figure 2. Validation of clones recognizing endogenous MerTK

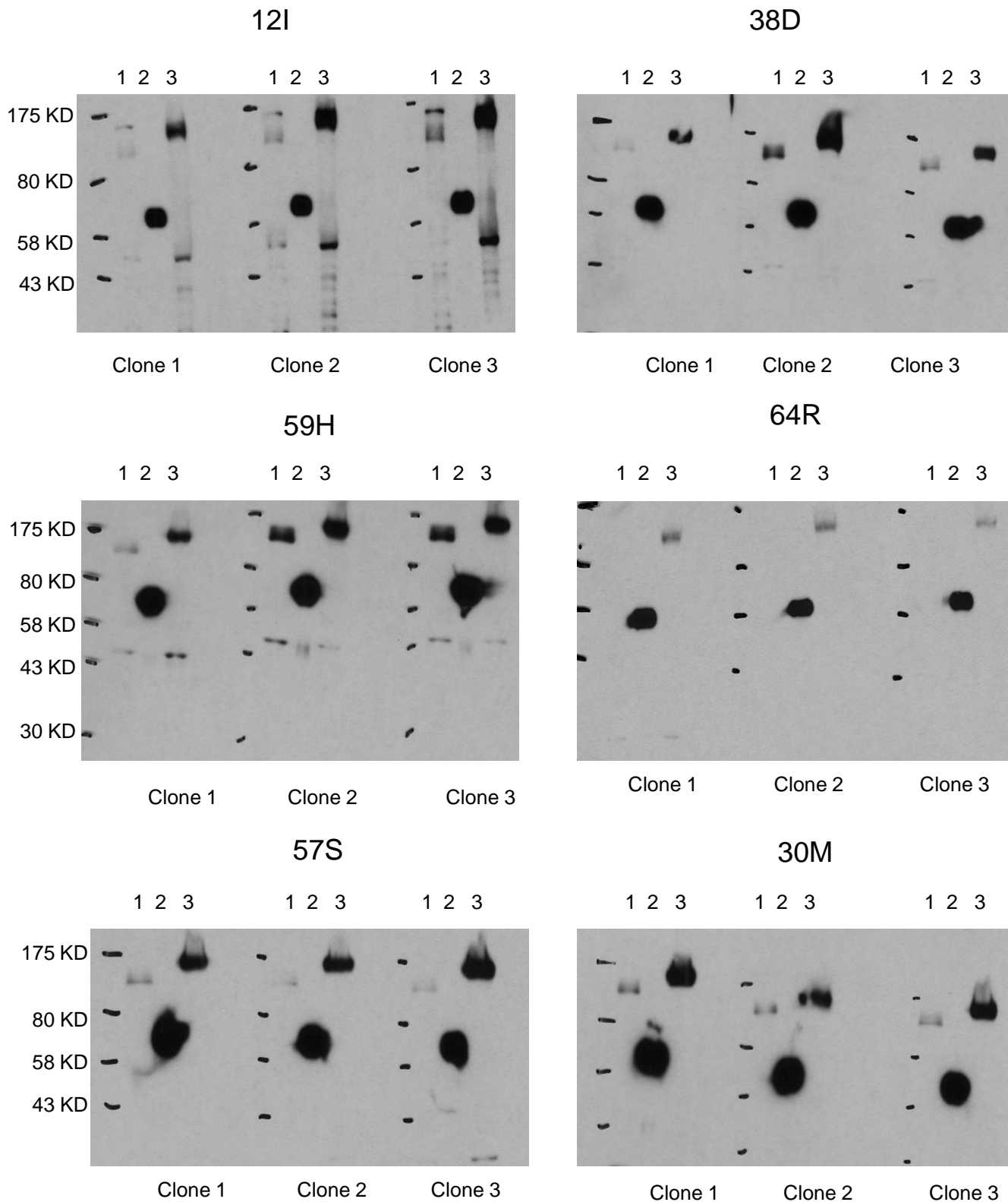


Figure 3. Validation of subclones recognizing three TAM receptors. 1. Protein lysates of 293 cells expressing pcDNA3-Axl-HA; 2. Purified GST-Tyro3-ICD. 3. Protein lysates of U373 cells stably expressing full-length MerTK.

Table 1. Summary of MerTK monoclonal antibody clones

clone	ELISA orig .	Western	subcloning	final clone	isotype	comments
57A	0.917	pos.				keep
15B	0.871	pos.	--			keep
88B	0.903	pos.	--			keep
38D	0.905	pos.	subclone			
59E	0.958	pos.	subclone			
87F	1.061	pos.	--			keep
5H	0.947	pos.	--			keep
58H	0.894	pos.	subclone			
12I	1.052	pos.	subclone			
30M	0.811	pos.	subclone			
15R	0.968	pos.	subclone			
64R	0.881	pos.	subclone			
78R	0.905	pos.	subclone			
28S	0.896	pos.	--			keep
30S	0.837	pos.				keep
49S	0.926	pos.	subclone			
57S	0.852	pos.	subclone			
71S	0.863	pos.	--			keep

Yellow: Clones recognizing endogenous MerTK

Blue: Clones recognizing all three overexpressed TAM receptors

7. Acknowledgments

I would like to sincerely thank my supervisor, Dr. Brian Hemmings FRS for giving me the opportunity to do my PhD in his laboratory, for letting me work on this challenging project, and for shaping my scientific thoughts and intellectual skills throughout the past years.

I would like to thank Pier Morin, who performed the microarray analysis and provided the basis of my PhD project. I would also like to thank the current GBM team, especially Gerald Moncayo and Michal Grzmil as well as all the other members of the Hemmings lab for their constructive suggestions and encouragement. A special thank goes to Gongda Xue for his consistent help, including scientific discussions, experiment design as well as manuscript correction.

I am very grateful to my thesis committee members Prof. Nancy Hynes, Prof. Kurt Ballmer and Prof. Adrian Merlo for continuous support during the course of my thesis. I would like to thank Prof. Stephan Frank for helping with the histological analysis of GBM samples and squeezing time for valuable discussions and comments on my manuscript. I would also like to thank all the other collaborators for their constant support in the past years, ranging from the provision of materials and scientific discussions to constructive comments on the manuscript.

I am extremely thankful to my husband Ying Yuan for his patience, understanding and encouragement during my PhD. I am also very grateful to my families in China. This thesis would not be possible without their love and consistent support. I feel very lucky to have my friends present in my life. Thank you so much for sharing with me your happiness and frustrations!

And, last but not least, I am very grateful to all the patients who contributed to this research.

8. Curriculum Vitae

Personal information

Yuhua Wang

Unterbaselweg 16, D-79576,

Weil am Rhein, Germany

Nationality: Chinese

Date of birth: 13/01/1982

yuhua.wang@fmi.ch

Education and Professional Training

05/2006 - now

PhD (Cell Biology), University of Basel, Switzerland

09/2006 - 02/2007

Internship at Max-Planck Institute of Immunobiology, Freiburg, Germany

09/2004 - 06/2006

Masters student, National Key Laboratory of Molecular and Medical Virology, Wuhan

University, Wuhan, China

09/2000 - 06/2004

BSc in Biology, Sichuan University, Chengdu, China

Publications

1. **Wang Y**, Moncayo G, Frank S, Morin P Jr, Xue G, Grzmil M, Lino MM, Merlo A, Clément V, Hemmings BA. Mer receptor tyrosine kinase promotes tumor cell invasion and survival in glioblastoma multiforme. (*Oncogene* - Under revision)

2. Grzmil M, Morin P Jr, Lino MM, Merlo A, Frank S, **Wang Y**, Moncayo G, and Hemmings BA. (2011). MAP Kinase-Interacting Kinase 1 Regulates SMAD2-Dependent TGF- β Signaling Pathway in Human Glioblastoma. *Cancer Research*. 71:2392-2402

Conferences Attended and Presentations

11/2011 The NCRI Cancer Conference, Liverpool, UK

Poster presentation

9/2011 TOR, PI3K and Akt Conference, Basel, Switzerland

Poster presentation

09/2010 FMI 40th Anniversary Symposium, Basel, Switzerland

Poster presentation

2007-2011 FMI Annual Meeting

Poster presentation